Acta Oceanol. Sin., 2021, Vol. 40, No. 7, P. 198–280
https://doi.org/10.1007/s13131-021-1730-5
http://www.hyxb.org.cn
E-mail: ocean2@hyxb.org.cn

Holocene sea level trend on the west coast of Bohai Bay, China: reanalysis and standardization

Jianfen Li[1, 2], Zhiwen Shang[1, 2], Fu Wang[1, 2], Yongsheng Chen[1, 2], Lizhu Tian[1, 2], Xingyu Jiang[1, 2],
Qian Yu[3, 4], Hong Wang[1, 2]*

[1] Tianjin Center, China Geological Survey, Tianjin 300170, China

[2] Key Laboratory of Coast Geo-Environment, China Geological Survey, Tianjin 300170, China

[3] Key Laboratory for Coast and Island Development (Nanjing University), Ministry of Education, Nanjing 210023, China

[4] School of Geographic and Oceanographic Sciences, Nanjing University, Nanjing 210023, China

Received 2 April 2020; accepted 14 August 2020

© Chinese Society for Oceanography and Springer-Verlag GmbH Germany, part of Springer Nature 2021

Abstract

Using 110 newly revised Holocene sea level indicators categorized into three types, sediments (67), shelly cheniers (27) and oyster reefs (16), this paper firstly provides a Holocene relative sea level curve, based on multiple approaches of litho- and biostratigraphies and sedimentary faces analysis, for the west coast of Bohai Bay, China. Following considerations, including indicative meaning, the paleo tidal pattern and range and conversion from mean tidal level to mean sea level, an apparent relative mean sea level (RMSL) curve was further reconstructed. After systematical calibration using CALIB, those of the 48 reworked samples were further corrected for the residence-time effect. Similarly, the younger ages for another 35 samples were chosen at the subsample level. These result in a younger-oriented shift for about 0.5 ka. Three local spatial factors, including neotectonic subsidence (average rate about 0.1 mm/a), self-compaction of unconsolidated sediments (between a few decimeters to about 6 m) and subsidence due to groundwater withdrawal (between a few centimeters to about 2.5 m), were quantitatively corrected. Finally, the amended RMSL curve after eliminating all these local temporo-spatial factors is very likely to show non-existence of mid-Holocene highstand and imply potential influences of both ice-volume equivalent sea level and regional glacial isostatic adjustment. Although it is still unable to divide both global and regional factors, the slowdown of sea level rise, in 7.5 –6.8 ka with a maximum height less than +1 m, may constrain the model effort in the near future.

Key words: cheniers, oyster reefs, sediments, temporospatial corrections, local RMSL

Citation: Li Jianfen, Shang Zhiwen, Wang Fu, Chen Yongsheng, Tian Lizhu, Jiang Xingyu, Yu Qian, Wang Hong. 2021. Holocene sea level trend on the west coast of Bohai Bay, China: reanalysis and standardization. Acta Oceanologica Sinica, 40(7): 198–280, doi: 10.1007/s13131-021-1730-5

1 Introduction

Local relative sea level changes contain rich information on the mechanisms that reflect the spatial and tempo-

Foundation item: The National Natural Science Foundation of China under contract Nos 41372173, 41476074 and 41806109; the China Geological Survey Project under contract Nos DD20189506 and DD20211301.
*Corresponding author, E-mail: whong@cgs.cn

ral variations of the global sea level picture and constrain history of ice melting and isostasy. However, such information is useful only if the resolution of the data (i.e., the sea level indicators, sea level index points) is sufficiently high.

Holocene sea level change on the west coast of Bohai Bay, China, represents a typical example. This issue has been investigated intermittently for the last four decades, initiated by litho- and biostratigraphical studies (Wang, 1964; Zhao et al., 1978; Yang et al., 1979). Zhao and Zhang (1984), Xia (1981), Xie (1986), Xu (1994), Wang (1994) and Xie et al. (2012) preliminarily reconstructed the history of relative sea level change for Bohai Bay and/or other sectors along the northern mainland coast of China. These studies were evaluated by Pirrazoli (1991) in his atlas of sea level curves. However, as Woodroffe and Horton (2005) have indicated, the spatial and temporal uncertainties of these early indicators were too large, in particular, these indicators do not meet the generally acknowledged criteria established by van de Plassche (1982, 1986), Murray-Wallace and Woodroffe (2014) and Shennan et al. (2015).

For example, ^{14}C dates from bulk-samples were presented as measured values (without isotope fractionation correction) and were not systematically calibrated for the regional marine reservoir effect and fluctuations in the atmospheric ^{14}C activity (Wang et al., 2004; Wang and Fan, 2005). The influence of residence time effects on reworked samples was not recognized or corrected for (Shang et al., 2016).

The vertical spatial accuracy of the early indicators was on the order of decimeters or meters (Zhao and Zhang, 1984; Wang, 1994). Moreover, the approaches used to measure the elevations of several of the indicators were oversimplified. For example, many researchers believed that shelly cheniers formed along shorelines at high tidal positions (Zhao et al., 1980; Zhao and Zhang, 1984; Liu and Walker, 1989; Xu, 1994). Therefore, half of the tidal range or 2 m should be subtracted from the elevation measured to determine the contemporary mean sea level (MSL) (Zong, 2004; Sun et al., 2015). However, other researchers have found that the subsurface of shelly cheniers may dip seawards, with a 1–2 m vertical difference between the rear and front ends (i.e., between the landward and seaward edges), into a muddy intertidal flat (Cai, 1981; Xia, 1981; Wang, 1994; Wang et al., 2000a, b, c; Su et al., 2011). Therefore, one must carefully consider the depositional position of a chenier indicator and its relationship with the tidal environment or use a wider vertical error range if one cannot accurately determine its depositional position (Su et al., 2011). Recently, several case studies were able to precisely define the subsurface slope of cheniers and the relationship between the chenier and the tidal range for such indicators found just above the chenier subsurface① (Su et al., 2011; Wang et al., 2011a; Li et al., 2016a, b).

Another method for determining the indicative meaning is using the top surface of oyster reefs, mainly those formed by *Crassostrea gigas*. Early studies suggested that the growth of *C. gigas* reefs was controlled by low tidal levels and the reefs cannot build above low tide. Therefore, half of the tidal range should be added to the elevation of the surface to reconstruct mean tidal level (MTL) (Zhao and Zhang, 1984). However, recent studies have reconfirmed that the elevation of the top surface of *C. gigas* reefs is mainly controlled by MTL, but not low tides (Wang, 1994; Zhang, 2004; Wang et al., 2006, 2011a, b, c). This has been shown by conchologists such as Okutani (2000).

Other than cheniers and oyster reefs, most sea level indicators are embodied in sediments; these types of sea level indicators include basal peat layers, which previously have been used by the local researchers (Zhao and Zhang, 1984) and the authors (Wang, 1994; Li, 2010; Wang et al., 2011a). Recently, several new efforts to integrate results from the area were restricted to basal peat layers obtained from cores in the coastal lowland and event-typed pulses of relative sea level changes found in cores in the adjacent shallow sea (Tian et al., 2017; Wang et al., 2020b).

In this paper, we attempt to establish an improved data set of the Holocene sea level indicators of the area; and the materials were obtained from sediments, shelly cheniers and oyster reefs (we reevaluated our previous data in Li et al. (2015) with a set of newly obtained data for the analysis). On such a basis, we establish a new local relative mean sea level (RMSL) curve, with systematic considerations for the local factors affecting the RMSL and discussions for the spatio-temporal position of the turning-phase of sea level change and possible constraints for the glacial isostatic adjustment (GIA) influence on the local RMSL trend. Finally, we try to approach potential ability to identify future research directions.

2 Regional setting

The Bohai Sea is an inner sea of China, including its three embayments, i.e., Liaodong Bay, Bohai Bay and Laizhou Bay (Fig. 1). Our study area, the coast of Bohai Bay, is located in the west Bohai Sea, with a muddy coastal lowland being distributed over the northeast part of

①Shang Zhiwen, Li Jianfen, Wang Hong, et al. 2016. Report of the China Coastal Depositional Records on Climate Changes (in Chinese), 74–99
②Pei Yandong, Wang Hong, Li Fenglin, et al. 2008. Tianjin Coastal Investigation Report (in Chinese), 7–13
③Li Jijun, Zhai Zimei, Shen Jian, et al. 2009. The Report of Tianjin Urban Geological Survey (in Chinese), 32–260

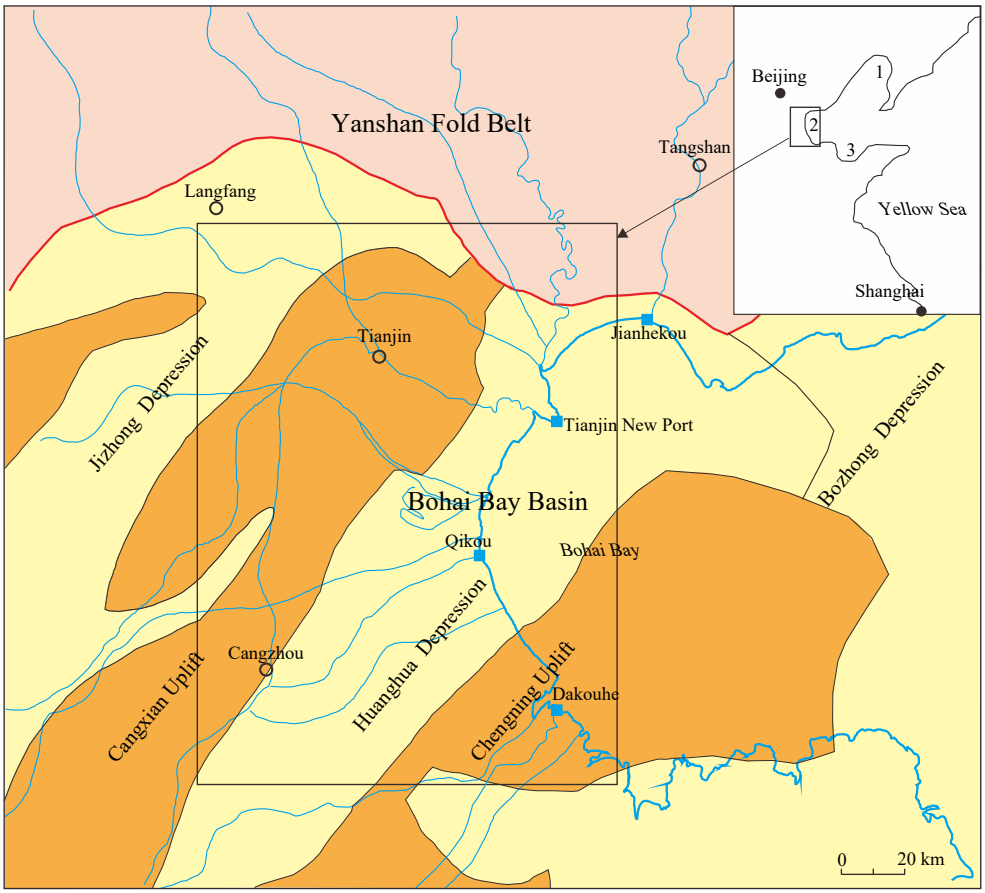

Fig. 1. Basement tectonic map of the study area, depicted by a black rectangle, mainly belongs to the Bohai Bay Basin (Zhang et al., 2010; Huang et al., 2014; Liu et al., 2016). Four tidal gauge stations, located at the mouths of four rivers, are shown by blue solid squares. Inset: 1. Liaodong Bay; 2. Bohai Bay; 3. Laizhou Bay (modified from Li et al., 2015).

the North China Plain (Fig. 1). Today, the coastal plain is generally lower than 5 m in elevation relative to National Vertical Datum 1985, with gentle slopes at around 1: 10 000. There are intertidal muddy flats, 3−5 km wide, with an average gradient of about 1:1 000[②] (Shang et al., 2016).

Geologically, the basement of study area, from the northwest to the southeast, includes the Jizhong Depression, the Cangxian Uplift, the Huanghua Depression and the Chengning Uplift, which are a set of secondary units of the Bohai Bay Basin (Fig. 1). Relative to the surrounding fold zones, the basin has slowly subsided since Paleogene rifting, being filled with mudstone, sandstone and psepholite, 3 000−5 000 m thick, during the Paleogene and sandstone and mudstone, 1 000−5 000 m thick, during the Neogene; in the Quaternary, fluvio-lacustrine muddy and sandy sediments were deposited with a maximum thickness of approximately 500 m[③] (Zhang et al., 2010; Chen et al., 2013; Huang et al., 2014).

Holocene sediments, about 15−25 m thick, superficially covered the entire study area and are divided into three parts: the lower and upper parts with flood plain and salt marsh-lagoonal facies, and the intercalated middle part with marine transgressive−regressive facies representing intertidal to shallow marine environments. The Holocene strata are mainly composed of silts and clays with a small amount of fine sands, showing a continuous stratigraphic sequence. All these coastal fine sediments are favorable for recording and preserving information of sea level changes. However, due to such very fine characteristics the late Pleistocene and Holocene brackish shallow aquifers in this coastal area were often semi-confined and confined with high levels of mineralization (Cao et al., 2016). It may affect the ages of sea level indicators concerned (see the following discussion of this paper).

Furthermore, we speculate that the Holocene tidal pattern in the Bohai Bay could be similar to present, and the

[④]Lambeck K. 2007. Paleo Reconstruction for China Sea. Lecture at Graduate School of Chinese Academy of Sciences, Beijing

[⑤]OkunoJ.2009.Glacio-andHydroisostasyandSeaLevelChangessincetheLastGlacialMaximum.LectureatEastChinaNormal University, Shanghai

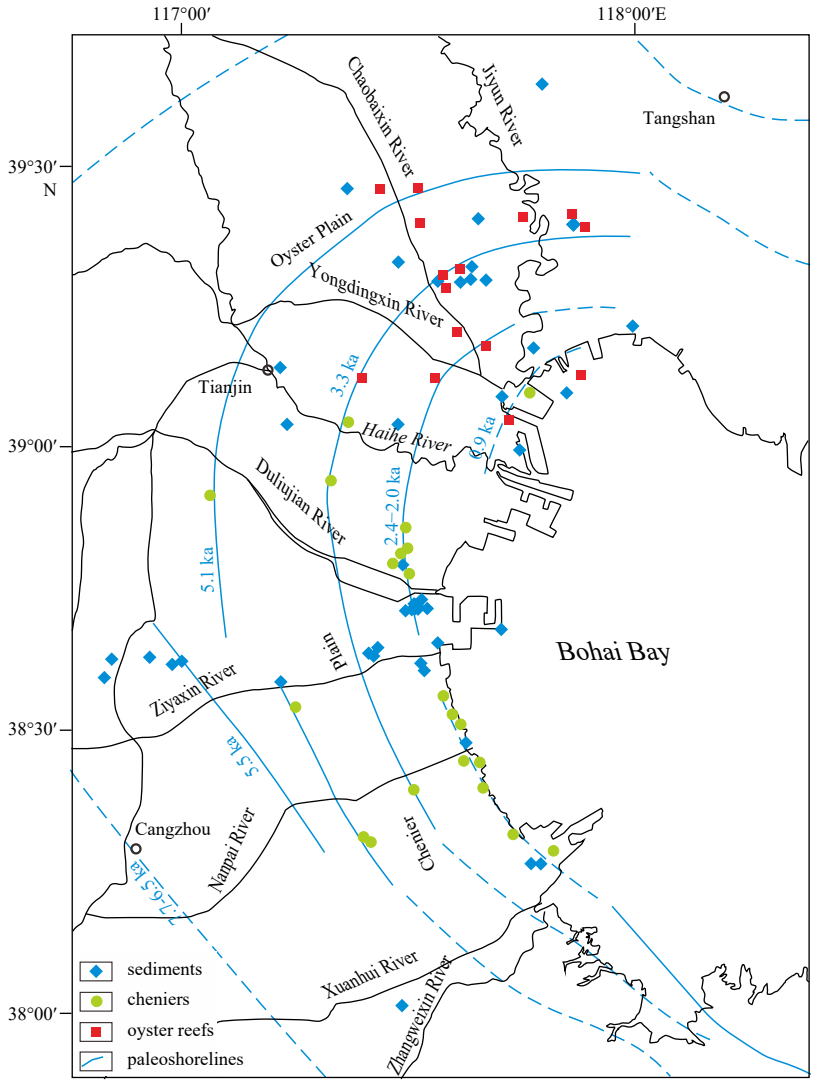

Fig. 2. Map showing the geographic distribution of the sea level indicators in the coastal lowland and contiguous shallow sea area of the west coast of Bohai Bay (modified from Li et al., 2015).

paleo tidal range is also similar if not even smaller (Shennan and Horton, 2002). This estimation is supported by the spatio-temporal distribution of Holocene shorelines showing an approximately concentric−circle configuration with present (Wang et al., 2010; Li et al., 2015; Shang et al., 2016). Therefore, the indicative meanings of Holocene sea level indicators are likely determined reasonably based on the present tidal regime (Fig. A1 and Tables A1−3).

At present, the annual average precipitation in the study area is about 600 mm (max. 897 mm, min. 332 mm), but the annual mean evaporation reaches about 1 740 mm (max. 2 673 mm). This striking contrast results in the presence of the salt-tolerant *Artemisia*-Chenopodiaceae-*Pinus* assemblage (Xu et al., 1986), including scattered *Cyperus rotundus* (?) and *Suaeda salsa* in the upper part of the intertidal zone. Such high evaporation directly causes poor development of vegetation in the salt marsh. For the recent decades, *Spartina alterniflora*, artificially imported from Jiangsu Province about 900 km southeast of the study area, has been thriving in the upper part of the intertidal zone. This newly intruded species modified the original characteristics of coastal vegetation.

3 Materials and methods

⑥DOE (Dagang Oil Exploration Bureau and State Information Center of Oceanography). 1991. Analytical Study on Marine Environmental Conditions of the West Bohai Bay (in Chinese), 1–11

⑦FDI (China Communications First Design Institute of Navigation Engineering and National Ocearnographical Information Center). 2006. Analytical Report on the Waves, Tides and Storm Surges for the East Port Area of Tianjin Port (in Chinese), 1–70

3.1 *Data sets of sea level analysis*

For the western Bohai Bay, the three major types of sea level indicators used in this study are sediments, cheniers and oyster reefs (Fig. 2). Two remarkable morphological features, the shelly cheniers of the Chenier Plain and the linear earthy mounds on the Oyster Plain, delineate the ancient shoreline positions and control the distributions of the sea level indicators (Wang et al., 2010; Shang et al., 2015; Shang et al., 2016) (Fig. 2).

Our previous work has determined 136 indicators from more than 530 radiocarbon-dated samples and their spatial positions (depth in cores and elevation/depth in outcrops) along the coast of Bohai Bay (Li et al., 2015). All the procedures for ensuring reasonable judgement of spatial and temporal information of relative sea level (rsl) indicators and further conversion to the corresponding RMSL have been conducted. Here, reference water level (RWL) and indicative range (IR) are based on van de Plassche (1986) and Shennan et al. (2015), with reference to the regionally generalized summary of Woodroffe and Horton (2005). Also, local residence-time corrections for both reworked shells and plant materials have been attempted (Shang et al., 2015; Shang et al., 2016; Li et al., 2015). Consequently, a RMSL band was obtained and compared preliminarily with the model-predicted regional relative sea level curves④⑤ (personal communication, Lambeck, 2014; Li et al., 2015).

In this study, we abandoned 34 "limited" indicators from the original 136 data (Li et al., 2015). These include (1) those sea level indicative meanings are relatively less clear. For example, the indicator Yujialing/TD356 was taken from a pit of bridge-pier. It could be estimated only in intertidal to subtidal depth because pier digging did damage to original reef sequence (Li et al., 2015) but now it is cautiously thought such a depth range estimated is too wide. (2) A vertical range between basal peat layer and overlying clearly marine-influenced sediment, identified by firaminifera, ostrocoda or diatom, is too large. For example, definite marine evidence was found 1 m or even near 2 m above the indicators ZH2/4/98Y083 or CH19/BA06817 (Li et al., 2015). Therefore, their capability indicating the contemporaneous sea level elevation is relatively weak. Afterwards, on the other hand, 8 newly revised data are added. Finally, 110 indicators are represented in this study.

Furthermore, a number of additional quantitative considerations for the local tidal regimes with estimation for the paleo tidal patterns, conversion from mean tidal level to MSL, standardization of different elevation systems and corrections for the local factors affected spatial characteristics including neotectonics, self-compaction and groundwater abstraction are given in this study.

3.2 *Determination of the validity of the sea level indicators*

Based upon the studies on the Holocene basal peat in core sequence and the modern coastal vegetation zonation in the southern Changjiang River Delta, together with the present tidal information from the five local gauge stations there, the Holocene basal peat was formed between the highest high water (HHW) and mean high water (MHW) (Wang et al., 2012b, 2013). Following this judgement, we chose an average 4.10 m of the observed highest high tidal ranges (in period of 1960−1979, Tanggu Station) and an average of 5.16 m for the predicted astronomical tidal ranges (four stations in the west of Bohai Bay) (Liu et al., 1986) and mistakenly used an average 4.63 m of both values as an estimated approximate maximum range of the local HHW and the lowest low water (LLW) (Li et al., 2015). Then, to compare with the 2.5 m mean tidal range (Liu et al., 1986), a vertical difference of 1.05 m (i.e., a half of difference between HHW−LLW and MHW−MLW ranges) was obtained for the IR for the local basal peaty samples and the midpoint RWL is 1.775 m above MSL. Finally, an indicative meaning of (1.8±0.5) m (rounded from (1.775±0.525) m) was used to be subtracted from the peaty sample's altitude to reconstruct RMSL (Li et al., 2015).

However, the following conditions should be considered in applying this method for the basal peat indicators. (1) The basal peat layers are a proxy of the vertical space between mean higher high water (MHHW) and MHW, or mean high water springs (MHWS) and MHW (van de Plassche, 1982; Shennan et al., 1983; Törnqvist et al., 1998; González and Törnqvist, 2009), but not between HHW and MHW. Even for Wang and her co-authors themselves, the IR, has been changed from HHW−MHW to MHWS−MHW now (Wang et al., 2018). (2) A potential mistake was not being aware of the difference between MTL and MSL and assuming they are equal (Li et al., 2015) even though the local MTL is actually approximately 15 cm lower than the MSL when higher tides are taken into consideration⑥⑦.

In this study, we changed to use vertical space between MHHW and MHW as IR for the basal peat layers. Consequently, the reconstructed RMSL is about 0.5−0.7 m higher than using 1.8 m and the IR is much narrower than in our previous paper (Li et al., 2015) (Table A3). Taking the same peat layer in the bayhead area as an example, a newly reconstructed RMSL will be 54 cm higher because RWL+IR, (1.26±0.05) m, is subtracted in this study in-

⑧SMG(TianjinAdministrationofSurveying,MappingandGeoinformation).1998.NoticeforStartUsingthe1972TianjinDagu Elevation System and Converting with the National Datum (in Chinese)

stead of subtracting (1.8±0.5) m. For the south periphery area, the difference is even larger, up to 0.7 m; i.e., compare the (1.1±0.03) m value in this study to the (1.8±0.5) m from Li et al. (2015) (Table A3).

For the other sediment indicators, either at approximately high waters, low waters or just in intertidal depth, their corresponding indicative meanings are given for bayhead and periphery, respectively (Table A3). In general, those formed at high waters, 1.3 m or 1.1 m should be subtracted; those formed at low waters, 1.15 m or 1.05 m should be added; those formed particularly at approximately mean lower low water (MLLW), 1.6 m or 1.45 m should be added, respectively, for bayhead or southeast periphery (Table A3). However, in our previous study, 1.5 m (a half of mean high tidal range) or 2.3 m (a half of the mistakenly recognized maximum tidal range of 4.63 m in Li et al. (2015)) were simply subtracted or added, respectively.

For the indicators, which are known formed in the intertidal depth but without tangible evidence to indicate their precise positions, we have indicated a vertical range of their intertidal depth. Therefore, its estimated RMSL is just their existing elevation with a large error of ±1 m. Such a treatment is the same as performed previously (Li et al., 2015).

In Li et al. (2015), the chenier samples collected from literature were commonly recognized to be from the intertidal zone only; therefore, no vertical compensation was needed. However, with further consideration on sedimentary facies now, the concrete sampling positions (either above the front-, the mid- or the rear-base) are determined when possible. As a result, for those formed above the mid- and rear-parts of the subsurface, certain compensations are given (Fig. 3; Tables A3 and A4). The oyster reefs' samples were taken exactly from the reef-top enable to indicate mean tidal level directly. Then, adding compensation of 15 cm, a converted RMSL can be estimated, then with an error ±0.7 m as practically observed undulation of the flat topography (Tables A3 and A4).

3.3 *Determination of the local tidal regime*

Tidal terms used in this study refer to those from van de Plassche (1986), Lin and Sun (1987) and Shennan (2015). The present tides in the west coast of Bohai Bay have an unequal semidiurnal pattern[⑥⑦] and thus, the "mixed tidal pattern" (Shennan, 2015) was used. The data of the present local tidal ranges, measured in four gauge stations from north to south along the west Bohai Bay, were collected and carefully collated (Figs 1 and A1; Tables A1 and A2).

Studies are rare about the local paleo tidal regime in the study area. Given an example of both the Humber and the Wash embayments, Shennan and Horton (2002) further corrected the MSL elevation of the sea level indicators, based on the modeled paleo tidal ranges of 6 ka and 3 cal ka BP, which are 2.5 m or 1.6 m, respectively, less than a half of the present high tidal ranges. However, Shennan and Horton (2002) also indicated that for those of open coasts, difference between the present and the paleo tidal ranges are relatively small. The paleo morphology of the west Bohai Bay, delineated as concentric-circles of the paleoshorelines determined by both the chenier and the earthymoundchains(Wangetal.,2010;Shangetal.,2015,2016) (Fig. A1), was quite similar with its present configuration. Therefore, the present tidal ranges (Tables A1 and A2) were used for the Holocene period.

The present shoreline of Bohai Bay had been completed continuously during the last 1.5 cal ka BP, following the formation of Chenier I (Wang et al., 2010; Shang et al., 2016). Therefore, the indicative meaning of samples, younger than 1.5 cal ka BP and distributed along the present shoreline, are derived based on the present tidal regime. However, prior to 1.5 ka, the paleo Bohai Bay extended further inland, and the paleo bayhead directed slightly northwestwards to the Oyster Plain with an extensive south periphery (Fig. A1). Sea level indicators older than 1.5 ka should comply with the paleo tides and paleo morphology, with estimated tidal ranges given in Table A3.

A small difference that should not be ignored between MTL and MSL is approached in this study, although we were not aware of this difference in our previous work or in all the early literature. According to the tidal gauge station in Tanggu (Tianjin New Port), in the present bayhead area, the MTL between MHHW and MLLW is 15−16 cm lower than the local MSL, while the MTL between MHW and MLW is only 2−2.5 cm lower than the local MSL[⑥⑦]. On the other hand, the local MSL in Tanggu Station is only 2 cm lower than the national MSL of National Vertical Datum 1985[⑥⑦]. We think therefore that interchangeability between the local and the nationwide MSLs is satisfied in this study. However, when using either MHHW or MLLW as being the RWL, a difference of about 15 cm between MTL and MSL must be taken into account (Tables A2 and A3). For example, at bayhead area, if a sea level indicator is determined as MHHW or MHW, (1.3±0.5) m should be subtracted for restoring MSL; however, if an indicator was formed at MLLW, (1.6±0.5) m should be added for its contemporaneous MSL (Table A3). Another example is that the actually observed elevation of reef-top for each oyster reef is indeed a proxy of MTL elevation, and thus, 15 cm should be added to MSL reconstruction (Tables A3 and A4.3: see the notes of the indicator No. 95). In a word, simply using a half of tidal range as MSL

⑨ShangZhiwen,SuShengwei,WangHong,etal.2013.ReportofNewDiscoveriesontheCheniersandOysterReefsinCoastofBohai Bay (in Chinese), 1–104

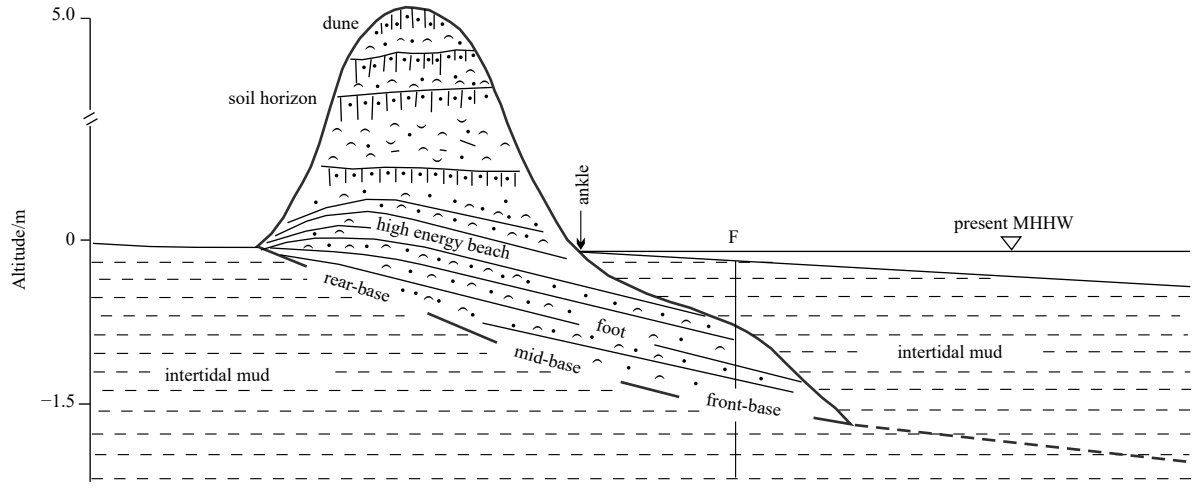

Fig. 3. Schematic illustration of a sedimentary model of the shelly cheniers in the Chenier Plain, west coast of Bohai Bay. Bar F, exposing the foot, was excavated in the wall of a shrimp pond and further Eijkelkamp penetrated, as shown in Figs 4a and b, while above the mid- or the rear-part can be seen in Figs 4c or f, respectively.

as we did before would provide about 15−30 cm deviation during MSL reconstruction in the coast of Bohai Bay.

3.4 *Unification of different elevation systems*

During the last two decades, we have used the National Vertical Datum 1985 to determine the elevation of our own samples. However, many previously published data, especially those before the 1990s, were based on different local datum systems or the old national system. In our former paper (Li et al., 2015), we have converted all the elevation values of the previously published data, relative to 1951 or 1972 local datum systems, into the National Vertical Datum 1985 by subtracting 1.543 m or 1.668 m from those original values, respectively; while for those values of the 1956 national system, 0.029 m should be subtracted to the National Vertical Datum 1985, based on an authoritative document issued by SMG⑧. In this paper, the same procedure is still performed for all the indicators used.

4 Results

4.1 *Sea level indicators from surficial/cored sediments*

We use the vertical space between MHHW and MHW as the growing space for basal peat. Thus, the newly revised indicative meaning is (1.255±0.045) m (i.e., (1.26±0.05) m) for both the present and ancient bayhead areas and (1.105±0.025) m (i.e., (1.1±0.03)) m for the ancient southeast periphery (Table A3). Those basal peat layers, formed in the present and ancient periphery sectors, will be treated as the samples in bayhead but based on their own tidal properties given in Table A2, although only small differences exist in between the bayhead and periphery subareas. The indicative meanings for these basal peat layers are (1.1±0.03) m for the south periphery and (1.15±0.03) m for the north periphery (Table A3). Each indicator was processed using the same procedure but its own tidal property and there is no need to go into more details in the following context. Detailed descriptions can be found in Appendix A.

The upper peaty layer, directly overlying on the Holocene marine and brackish sediments, was much less developed and preserved than the basal peat in the study area. However, a number of proxies, including organic-rich soil horizons and peaty mud and hydromorphic soil horizons in lagoonal-salt marsh environments, were probably discontinuously influenced by high tidal levels. Therefore, the upper peaty layers and proxies were treated in the same way as the basal peat layers were in this study.

The depositional mechanisms of the *in situ* thin organic-rich layers intercalated with marine-influenced, brackish muddy sediments are similar to those of the upper peat layers; their indicative meanings further support these interpretations. For example, indicator No. 53, a darkish organic-rich muddy layer less than 5 cm thick, intercalated with brackish muddy sediments, has a foraminifera assemblage consisting of 12 tests of *Nonion glabruum* and a single test of *Ammonia beccarii*, indicating a relatively weak influence from high water levels. Therefore, such intercalated thin organic-rich layers are treated in the same way as the peat layers are in their RMSL reconstruction (Table A4.1).

The other sedimentary indicators are composed of various marker layers. Lithostratigraphical logging, facies analysis and micro paleontological studies can determine indicative meanings. For indicators formed at MHHW, 1.3 m was subtracted, with an error ±0.5 m; for indicators

⑩ Wang Hong, Li Jianfen, Yan Yuzhong, et al. 2002. Formation and evolution of the oyster reefs on the Oyster Plain, Bohai Bay, Special Report for the Huaidianxiang Sheet (J50E005015, 1: 50, 000) (in Chinese), 1–57

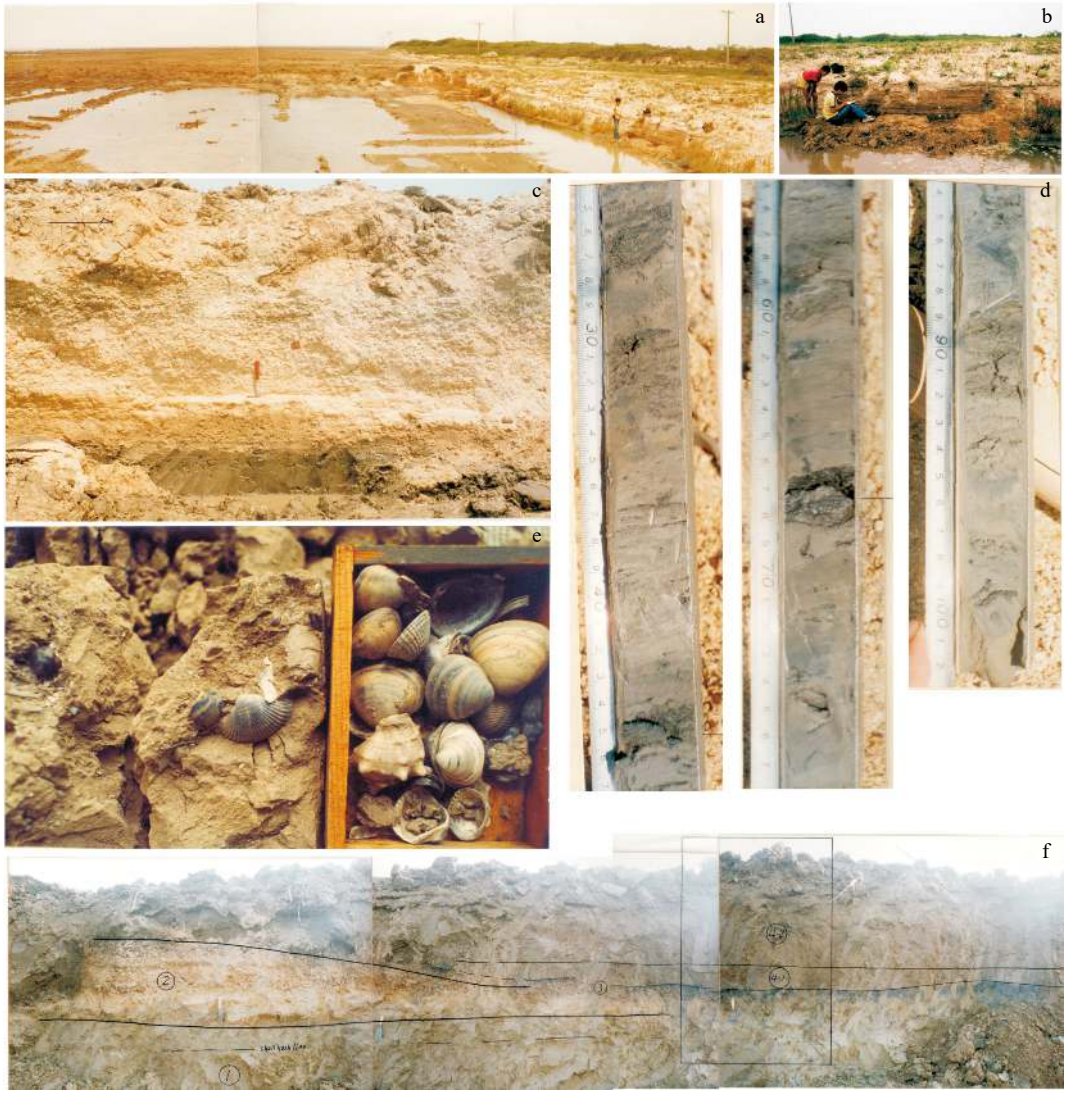

Fig. 4. Photos showing the shelly cheniers and underlying and overlying muddy sediments in the Chenier Plain, the west coast of Bohai Bay. a. Chenier I, Houtangpu site, its crest covered by Jujuba shrubs, was perched on the surrounding muddy coast and formed the present native shoreline since last about 1 cal ka BP (Wang et al., 2000b). An excavation wall of a shrimp pond (bar F in Fig. 3), dug in the upper part of the present muddy tidal flat, shows the sediments above the front-base of the shelly chenier. b. Details of the wall in Fig. 4a. Thin layers, alternatively consisting of shell fragments and muddy shell hash, were revealed in this wall section. The indicator No. 84 (Table A4.2) was taken from the lower part of the wall-section. Eijkelkamp augering revealed a meter thick, muddy shell hash sediments, which show the very bottom of the chenier above its front-base and the underlying tidal mud. c. Chenier II-2 and the underlying mud, Gongnongcun, Shanggulin site, subsurface of the mid-part of chenier was visible about 30 cm below hammer. d. The underlying mud, below the subsurface in Fig. 4c, was further Eijkelkamp augured to a depth of 102 cm (from left-top to right-bottom), showing intertidal environment. The indicator No. 79 (Table A4.2), articulated *in situ Sinonovacula constricta* shells, was taken from the top of this underlying mud. e. The top of the underlying mud beneath the front-base, Chenier II-2, Apple Garden, Shanggulin site, was mixed with reworked single valves of *Mactra veneriformis, Scapharca kagoshimensis* and gastropoda *Rapana*, see the shells washed clean in a wooden box at right side, i.e., the indicator No. 75 (Table A4.2). f. Chenier II-1, Papadi, Shanggulin site, the rear-part of chenier body, showing fade-out landward (to right side), was covered by a thin darkish upper peat layer (i.e., indicator No. 23, Table A4.1). The geographical distribution of the sites here can also be found in Shang et al. (2016).

formed at MHW, 1.21 m was subtracted (Table A2). Here, we simply used (1.3±0.5) m for both MHHW and MHW for the bayhead samples (Table A3). For those samples formed at approximately MLLW, (1.6±0.5) m was added, while for those formed at approximately MLW, (1.15±0.5) m was added for bayhead samples (Tables A2 and A3).

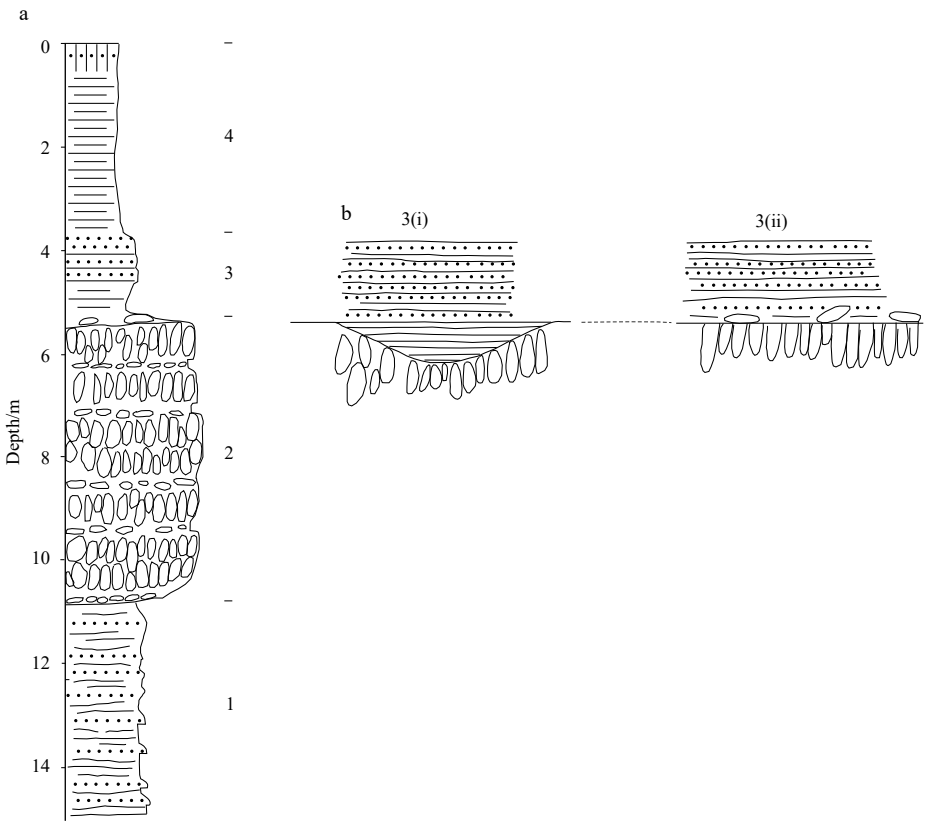

Fig. 5. Schematic illustration of a sedimentary model for Holocene *Crassostrea gigas* reefs in the Oyster Plain, northwest coast of Bohai Bay. a. Reef body and its underlying and overlying muddy sediments. The reefs, about 2−6 m thick, were mainly composed of *C. gigas* shells, with a binary structure of the normal vertical building-ups of almost exclusively vertical posed and articulated individuals, and the horizontally intercalated muddy layers mixed with distorted individuals laying up horizontally. Such cyclicity, mostly repeated 6−7 times in the Oyster Group III only, about 5.8−4 cal ka BP, is a remarkable characteristic, although whether this characteristic was a response to sea level fluctuations still remains an open question (Wang et al., 2006). In this study, we picked the shell samples from the reef-top only as indicating MTL (mean tidal level). b. Two extreme and opposite patterns of the transition from reef top to the overlying upper intertidal muddy sediments: Bed 3(i) tranquil accumulation occurred first in the small depressions on the top surface and the shell-margin (ventral margin) of the individuals at the very top was still intact; Bed 3(ii) erosion and then deposition, the shell-margin on the very top was sharply truncated and a few individuals were removed by strong tides and then paved horizontally.

The indicative meanings of samples formed in an intertidal zone are the altitudes of the samples, with an error ±1 m. For example, sample No. 7, a thin layer of lagoon-salt marsh sediments in the ancient bayhead area was formed by a flooding event, revealed by its foraminifera assemblage (Li et al., 2004) (Table A4.1). Therefore, 1.3 m, the vertical difference between MHHW−MTL (Table A2) was subtracted to reconstruct the RMSL (note that the relationship between the local MTL and MSL is described in Section 3.3).

4.2 *Sea level indicators associated with cheniers*

In earlier studies, the subsurface (i.e., the base, the bottom) of a chenier was thought to be spread along or above the MHHW shoreline, on which reworked shells and shell hash, mixed with fine sand and mud, accumulated (Russell and Howe, 1935; Price, 1955; Wang, 1964; Otvos and Price, 1979; Reineck and Singh, 1980; Zhao and Zhang, 1981; Zhao et al., 1980; Gu et al., 1983; Li and Li, 1987; Zhao, 1989; Wang and Ke, 1989; Liu and Walker, 1989; Xu, 1994).

However, several other researchers argued that the subsurface of chenier formed in intertidal zone, especially during its initial stage (Woodroffe et al., 1983; Weill et al., 2012) and dipped seaward (Neal et al., 2002; Rodríguez-Ramírez and Yáñez-Camacho, 2008; Weill et al., 2012). The vertical difference between its seaward front and landward rear of the subsurface is 1−2 m (Rodríguez-Ramírez

⑪WangHong,WangYunsheng,YanYuzhong,etal.2002.ReportofBaishuitou-QikouzhenSheets(J50E008015,J50E009015,1:50 000) (in Chinese), 1–128

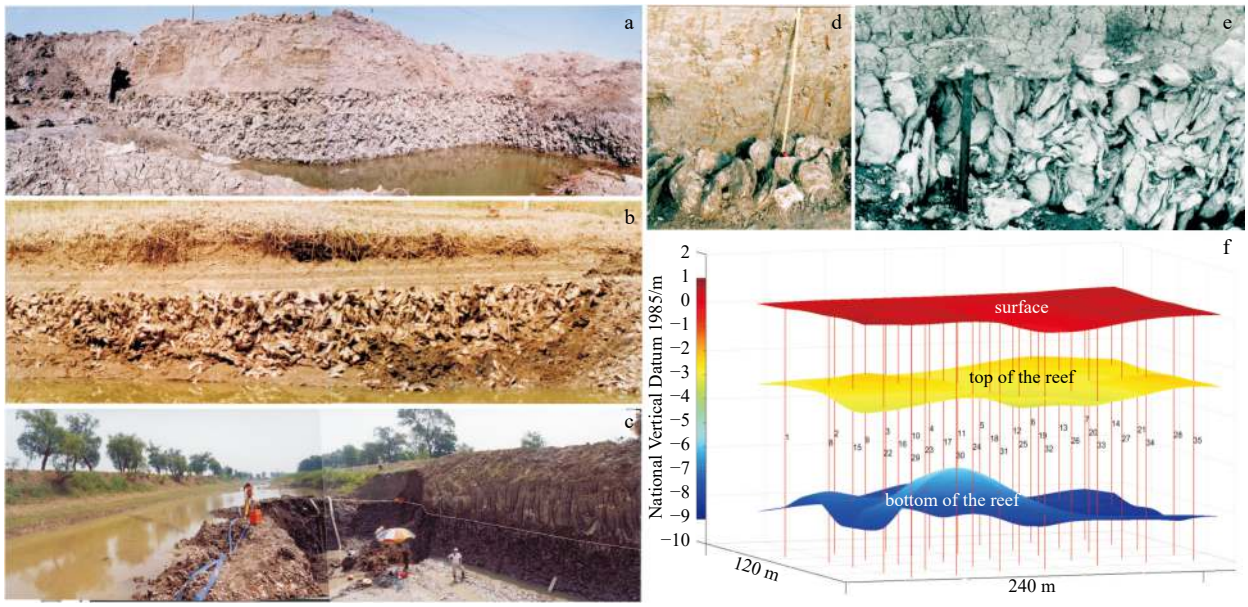

Fig. 6. Buried Holocene *Crassostrea gigas* reefs, Oyster Plain, the northwest coast of Bohai Bay. a. Section 1, Dawuzhuang site, one of the largest reefs in Oyster Plain, was intermittently excavated from the 1990s to 2010s. By the end of digging work in the mid-2010s, the totally excavated area was about 150 m×100 m. Following such excavations, 11 sections were set up to study the reef itself and the overlying and underlying muds by our group (Fan, 2008, 2010; Liu, 2010; Wang et al., 2011c). Leveling shows the reef-top at 7 sections undulated in between −3.22 m and −1.94 m (undulation range 1.28 m), with an average elevation −2.48 m of National Vertical Datum 1985 (unpublished data). The indicator No. 97 was taken from the top part in this reef (Table A4.3). b. Biaokou site (Wang et al., 1995, 2006). The most concomitant species, *Trapezium liratum,* indicator No.101, was taken from 5 cm below the top surface in this reef (Table A4.3). c. Zengkouhe site. Dr. D. Surge, North Carolina University, stood on the bottom of excavating pit and Dr. Shang, one of the authors, stood with total station on a temporarily piled-dyke during the 2006 summer field work. Note a thin white line illustrating the boundary between the reef and the overlying muddy sediments, while the subsurface of reef was still a few decimeters below the pit bottom[12][13]. The indicator No. 100 was taken from this reef (Table A4.3). d. The first type of transition (see 3(i) in Fig. 5b) from reef to the overlying intertidal mud revealed by Section 2, Dawuzhuang site, after carefully cleaning, no truncation was found from the ventral margin of the very top shells (except the one in the front of box ruler was artificially cut by cleaning). The lower part of overlying mud without laminar bedding structure is due to the stagnant qranquil microenvironment (i.e., the small depression), and gradually changed upwards to irregularly interbedded clayey and silty-fine sandy laminae, which are typically intertidal bedding structures. e. The second type of transition (see 3(ii) in Fig. 5b), Beihuaidian site. The shell margin was obviously truncated and even a few individuals were removed and paved on the boundary by strong floodings. f. A result for the Oyster-Museum-choosing-site investigation conducted in an area between Biaokou and Zengkohe sites. A three-dimensional diagram, based on 35 cores (the red vertical lines) in the area of 120 m×240 m, shows the reef-top (yellow) and reef-bottom (blue) depths, respectively. Ground surface, leveled against National Vertical Datum 1985, is shown by red color. The elevation of the reef-top observed undulates between −3.52 m and −2.26 m (Qin et al., 2017).

and Yáñez-Camacho, 2008; Weill et al., 2012) or 2−3 m (Hijma et al., 2017). On the coast of Bohai Bay, several previous studies indicated that the seaward front of the subsurface declines into the intertidal zone and is buried by late intertidal muddy sediments. The seaward front of the subsurface was >2 m lower than its landward rear, with slope ratio of 13 ‰−19 ‰ (Xia, 1981; Xie, 1986; Cai, 1981; IOG, 1985).

Figure 3 shows a comprehensive model of the local shelly cheniers based on our own investigations (Wang, 1994; Wang and van Strydonck, 1997; Wang et al., 2000a, b, c; Su et al., 2011), which have provided more sedimentary evidence for the indicative meaning of the local cheniers.

Leveling investigations of the subsurface, using an Eijkelkamp gouge corer (25 mm or 50 mm in diameter) and a total survey station, revealed that the chenier subsurface

[12] Shang Zhiwen, Fan Changfu, Wang Hong, et al. 2007. Comprehensive Report to Tianjin Paleo Coast and Wetland State Natural Conservation Area: Second-Phase Geological Investigations for Oyster Reefs (in Chinese), 1–55

[13] Shang Zhiwen, Li Jianfen, Wang Hong, et al. 2016. Report of the China Coastal Depositional Recoreds on Climate Changes (in Chinese), 1–100

dips seaward with slope ratio of 5 ‰–20 ‰ (maximum 22‰–27‰), based on 22 Eijkelkamp-core sections conducted perpendicular to five chenier chains (Cheniers IV-1, III, II-1, II-2 and I) at an average surveying distance of 105 m and a mean vertical difference between the seaward and landward ends of about 1 m⑨ (Su, 2012a; Su et al., 2011; Wang et al., 2000a, b, c; Wang et al., 2020a).

As described in the first section of this paper, correctly using shelly cheniers as sea level indicators requires knowledge of the sampling position. The subsurface of the chenier body tilts seawards and can be separated into three parts: the front-, mid- and rear-base. Only samples taken closely above the subsurface can be used because the subsurface and the sediments immediately above it have a connection to tidal levels. Therefore, most of our chenier samples were collected immediately above the subsurface and a few were collected from the very top of the underlying muddy sediments. Sediment above the front-part, i.e., the foot of the chenier, is wedged into intertidal muds and is ideal for sampling because this part was undoubtedly deposited in the intertidal zone and can be used as index point directly indicating intertidal depth. However, the sediments above the mid- and the rear-part of the subsurface need microfossil information for interpretation; e.g., the mid-part of Chenier III in Jugezhuang site (Li et al., 2016b; the indicator No. 71 for example in this study). Radiocarbon-dated shells, taken from the mid- to upper parts of chenier body, accumulated from strong waves during storm surges and generally are difficult to precisely and convincingly use to reconstruct contemporaneous sea levels. The previously dated samples collected from the mid- and upper parts of cheniers were distinguished (Wang and van Strydonck, 1997) and abandoned (Li et al., 2015) (Fig. 3).

Along the coast of Bohai Bay, many pits, dug two decades ago by the local fishermen for shrimp culture in the present muddy upper tidal flat, expose the buried foot of Chenier I in the bayhead and its south periphery (Figs 4a and b). This deposit contains shelly fragments (commonly a few millimeter to 1 cm) mixed with silt and clay and is poorly sorted, showing roughly wavy bedding of alternation between shell hash-dominated and mud-dominated layers (a few centimeter thick each), with peculiar penecontemporaneous gravity-deformation (irregular convolute-bedding). The color is dark and indicates a reducing environment (even shells and foraminifera tests were dip-dyed to a dark color).

Moreover, numerous reworked shell hash and broken shells, several of which are still distinguishable as *Mactra veneriformis, Scapharca* sp., *Rapana, Solen* sp., and *Glos-*

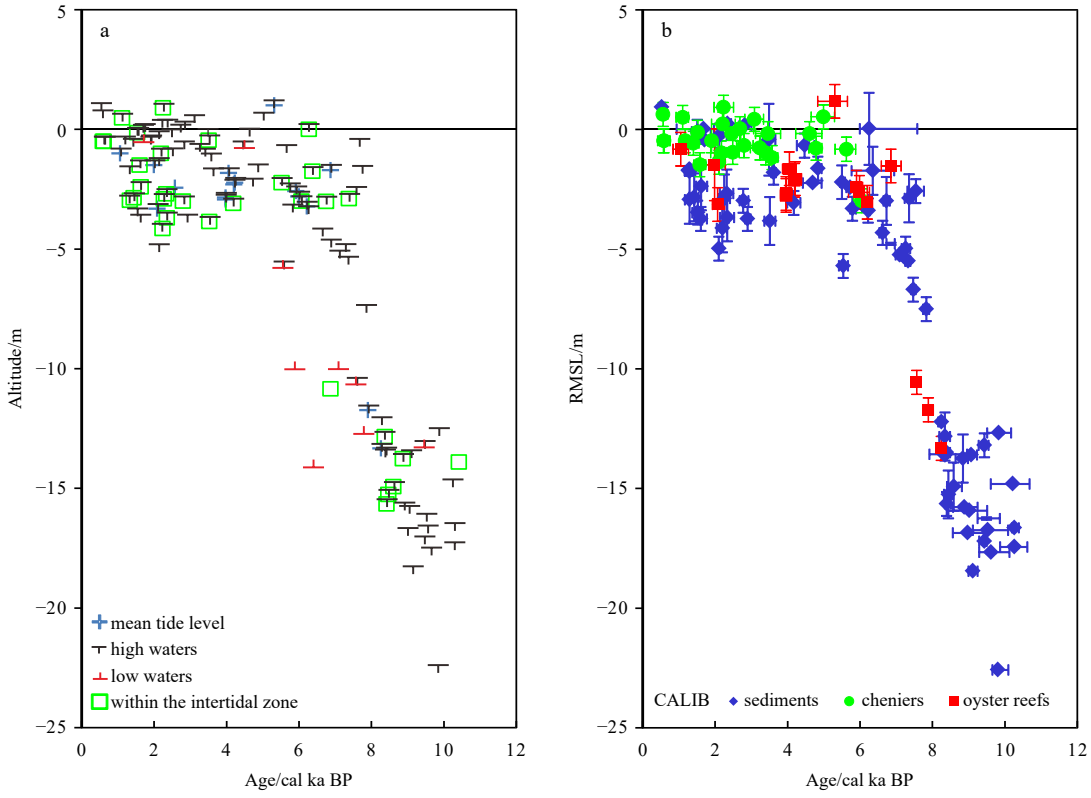

Fig. 7. The primary evidence of the sea level change on the west coast of Bohai Bay. a. Distribution of the observed relative sea level (rsl) indicators, with the various symbols indicating different water levels as high (⊤), low (⊥), intertidal (□) and the mean tidal (+). b. Distribution of the relative mean sea level (RMSL) indicators, derived quantitatively from their originally observed rsl with the specific indicative meanings, shown as the three major types of sediments, cheniers and oyster reefs.

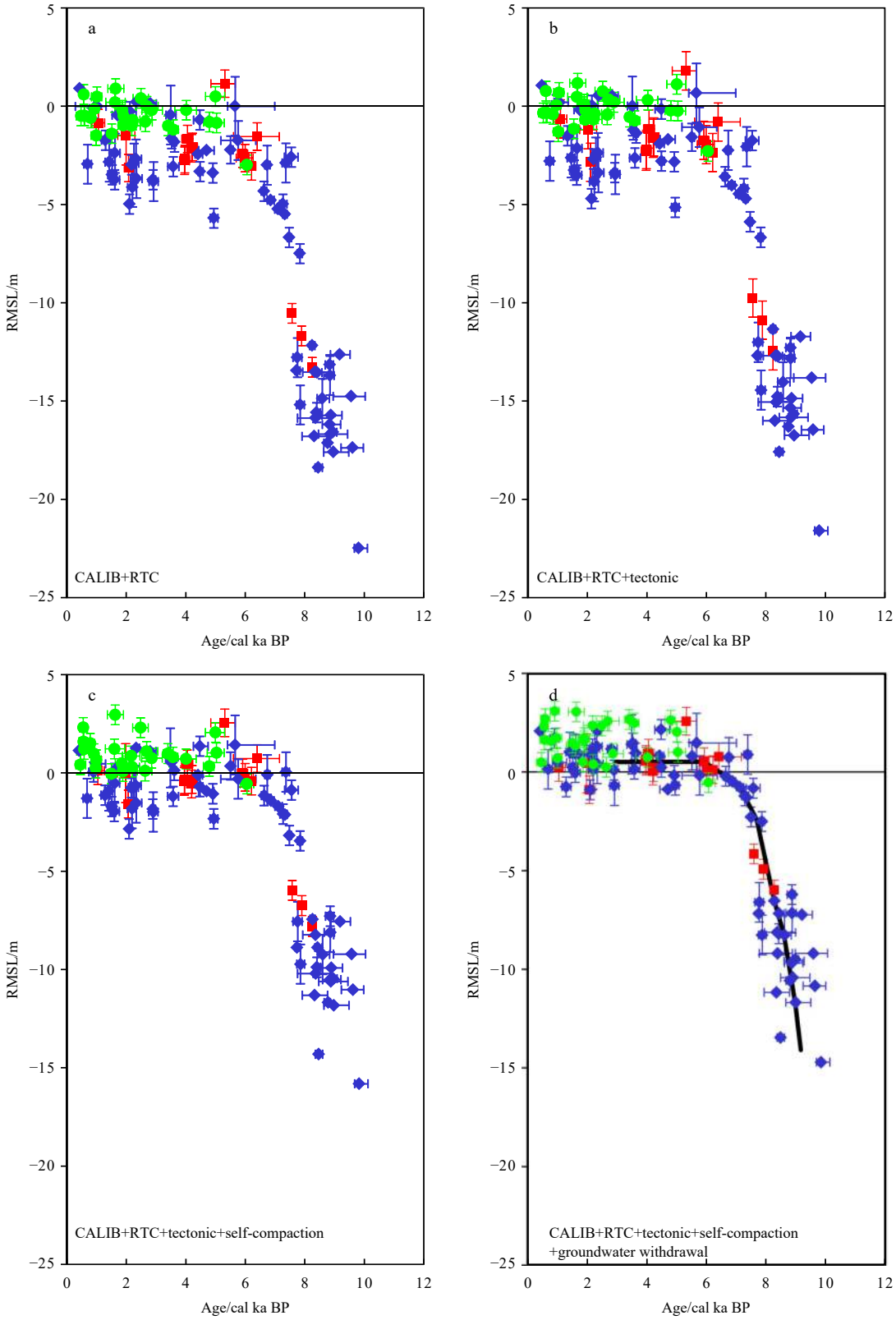

Fig. 8. A series of temporospatial calibrations for the observed RMSL indicators on the west coast of Bohai Bay, China. a. Correction for the local residence time effects (RTC) for the 48 indicators, and the younger-age-selection at the subsample level for another 35 indicators are added to Fig. 7b. To date, two steps for time calibrations, CALIB+RTC corrections, have been completed in this study. b. A correction for the neotectonic subsidence, by compensating 0.1 mm/a, is added to Fig. 8a. c. A correction for the self-compaction of unconsolidated sediments is added to Fig. 8b. d. Further correction for the subsidence due to groundwater withdrawal is added to Fig. 8c. To date, all the local factors influencing the temporospatial distribution of the RMSL indicators have been corrected. Then, a solid black line describes approximately a local RMSL curve in the study area.

saulax sp., and other marine mulloscs, were mixed with the underlying muddy sediments beneath the front-base. Thus, the top of the underlying muddy sediments below the front-base indicated the intertidal depth. Both samples, taken from the chenier foot and the top of its underlying mud, indicated the intertidal depth and their indicative meaning is the sample altitude ±1 m (Table A3).

In contrast to the underlying mud immediately below the front-base, muddy sediments beneath the mid-part, especially beneath the rear-part, were less influenced by sea water. These muddy samples and the shell samples taken from above the mid- and rear-part are thus preferable for study of microfossil assemblages. Here, we present a case study. Continuous Eijkelkamp core sampling from the underlying mud upward to the lower part of shelly chenier was conducted across the mid-part of the subsurface (Fig. 3) in Section J341-13, Jugezhuang site, Chenier III (Li et al., 2016b; Su et al., 2011). Foraminifera from the top of the underlying mud resulted in 79−692 tests per10 g dry sample, composed of *Ammonia beccarii* vars.−*Elphidium nakanokawaense*−*Nonion glabrium* assemblage with *A. granuloumbilica* and *A. takanabensis*, which is quite similar to the present tidal flat assemblage of L3 between MHW and MHWN (Li et al., 2016a). For the samples immediately above the subsurface in this core, 2 016−6 979 tests per 10 g dry samples, mainly consisting of *A. beccarii* vars.−*A. confertitesta* assemblage with small amount of *E. simples, A. granuloumbilica, A. anntetens, Pseudononionella variabilis, P. tuberculatum* and so on, were found and are similar to the present tidal flat assemblages L2 and L1, found at approximately MHW−MHHW (Li et al., 2016a). Therefore, the samples taken immediately above the mid-part of subsurface can be roughly recognized as representative of approximately MHW. Correspondingly, the indicative meaning is calculated by subtracting (1.2±0.5) m (rounded from 1.21 m) from bayhead sites and subtracting (1.1±0.5) m (rounded from 1.08 m, Tables A2 and A3) from south periphery sites. For the samples taken immediately above the rear-base, (1.3±0.5) m or (1.1±0.5) m should be subtracted for the bayhead and south periphery sites, respectively (Tables A2 and A3).

4.3 *Sea level indicators with oyster reefs*

Crassostrea gigas has been found from the East Siberian coast, Hawaii, Japan, through the Chinese coast, to Vietnam and Thailand, and lives in shallow waters to the intertidal zone (Johnson and Foster, 1951; Kira, 1975; Scarlato, 1981; Chonglakmani et al., 1983; Wang, 1994; Okutami, 2000; Wang et al., 2006). Relative to the genus *Ostrea*, which prefers deeper water, the species of *Crassostrea* can grow from subtidal to intertidal depths in shallow bays, estuaries, tidal-influenced mouth-channels and lagoons (Stenzel, 1971; Hopkins, 1979). *Crassostrea* requires higher summer water temperatures to successfully propagate (spawning, fertilization and larval growth) since they are all nonincubatoric. However, they can tolerate extreme low temperatures in the winter season. Therefore, accumulating in intertidal zone or very shallow water is normal for the species of genus *Crassostrea* (Stenzel, 1971). *C. virginica*, crowded with dense clusters of living and dead specimens in the intertidal zone, can be seen along the coast from the southern Atlantic states to the Gulf, USA. An extreme example is in estuary near Wadmalaw Island, South Carolina, where the living reefs of *C. virginica* are exposed twice daily during normal low tides (Stenzel, 1971; Hopkins, 1979; Davis and Fitzgerald, 2004). We found that the top of living *C. gigas* reefs can reach an elevation of MTL in the intertidal zone of Dashentang, Tianjin (Wang et al., 2011c). Similarly, in the intertidal area of the Xiaomiaohong site, Yellow Sea, Jiangsu Province, about 900 km south of the study area, the modern *C. gigas* reefs grow to MTL (Zhang, 2004).

Figure 5 shows a comprehensive model of the local oyster reef build-up based on our investigations[10] (Wang, 1994; Wang et al., 2006, 2011b, c, 2012a; Fan, 2008, 2010; Liu, 2010; Li et al., 2020), which have provided more sedimentary and ecological evidence of its indicative meaning.

Bed 1. Thin layered and/or laminated alternation between muddy (clayey and silty) and fine sandy−silty sediments, brownish gray to black brown (10YR 6/1−3/1), mixed with scattered marine shells such as articulated *Scapharca kagoshimensis, Mactra veneriformis, Dosinia* sp., *Cyclina sinensis, Potamocorbula laevis* and their broken valves, and gastropoda shells Terebridae and *Nassarius* sp., etc. It was undoubtedly a marine environment.

Bed 2. Oyster reef, densely populated, vertical growing *in situ* articulated oysters, *Crassostrea gigas* shells, with horizontally intercalated layers of disturbed individuals (mainly still articulated but a few disarticulated due to reworking), indicates alternation between tranquil and relatively unstable environments during the reef building. *Trapezium liratum* shells, articulated, were the most common concomitant species; also less common are *Rapana, Scapharca kagoshimensis, Ruditapes philippinarum*, *Cerithidea* sp., *Assiminea* sp., *Stenothyra* sp. and occasionally crab chelae and even teeth of *Actobates* sp. Clayey mud filled in between the crowded individuals, representing about 10%−20% of the normal growth layers, but

[14] YangJilong,XiaoGuoqiang,WangQiang,etal.2015.StratigraphicalComparisionofDeepDrillingbetweenSubsidingCoastsandLacustrine Basins (in Chinese), 1–126

[15] IGM (Institute of Geoenvironment Monitoring). 2016. Report on Ground Subsidence of Key Areas in North China Plain, CGS internal Report (in Chinese), 1–240

[16] GSC (Tianjin Office of Ground Subsidence Control). 2015. The 2014 Annals of Tianjin Land Subsidence (in Chinese), 1–20

>50% of the disturbed horizontal layers.

Bed 3. Clayey and silty mud, brownish gray (10YR 6/1−4/1), with scattered broken shells and articulated larvae of *Potamocorbula laevis. Corbicula fluminea,* and Terebridae and *Cerithidea* sp. also existed. A few *Solen* sp. shells are articulated and in a vertical *in situ* position. Usually, this mud deposit coarsens upward, especially when found in small depressions on the reef-top, implying less sedimentation in such depressions to normal accretion on an open tidal flat. In the small depressions, about 30−50 cm thick, nonlaminated, organic-rich clayey mud, brownish gray to dark brown (10YR 5/1−3/4), accumulated in a stagnant reducing microenvironment (Fig. 6d). The ventral margin of the shells on the upper most top of reef body is still sharp and without truncated and eroded traces. This implies a quiet transition from reef to overlying mud (Fig. 6d). Coarsing upward is present and a gradual change to alternate laminae of clay and silt-very fine sand or silty-sandy lenses, commonly <1 cm thick and less than 5−10 cm long, irregularly appear in the muddy matrix. These alternations and/or irregular silty-sandy lenses are typically of tidal bedding structure (Reineck and Singh, 1980; Davis and Fitzgerald, 2004). Nevertheless, the reef-top was sharply eroded and the ventral margin of the upper most shells was clearly truncated and some shell individuals were even removed from/horizontally paved on the reef top (Fig. 6e). These two circumstances, the change from reef to the overlying mud either conformably or erosionally, occurred at approximately MTL. However, most of the reef top was only slightly eroded and the samples taken from the very top of reefs are still able to indicate MTL.

A total thickness of Bed 3, i.e., between the reef-top and the upper boundary of the tidal bedding structure[11] (the last irregular silty/sandy lamina, LISL; Wang et al., 2006), was observed to be 1.2−2 m in Biaokou, 1.1−2.2 m in Beihuaidian, about 1 m in Lingtou, 1.4−2.4 m in Dawuzhuang, about 2.1 m in Binhaihu and 1−1.3 m in Konggang sites. Generally, the average thickness is 1.6 m (Wang et al., 2011c). The local mean high tidal range is about 3−2.8 m from the bayhead to the two periphery sides (Tables A1 and A2) and the reef top may build to MTL; therefore, a range of 1.6 m is an accommodation space that the high tides may provide to a vertically depositional capacity from the mean tidal level (i.e., the reef top) upward to approximately MHHW. This is counterevidence showing that the top surface of reefs was essentially controlled by MTL. Thus, the top surface of *C. gigas* reefs can be directly used as a MSL indicator after conversion from mean tidal level to MSL (see Section 3.3), with an undulation error ±0.7 m (see below).

Bed 4. Muddy sediments, dull yellow orange to dull yellowish brown (10YR 6/3−5/4), garlic structure, freshwater *Gyraulus* sp., *Bithynia* sp., *Metodontia* sp. and brackish articulated *Solen* sp., *Glauconome primeana* were scattered *in situ* in the muddy sediments. This represents a lagoonal-salt marshy environment with a few sea water flooding events (e.g., indicator nos 7 and 8, Table A4.1), and sometimes, a short gap existed in between this layer and the underlying intertidal mud deposition (Li et al., 2004).

The top of local *C. gigas* reefs is often slightly undulated. Leveling investigations for 19 spots at three buried reef sites, including Dawuzhuang (Fig. 6a), revealed that the top undulations for each site are 1.28 m, 1.4 m and 0.46 m, respectively (Fan et al., 2005; Liu, 2010; Wang et al., 2011c; Wang, 2012). Based on the maximum undulation of 1.4 m, we therefore use ±0.7 m as a vertical error when using the top-elevation of the reefs as MSL indicator.InXiaomiaohongsite,thetop-undulationissimilarlyas0.5−

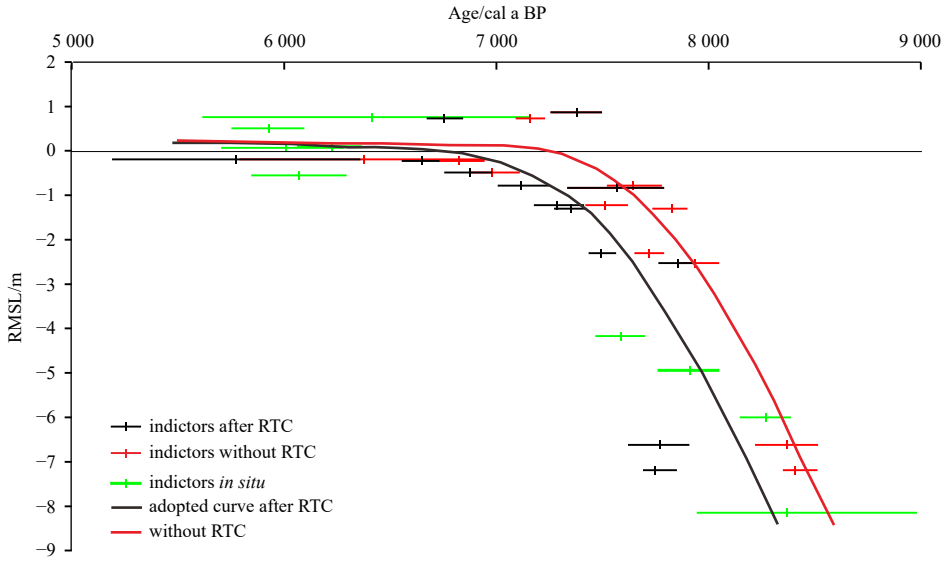

Fig. 9. Comparison of two inferred RMSL patterns shows that after RTC. A black curve is about 0.5 ka cal a younger than a red one without RTC in the time period of about 7.3−6.8 ka.

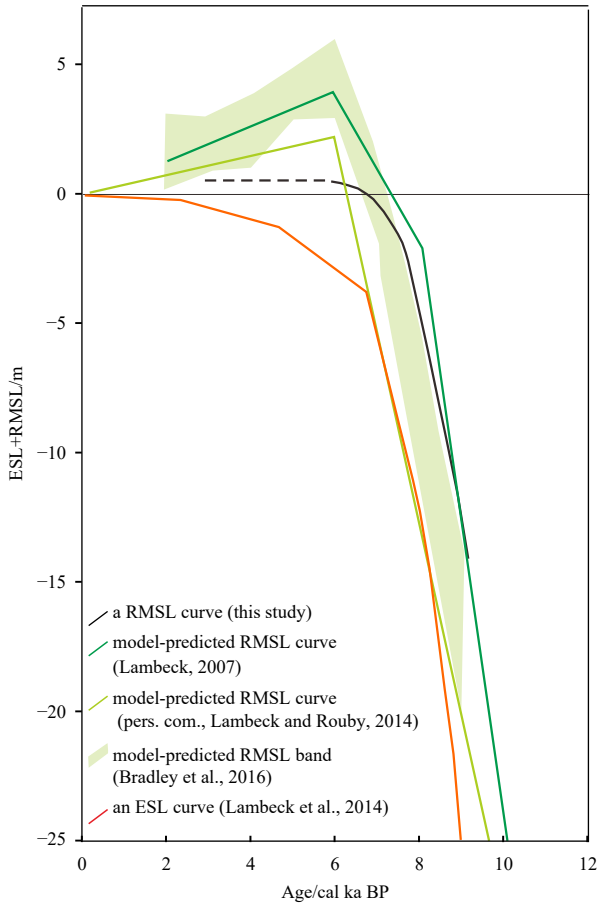

Fig. 10. A diagram illustrates our RMSL curve (black solid line) in this study, the ESL curve of Lambeck et al. (red solid line), the model-predicted RMSL curves of Lambeck④ and Lambeck et al. (personal communication, 2014) (two green lines), and a RMSL band (light green shadow), redrawing from Fig. 4a-BB (Bohai Bay) of Bradley et al. (2016).

1.0 m (Zhang, 2004). Recently, a choosing-the-site investigation for envisaged Oyster Reef Museum was carried out in Ninghe County, Tianjin (about 3 km east of Chaobaixinhe River, about 30 km down from the top-frame of Fig. 2). In total, 35 rotary drilling boreholes were implemented penetrating the reef body over an area of 240 m×120 m within an extensive reef. Observed elevations of the top surface revealed in all 35 cores was between −3.522 m and −2.260 m (National Vertical Datum 1985) and thus the maximum undulation is 1.26 m (Qin et al., 2017) (Fig. 6f). This result indicates that this newly investigated result is consistent with general estimate of 1.4 m obtained by the previous studies.

4.4 *Distribution of RMSL indicators*

All the ^{14}C ages of the 110 indicators are calibrated by CALIB Series 7 (Reimer et al., 2013) with ΔR=−178±50 a for the marine shell samples in Bohai Sea (Southon et al., 2002). For those nonconventional dates, which were obtained from the literature in the 1980s−1990s, lacking of δ^{13}C values, CALIB 3 (Stuiver and Reimer, 1993a, b) is first used with either the local empirical mean value of −2.68‰ PDB for marine shells (Wang, 1994; Wang and van Strydonck, 1997; Li et al., 2015) or recommended δ^{13}C values given by Mook and van de Plassche (1986) for other samples to fulfill the isotope fractionation correction and obtain their approximate conventional ages, and then, IntCal13 or Marine13 of CALIB Programmes 7 were used for further systematic calibration (Reimer et al., 2013; http://calib.qub.ac.uk/calib) (Table A4). The 2σ range of calibrated age and the median probability are listed simultaneously (Table A4). For graphical purposes (Törnqvist et al., 2015; Hijma et al., 2015), the median values are illustrated in this paper (Figs 7 and 8).

The spatial positions are depicted qualitatively by using a few different symbols. For instance, indicators of the peat layers, showing high waters between MHHW−MHW, are illustrated as "┬" in time-depth graph (Fig. 7a). Indicators that were formed around low waters, i.e., the lower part of the intertidal zone or the upper part of the contiguous subtidal environment, are illustrated as "┴". Those indicators, which are known to be formed in intertidal depth only, are drawn as "□". Some indicators may directly define the mean tidal level and must be converted to MSL (see Section 3.3), the top of oyster reefs demonstrates this case, being portrayed as "+" (Fig. 7a). For those marked layers, including archaeological proof (e.g., indicator No. 34, a layer in which a copper coin was found in Chuangganglu site), relevant symbols will be chosen from one of the above based on their facies descriptions. As the primary result that we actually observed, Fig. 7a serves as a foundation for the following explorations. First, based on the RWL and IR characteristics (Table A3) of each indicator, a temporospatial RMSL trend is derived (Fig. 7b, Table A4).

4.5 *Corrections for residence time effects*

Local residence time corrections (RTC) have been added to CALIB for reworked shells and several organic-rich bulk samples from our previous studies to decrease the age contamination (Shang et al., 2015, 2016; Li et al., 2015). In reworked marine shells, the average maximum residence time ranges from 1 100 cal a to 1 300 cal a, with the semi-empirical values of 600 cal a or 100 cal a for the original ^{14}C dates older or younger than 1 cal ka BP, respectively, based on the age comparison between 47 subsamples from 17 single layers in the study area (Shang et al., 2016). Similarly, for the terrestrial organic-rich bulk samples, an average maximum range of the residence time is 1 320 cal a, with the semi-empirical values of 660 cal a or 100 cal a for the original ^{14}C dates older or younger than 2 cal ka BP, respectively, based on the age comparison of 40 subsamples from 20 bulk ones (each bulk sam-

ple has two subsamples: >180 μm and <180 μm) (Li et al., 2015). In total, 48 marine and terrestrial samples were RTC treated directly (Table A4: Column 10).

As to those subsamples themselves, the younger/youngest ages were directly chosen, and 35 indicators were the case (Table A4: ticked "yes" in the Column 9). In reality, selecting the younger/youngest at the subsample level is a kind of RTC, as well. In total, of 110 indicators, 83 have been RTC corrected. Thus, a small shift in the temporal distribution towards a younger direction is revealed in Fig. 8a.

4.6 *Correction for neotectonic subsidence*

For a long time, some local researchers simply believed that the neotectonic subsiding rate should be equal to the sedimentation rate. As a result, a neotectonic subsiding rate of 1−2 mm/a was estimated according to the thickness of the local Pleistocene and Holocene sediments (Wang et al., 2003). Although this is not appropriate, quantitative estimation of the neotectonic subsidence has long been one of the thorniest problems for the local geologists.

Xu et al. (2005) found that during the Quaternary period, a total of five alluvial terraces were formed in the western and northern mountains surrounding the study area (Fig. 1), and the highest one had been raised to about 250 m above the present river surface. To a first order, this outcome might imply that an average neotectonic uplifting rate is about 0.1 mm/a in the mountain areas. Correspondingly, the local neotectonic subsidence in the contiguous plain, including our study area, might be at most about 0.1 mm/a.

During recent years, seismological and lithostratigaphical studies, spurred by petroleum exploration, offered a new perspective for better understanding the regional neotectonics. Following the studies of the postrift tectonic reactivation during the Neogene−Quaternary in the Bohai Bay Basin, by using the back-stripping method for 120 deep cores (Huang et al., 2014), Liu et al. (2016) indicated that the Bohai Bay Basin as a whole began to subside during this postrift phase until present day. As a depressional center of the whole basin, the Bozhong Depression, which is the east of the study area (Fig. 1), had an average subsiding rate of about 0.08 mm/a for the past 5 Ma (Pliocene and Pleistocene), while the Huanghua Depression was only about 0.035 mm/a (Huang et al., 2014; Liu et al., 2016). As to those secondary uplifting regions such as the Cangxian Uplift and Chengning Uplift, their subsiding rates were even lower than those of the Huanghua Depression (Fig. 1).

These estimations of neotectonic subsiding rates—being less than one-tenth of 1 mm/a—are definitely an order lower than what was previously acknowledged by some local researchers. Nevertheless, a correction for the neotectonics is an indispensable part of a sea level study in a relatively small area, and we therefore use 0.1 mm/a as a general subsiding rate to give an elevation correction of all the sea level indicators in this study (Fig. 8b, Table A4: the first line of Column 13).

4.7 *Correction for the self-compaction of sediments*

The actually measured data of the vertical distribution of the porosity in the study area consist of four varying values (Table A5)[③]. A decay in the local porosity shows that consolidation settlement nearly finished at approximately 400 m in depth, which coincides approximately with the average thickness of Quaternary sediments in the area[⑭]. It means that a decompacting correction is needed for the upper 400 m at least. On the other hand, based on these data[③] and average depths of several key layers (Table A5), approximate porosity values are estimated for the surface sediment, the Holocene basal peat, the hard soil horizon formed during the Last Glacial Maximum (LGM), and the base of Quaternary sediments as well (Table A6).

This approach is different from Pico et al. (2016), who used 1.68 km, a general estimate of total sediment thickness for the Bohai Sea and Yellow Sea region, as well as 63% of the surface porosity of clay sediment (Φ_0) and an exponential attenuation length of 3.7 km (i.e., 1/0.27 km) for the clay sediment column (z_0), both based on Guillocheau et al. (2012). Pico et al. (2016) then obtained a decompaction value of 8.04 m for an exemplified Core SYS-0701 at a depth of about 19.3 m (−52 m below sea surface and about 115 km out of the nearest present continental shoreline in the Yellow Sea (Liu et al., 2010)). Our result shows that a correction value is 5.62 m for the same depth of 19.3 m (Appendix B), which is less than the value of 8.04 m from Pico et al. (2016). Geographically, our study area is quite different with Core SYS-0701; therefore, the estimated value of 5.62 m for our study area seems to be reasonable.

Finally, all sea level indicators in this study are corrected for self-compaction by adding an appropriate value (Fig. 8c, Table A4: the second line of Column 13). A thickness of the modern artificially backfilling material is certainly not considered for this calculation. However, for those indicators taken from the cores drilled in the shallow sea, the thickness of the overlying water column should be included because it will play a similar function for compaction as the sediment overburden on the layers of the indicators. Such indicators include Nos 18, 19, 38, 106, 107 and 108.

The self-compaction of sediments can largely alter the altitude of relative sea level indicators, especially for thick peat layers that may be reduced by 90% of their original volume (Shennan and Horton, 2002). Shennan and Horton (2002) then suggested to select thin peat layers that lay on the Pleistocene sandy sediments as sea level indicators. However, in our study area, the whole late Pleistocene and Holocene sediments are mostly composed of muddy sediments. Compaction may influence all the sediments at var-

ious depth ranges, within which the Holocene sea level indicators must be involved.

4.8 Correction for subsidence by groundwater withdrawal

Although land subsidence had started sporadically in the urban area of Tianjin since the 1920s by the first ground water withdrawal (Wang et al., 2003), extensive subsidence began only after 1975 in the whole low-lying coast of Bohai Bay③⑮ (Xie et al., 2019). Isobath map of land subsidence for the past four decades of about 1975−2015, with high resolution lines as 100 mm or 200 mm spacing, indicates that the maximum subsidence has accumulated more than 3 m in this period in some crucial areas⑮⑯. Therefore, compensation for land elevation is needed for those indicators from the boreholes and pits, drilled or dug after 1975 in the subsiding places shown by GSC⑯ and IGM⑮. For example, Borehole BQ2, from which indicator No. 24 was obtained, is located in the isopach line 1 600 mm and was drilled in 2000 with the borehole elevation +1.57 m measured during the drilling process. If considering that the subsiding started in 1975, then the actual subsidence of this borehole until the drilling year of 2000 should be 1.0 m; i.e., the land surface of this borehole from its existing +1.57 m National Vertical Datum 1985 should be compensated to +2.57 m, and the elevation of indicator No. 24 should be correspondingly added by this value approximately. All the indicators influenced by this subsidence have been corrected (Fig. 8d, Table A4: the third line of Column 14).

To date, all the local factors have been removed step by step from the original RMSL pattern in Fig. 7b. As a result, a solid black line, arbitrarily hand-drawing in Fig. 8d, shows preliminarily a local RMSL curve in the study area.

5 Discussion

5.1 Turning-phase of Holocene sea level rise

In total, 21 indicators were found in the period of about 8.3−5.8 ka. They can be separated into two groups. The first group is not necessary for RTC, including two articulated, vertically stood razor shell indicators, Nos 59 and 82, and seven oyster indicators, Nos 95−98 and 106−108. Similarly, indicators Nos 3 and 67 are classified to this group because they are macroplant samples.

The second group is composed of redeposited samples and is RTC processed. This group includes eight organic-rich sediment indicators, Nos 53−56, 60−61, and 63−64. Their younger ages, given by their subsamples >180 μm, were used. Additionally, indicators Nos 1 and 44, reworked shell or peaty mud, fall under to this group. The ten RTC processed indicators of the second group, together with the first group, comprise a hand-drawn line for this period (Fig. 9: black line). However, if considering the ages contributed by the subsamples <180 μm of the second group, the further obtained approximate ages for their bulk samples (i.e., a mathematic mean of the ages of the two subsamples), and the originally non-RTC processed ages of the indicators Nos 1 and 44, then another curve by integrating Group 1 may be achieved (Fig. 9: red line). A comparison between the two lines shows an obvious geochronological uncertainty, and a trend that is about 0.5 cal ka younger likely exists. As a result, a change from slowdown to stop (i.e., nearly horizontal) seems to occur at about 6.8 cal ka BP rather than about 7.3 cal ka BP and the slowdown is likely to start from about 7.5 ka (Fig. 9).

After eliminating all the local temporospatially affected factors, an amended RMSL pattern illustrated by a solid black curve in Figs 8d, 9 and 10 only remains; theoretically, combined contributions of the eustatic change and the regional isostatic adjustment only remain, as well.

Lambeck et al. (2014) and Bradley et al. (2016) discussed the ice-volume equivalent sea levels (ESLs) and gave the crucial heights of about −5.4 m or about −5.8 m, respectively, at about 7 cal ka BP, which can be roughly recognized as the beginning of the slowdown and nearlly stopped at about 2 ka (Lambeck et al., 2014). However, such two time boundaries are about 7.5 ka and about 6.8 ka, respectively, aforementioned for the study area. Note all the ESLs are not RTC corrected. Among all the 968 original observation data (Lambeck et al., 2014), nearly 450 belong to various sediments, shells, beahrocks and cheniers, of which some ages are likely contaminated by redeposition and/or different at the subsample level. If we would do the RTC for these data, then a beginning of the slowdown, constrained by both ice sheet melting history and isostasy, would be even younger.

Additionally, the progressively improved GIA-modeled projections emphasized a mid-Holocene highstand, i.e., about 2−3 m higher than that at present for the west coast of Bohai Bay④ (personal communication, Lambeck, 2014). Bradley et al. (2016) also discussed a set of projected sea level curves being even about 4−6 m higher at approximately 6 cal ka BP for the same region. However, our RMSL curve is remarkably lower than the predicted curves after about 6 cal ka BP but also obviously higher than both the later predicted curve of Lambeck and Robby (personal communication, 2014) (Fig. 10: the light green one) and the band of Bradley et al. (2016) before about 6−7 cal ka BP (Fig. 10). Such double misfits are perhaps interesting for the existing explanations (Lambeck et al., 2014; Bradley et al., 2016) for the north coast of China. It may imply that comparing that the projected GIA-contributions④ (personal communication, Lambeck, 2014; Bradley et al., 2016) after 6 ka were likely overestimated but were underestimated before that for the region (Fig. 10).

5.2 Uncertainties given by spatial corrections

It is worthwhile to pinpoint that the monotonically seaward-dipping characteristic of the chenier subsurface in the coast of Bohai Bay is different with the convex form of subsurface due to the sink-down of chenier body at the Louisiana coast (Reineck and Singh, 1980: p.352). This difference for the subsurface form may imply that postdepositional self-compaction of the chenier itself and the immediately underlying sediments in the study area was not as strong as that at the Louisiana coast. For instance, indicator No. 71 (Table A4.2) has a compensation of 1.56 m for self-compaction based on its sampling depth of 4 m (Table A5). In total, among 27 chenier indicators, most of them are estimated to experience a self-compaction of about 0.5−2 m (Fig. 8c, Table A4.2: the second line of Column 13). However, if considering the fact that the subsurface was not of a convex type (Fig. 3), then the vertical compensations of about 0.5−2 m may be overestimated. If so, it may explain why the chenier indicators lie at much higher positions, often about 2−3 m above the present MSL (Fig. 8c). On the other hand, due to lacking practically tested data at this time, the compensation for subsidence by groundwater withdrawal that we used is only linear-transmitted to the depth at which indicators existed. Therefore, such compensation may also be overestimated. Nevertheless, if considering two such possible overestimations, it is even much more unfavorable for model-projections of the mid-Holocene highstand.

The early Holocene sea level rise was quickly with an average rate of about 1.4−0.7 cm/a in period of 9−7 cal ka BP (Lemback et al., 2014). Thus the vegetation pavement, forming the basal peat layer later on, may further horizontally extend inland from its original range between MHHW−MHW (Tables A2 and A3), at most, for about 1 km, considering intertidal gradient (the present gradient, see Section 2) if vegetation growth and sediment supply kept pace with the sea level rise. Nevertheless, on the other hand, high sea waters may not often reach such extended end. This is likely a reason that why top part of basal peat layer and/or muddy sediment immediately-above-basal-peat-layers lack definite paleo microbiological evidence for sea water existence and such basal peat layers sometimes can only be used as “limited” indicators.

5.3 *Uncertainties given by temporal corrections*

Twenty organic-rich bulk samples, taken from six cores from DC01 eastward to Q7, about 70 km apart (Shang et al., 2018), were all separated into two subsamples with boundary of 180 μm. Of them, 19 bulk samples, taken from last five cores, located in the range of Holocene marine transgression, show all $\delta^{13}C$ values are in between −19.2‰ and −27.0‰ PDB for the subsamples <180 μm, but $\delta^{13}C$ values of subsamples >180 μm are −24.5‰ to −28.3‰ PDB (Shang et al., 2018). All these 19 subsamples of <180 μm have older AMS ages than subsamples >180 μm, with older range of 170−8 530 cal a (an average 1 320 cal a) (Li et al., 2015; Shang et al., 2018). Thus, much heavier and much older for the subsamples <180 μm must have a regional significance. The heavier $\delta^{13}C$ the closer to the sea is obedient to marine influence (Törnqvist et al., 2015). However, the regional marine reservoir age of about 220 a, caused ΔR= −178±50 a (Southon et al., 2002), is unable to explain why the age-difference between the two subsample groups is so large.

Here, hydrogeological approach is likely to tackle this puzzle. Due to very fine sediments, semi-confined and confined groundwater aquifers exist in the coastal lowland of the study area, which may contain isolated water bodies as old as, at least, several thousand years (Cao et al., 2016; personal communication, Han, 2019). The finer subsamples have larger absorption and their ages can be relatively older.

6 Conclusions

In this study, a total of 110 indicators are classified into three categories: sediments (67), cheniers (27) and oyster reefs (16). Thorough examinations of the indicative meaning for each indicator have been performed with particular descriptions for cheniers and oyster reefs. With reasonable estimation for the paleo tidal pattern and relationship between MTL and MSL, procedures from the observed rsl to RMSL have been completed.

RTC caused more than two-thirds of the whole data to have a younger-oriented shift. Three additional corrections for spatial factors such as neotectonics, self-compaction and groundwater withdrawal are further scrutinized. Consequently, about 0.1 mm/a has been used as the local neotectonic subsiding rate; a few decimeters to nearly 6 m have been compensated for self-compaction on different depths; a few centimeters to nearly 2.5 m have been reimbursed for subsidence by groundwater withdrawal. Finally, a local RMSL curve, eliminated all the local factors, has been speculated, and a slowdown is in between about 7.5−6.8 cal ka BP. None of the obvious mid-Holocene highstand was found, and a likely stable RMSL at <+1 m lasted from about 6.8 ka until about 3 ka before the present.

This new attempt for Holocene sea level reconstruction on the west coast of Bohai Bay may provide a new constrained platform for further modeling efforts in the coming future.

Acknowledgements

The authors acknowledge the numerous researchers provided original data during the last decades, among whom Zhiren Xie (Nanjing Normal University, Nanjing) is particularly thanked for his consistent encouragement. We greatly appreciate Kurt Lambeck (The Australian National University) for his guidance in aspect of the GIA pre-

dicted curves in the study area, and acknowledge Lei Huang (Northwest University, Xi 'an) and Sarah L. Bradley (Utrecht University) for discussions of the regional neotectonics and isostatic approach. Thanks are given to Shu Gao (Nanjing University, Nanjing) for his suggestions of significant reorganizing of the manuscript. Two anonymous reviewers are truly indebted for their valuable review and constructive comments.

References

Bradley S L, Milne G A, Horton B P, et al. 2016. Modelling sea level data from China and Malay-Thailand to estimate Holocene ice-volume equivalent sea level change. Quaternary Science Reviews, 137: 54–68, doi: 10.1016/j.quascirev.2016.02.002

Cai Aaizhi. 1981. A preliminary study of the origin of the cheniers of Bohai Gulf. Studia Marina Sinica (in Chinese), 18: 117–132

Cao Guoliang, Han Dongmei, Currell M J, et al. 2016. Revised conceptualization of the North China Basin groundwater flow system: Groundwater age, heat and flow simulations. Journal of Asian Earth Sciences, 127: 119–136, doi: 10.1016/j.jseaes.2016.05.025

Chen Yukun, Zhao Guomin, Yan Chengguo, et al. 2013. Active Fault Surveying and Risk Evaluation on Earthquakes in Tianjian City (in Chinese). Beijing: Science Press, 48–67

Chonglakmani C, Ingavat R, Piccoli G, et al. 1983. The last marine submersion of the Bangkok area in Thailand. Memorie di Scienze Geologiche, 36: 343–352

Davis R A Jr, Fitzgerald D M. 2004. Beaches and Coasts. Oxford: Blackwell Publishing, 263–277

Fan Changfu. 2008. Paleo-environment recorded by the Holocene buried oyster reef on the west coast of the Bohai

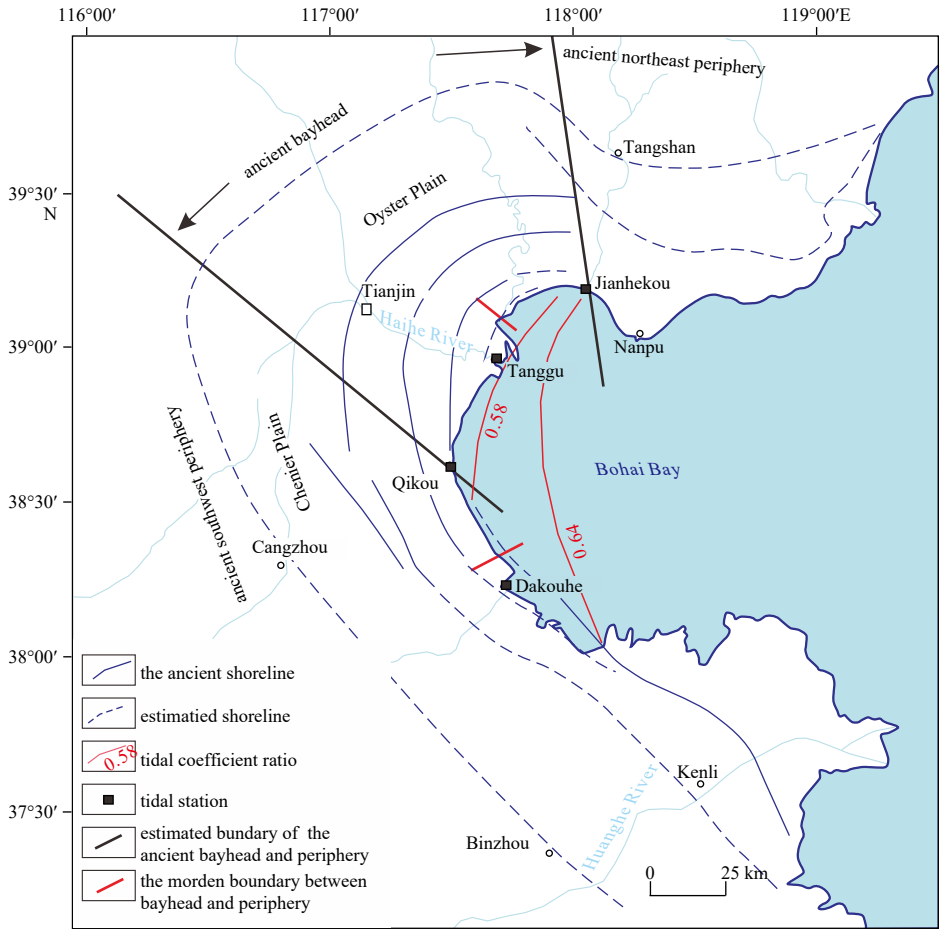

Fig. A1. Comprehensive diagram shows tidal gauge stations and the paleo bayhead evolution since the early mid-Holocene. Bayhead migrated gradually from the Oyster Plain in about 7 ka BP southeastward to the Chenier Plain and, finally, the present bayhead is located in the Jiyun River−Nanpai River section. Thin red lines, 0.58 and 0.64 of $[(H_{O_1}+H_{K_1})/H_{M_2}]$ in the shallow sea area, show less notable semidiurnal pattern⑥. Dotted+solid blue lines on the coastal lowland are paleoshorelines, determined by chains of both cheniers in the Chenier Plain and earthy mounds in the Oyster Plain. The earthy mound chains were alternated with the buried oyster reefs (Wang et al., 2006, 2010). Two red bars are approximate boundary separating modern bayhead and both sides of periphery while the thick black lines are rough boundary between the speculated ancient bayhead and peripheries.

Table A1. The type of tides and tidal information collected from four gauge stations in the Bohai Bay⑥⑦ (Liu et al., 1986; HPL, 2007; EBC, 1989; HPL, 2007; Sun and He, 2013)

Tidal ranges	Northeast periphery (Northeast of Jiyun River Mouth)	Bayhead (Jiyun River Mouth−Napai River Mouth)		Southeast Periphery (Southeast of Nanpai River Mouth)
	Jianhekou Station	Tanggu Station	Qikou Station	Dakouhe Station
Mean tidal range (MHW−MLW)	about 2.3 m	(1) 2.51 m, (2) 2.28 m, (3) 2.48 m, (4) 2.40 m average: about 2.42 m	(1) 2.51 m, (2) 2.3 m	(1) 2.34 m, (2) 2.15 m, (3) 2.30 m average: about 2.26 m
Mean high tidal range (MHHW−MLLW)	2.80 m	(1) 3.02 m, (2) 2.82 m, (3) 2.9−2.8 m average: about 3.0 m	(1) 3.11 m	(1) 2.88 m, (2) 2.7 m, (3) 2.79 m average: about 2.79 m
Mean high water (MHW)	about +1.13 m	(1) +1.13 m, (2) +1.20 m, (3) about +1.23 m average: about +1.21 m	(1) +1.23 m, (2) about +1.23 m	about +1.08 m
Mean higher high water (MHHW)	about +1.18 m	(1) +1.26 m (2) +1.34 m average: about +1.3 m	(1) about +1.23 m, (2) about +1.36 m	+1.13 m
Mean low water (MLW)	about −1.12 m	(1) −1.15 m, (2) about −1.17 m average: about −1.16 m		about −1.07 m
Mean lower low water (MLLW)	about −1.52 m	(1) −1.56 m, (2) −1.66 m average: about −1.61 m		−1.47 m
Observed highest high weter (HHW)		(1) +3.31 m, (2) +3.15 m, (3) +3.11 m average: +3.19 m		

Note: All the average values are calculated by this study and reaffirmed in Table A2.

Table A2. Summary of the tides and geographic distribution for both the present and Holocene tidal situations in the Bohai Bay region, based on Table A1 and paleo geomorphology described in the main text and Fig. A1

Tidal properties	The present tides and bay morphology			Analogous Holocene tides and paleo bay morphology	
	northeast periphery (Northeast of Jiyun River Mouth)	bayhead (Jiyun River Mouth−Nanpai River Mouth)	southeast periphery (Southeast of Nanpai River Mouth)	paleo bayhead (Nanpai River Mouth−north most limit of the data)	south periphery (Southeast of Nanpai River Mouth)
Mean range	2.3 m	2.42 m	2.26 m	2.42 m	2.26 m
Mean high range	2.80 m	3.0 m	2.79 m	3.0 m	2.79 m
MHW	+1.13 m	+1.21 m	+1.08 m	+1.21 m	+1.08 m
MHHW	+1.18 m	+1.3 m	+1.13 m	+1.3 m	+1.13 m
MLW	−1.12 m	−1.16 m	−1.07 m	−1.16 m	−1.07 m
MLLW	−1.52 m	−1.61 m	−1.47 m	−1.61 m	−1.47 m

Sea (in Chinese) [dissertation]. Nanjing: Nanjing University

Fan Changfu. 2010. Plaeo-environment recorded by the mid-Holocene buried oyster reef on the west coast of the Bohai Sea (in Chinese) [dissertation]. Beijing: Chinese Academy of Geological Sciences

Fan Changfu, Li Jianfen, Wang Hong, et al. 2005. Age and paleoenvironmental change of Dawuzhuang oyster reef on the northwest coast of Bohai Bay. Geological Survey and Research (in Chinese), 28(2): 124–129

González J L, Törnqvist T E. 2009. A new Late Holocene sea-level record from the Mississippi delta: Evidence for a climate/sea level connection?. Quaternary Science Reviews, 28(17–18): 1737–1749

Table A3. The indicative meanings (RWL and IR) of the Holocene sea-level indicators on the west coast of Bohai Bay

Types of indicators	Modern and ancient bayhead	Modern and ancient southeastern periphery	Modern northeastern periphery (rarely used) [1)]
Peaty layers	subtracting (1.26±0.05) m	subtracting (1.1±0.03) m	subtracting (1.15±0.03) m
Other sediments	(1) when indicating MHHW or MHW: subtracting (1.3±0.5) m, (2) when indicating MLLW: adding (1.6±0.5) m, (3) when indicating MLW: adding (1.15±0.5) m, (4) when indicating intertidal zone only: sample's altitude ±1 m	(1) when indicating MHHW or MHW: subtracting (1.1±0.5) m, (2) when indicating MLLW: adding (1.45±0.5) m, (3) when indicating MLW: adding (1.05±0.5) m, (4) when indicating intertidal zone only: sample's altitude ±1 m	(1) when indicating MHHW or MHW: subtracting (1.15±0.5) m, (2) when indicating MLLW: adding (1.5±0.5) m, (3) when indicating MLW: adding (1.1±0.5) m, (4) when indicating intertidal zone only: sample's altitude ±1 m
Cheniers	(1) front-part: sample's altitude ±1 m, (2) above the mid-subsurface: subtracting (1.2±0.5) m, (3) above the rear-subsurface: subtracting (1.3±0.5) m	(1) front-part: sample's altitude ±1 m, (2) above the mid-subsurface: subtracting (1.1±0.5) m, (3) above the rear-subsurface: subtracting (1.1±0.5) m	(1) front-part: sample's altitude ±1 m, (2) above the mid-subsurface: subtracting (1.1±0.5) m, (3) above the rear-subsurface: subtracting (1.2±0.5) m
Oyster Reefs [2)]	(The reef-top-elevation+0.15 m) ± 0.7 m	–	–

Note: All the values, based on Table A2, were rounded to the nearest 5 or 10. [1)] Indicative meanings for the northeastern periphery are also listed though this coastal sector is rarely dealt with in this study. [2)] Elevation of the top of oyster reef indicates mean tidal level (MTL) directly and 0.15 m is added to reconstruct a corresponding MSL.

Gu Jiayu, Yan Qinshang, Yu Zhiying. 1983. The cheniers of the northern coastal plain of Jiangsu province. Acta Sedimentologica Sinica (in Chinese), 1(2): 47–59

Guillocheau F, Rouby D, Robin C, et al. 2012. Quantification and causes of the terrigeneous sediment budget at the scale of a continental margin: a new method applied to the Namibia-South Africa margin. Basin Research, 24(1): 3–30, doi: 10.1111/j.1365-2117.2011.00511.x

Hijma M P, Engelhart S E, Törnqvist T E, et al. 2015. A protocol for a geological sea-level database. In: Shennan I, Long A J, Horton B P, eds. Handbook of Sea-Level Research. West Sussex: John Wiley & Sons, 536–553

Hijma M P, Shen Z X, Törnqvist T E, et al. 2017. Late Holocene evolution of a coupled, mud-dominated delta plain-chenier plain system, coastal Louisiana, USA. Earth Surface Dynamics, 5(4): 689–710, doi: 10.5194/esurf-5-689-2017

Hopkins S H. 1979. Oysters. In: Fairbridge R W, Jablonski D, eds. The Encyclopedia of Paleontology, Encyclopedia of Earth Sciences, VII. Kansas: The Universtity of Kansas, 505–514

Huang Lei, Liu Chiyang, Wang Yingbin, et al. 2014. Neogene-Quaternary postrift tectonic reactivation of the Bohai Bay Basin, eastern China. AAPG Bulletin, 98(7): 1377–1400, doi: 10.1306/03071413046

IOG (Institute of Geology of Dagang Oil Field, Academy of Marine Oil Prospection, Institute of Oceanography of Tongji University). 1985. Sedimentary Systems of the Alluvial Fan and Delta of the Luanhe River (in Chinese). Beijing: Geological Publishing House, 84–94

Johnson J H, Foster H L. 1951. Recent molluscan association with paleontologic and stratigraphic implications: geological notes. AAPG Bulletin, 35(11): 2430–2431

Kira T. 1975. Shells of the Western Pacific in Color (in Japanese). 2nd ed. Osaka, Japan: Hoikusha Publishing Co. Ltd., 143–144

Lambeck K, Rouby H, Purcell A, et al. 2014. Sea level and global ice volumes from the Last Glacial Maximum to the Holocene. Proceedings of the National Academy of Sciences of the United States of America, 111(43): 15296–15303, doi: 10.1073/pnas.1411762111

Li Jianfen. 2010. Distribution characteristics of the modern foraminifera assemblages and their geoenvironmental records in the West Bohai Bay (in Chinese) [dissertation]. Beijing: China University of Geosciences (Beijing)

Li Shaoquan, Li Guangxue. 1987. Cheniers in Huanghe River delta. Marine Geology & Quaternary Geology (in Chinese), 7(S): 103–111

Li Jianfen, Shang Zhiwen, Chen Yongsheng, et al. 2020. Research status and protection suggestions on oyster reef in Bohai Bay. Geological Survey and Research, 43(4): 317–333

Li Jianfen, Shang Zhiwen, Jiang Xingyu, et al. 2016a. Sea-level indicated by foraminifera assemblages living in the open muddy flats with or without influence of the chenier ridges in Bohai Bay coastal area. Geological Bulletin of China (in Chinese), 35(10): 1578–1583

Li Jianfen, Shang Zhiwen, Wang Fu, et al. 2015. Holocene sea level change on the west coast of the Bohai Bay. Quaternary Sciences (in Chinese), 35(2): 243–264

Li Jianfen, Su Shengwei, Shang Zhiwen, et al. 2016b. Sea level reconstruction based on foraminifera assemblages: A paradigm obtained in Jugezhuang Chenier, Bohai Bay, and

its underlying muddy sediments. Geological Bulletin of China (in Chinese), 35(10): 1584–1589

Li Jianfen, Wang Hong, Li Fenglin, et al. 2004. Holocene geoenvironmental changes at the Xingtuo section in the central part of the Oyster Reef plain, Bohai Bay. Geological Bulletin of China (in Chinese), 23(2): 169–176

Lin Guande, Sun Henglun. 1987. Sea Level (in Chinese). Beijing: Geological Publishing House, 3–24

Liu Huimin. 2010. Dawuzhuang oyster reef: Its reef-mud transformation and the geoenvironmental changes on the northwest coast of Bohai Bay (in Chinese) [dissertation]. Changchun: Jilin University

Liu Qiongying, He Lijuan, Huang Fang, et al. 2016. Cenozoic lithospheric evolution of the Bohai Bay Basin, eastern North China Craton: constraint from tectono-thermal modeling. Journal of Asian Earth Sciences, 115: 368–382, doi: 10.1016/j.jseaes.2015.10.013

Liu Jian, Saito Y, Kong Xianghuai, et al. 2010. Delta development and channel incision during marine isotope stages 3 and 2 in the western South Yellow Sea. Marine Geology, 278(1–4): 54–76

Liu Cangzi, Walker H J. 1989. Sedimentary characteristics of cheniers and the formation of the Chenier plains of East China. Journal of Coastal Research, 5(2): 353–368

Liu Aiju, Zhang Yanting, Huang Yichang. 1986. The tide characteristics along the coast of Hebei Province. Journal of Oceanography of Huanghai & Bohai Seas (in Chinese), 4(3): 1–7

Mook W G, van de Plassche O. 1986. Radiocarbon dating. In: van de Plassche O, ed. Sea-Level Research: A Manual for the Collection and Evaluation of Data. Dordrecht: Springer, 525–560

Murray-Wallace C V, Woodroffe C D. 2014. Quaternary Sea-Level Changes: A Global Perspective. Cambridge: Cambridge University Press, 1–484

Neal A, Richards J, Pye K. 2002. Structure and development of shell cheniers in Essex, southeast England, investigated using high-frequency ground-penetrating radar. Marine Geology, 185(3–4): 435–469

Okutani T. 2000. Marine Mollusks in Japan (in Japanese). Tokai: Tokai University Press, 924–925

Otvos E G Jr, Price W A. 1979. Problems of chenier genesis and terminology —an overview. Marine Geology, 31(3 –4): 251–263

Pico T, Mitrovica J X, Ferrier K L, et al. 2016. Global ice volume during MIS 3 inferred from a sea-level analysis of sedimentary core records in the Yellow River Delta. Quatenary Science Reviews, 152: 72 –79, doi: 10.1016/j.quascirev.2016.09.012

Pirrazoli P A. 1991. World Atlas of Holocene Sea-Level Changes. Amsterdam: Elsevier, 117–125

Price W A. 1955. Environment and formation of the chenier plain. Quaternaria, 2: 75–86

Qin Lei, Shang Zhiwen, Li Yong, et al. 2017. Temporo and spatial distribution of the oyster reef in Biaokou to Zengkouhe area. Geological Survey and Research (in Chinese), 40(4): 306–310

Reimer P J, Bard E, Bayliss A, et al. 2013. Intcal13 and Marine13 radiocarbon age calibration curves 0−50,000 years cal BP. Radiocarbon, 55(4): 1869 –1887, doi: 10.2458/azu_js_rc.55.16947

Reineck H E, Singh I B. 1980. Depositional Sedimentary Environments. Berlin: Springer-Verlag, 114–128, 352–359

Rodríguez-Ramírez A, Yáñez-Camacho C M. 2008. Formation of chenier plain of the Doñana marshland (SW Spain): Observations and geomorphic model. Marine Geology, 254(3–4): 187–196

Russell R J, Howe H V. 1935. Cheniers of southwestern Louisiana. Geographical Review, 25(3): 449 –461, doi: 10.2307/209313

Scarlato O A. 1981. The Bivalve Molluscs in the Temperate Latitudes of Western Part of the Pacific Ocean (in Russian). Leningrad: Leningrad Press, 253–254

Shang Zhiwen, Chen Yongsheng, Jiang Xingyu, et al. 2015. New discovery of a fishing site during Western Han Dynasty and an enlightenment for the "Western Han Dynasty's Transgression" on the west coast of Bohai Bay. Geological Review (in Chinese), 61(6): 1468–1481

Shang Zhiwen, Wang Fu, Fang Jing, et al. 2018. Radiocarbon ages of different fractions of peat on coastal lowland of Bohai Bay: marine influence?. Journal of Oceanology and Limnology, 36(5): 1562 –1569, doi: 10.1007/s00343-019-7091-7

Shang Zhiwen, Wang Fu, Li Jianfen, et al. 2016. New residence times of the Holocene reworked shells on the west coast of Bohai Bay, China. Journal of Asian Earth Sciences, 115: 492–506, doi: 10.1016/j.jseaes.2015.10.008

Shennan I. 2015. Handbook of sea-level research: framing research questions. In: Shennan I, Long A J, Horton B P, eds. Handbook of Sea-Level Research. West Sussex: John Wiley & Sons, Ltd., 3–25

Shennan I, Horton B. 2002. Holocene land- and sea-level changes in Great Britain. Journal of Quaternary Science, 17(5–6): 511–526

Shennan I, Long A J, Horton B P. 2015. Handbook of Sea-Level Research. West Sussex: John Wiley & Sons, Ltd., 1–581

Shennan I, Tooley M J, Davis M J, et al. 1983. Analysis and interpretation of Holocene sea-level data. Nature, 302(5907): 404–406, doi: 10.1038/302404a0

Southon J, Kashgarian M, Fontugne M, et al. 2002. Marine reservoir corrections for the Indian Ocean and Southeast Asia. Radiocarbon, 44(1): 167 –180, doi: 10.1017/S0033822200064778

Stenzel H B. 1971. Mollusca 6, Bivalvia. In: Moore R C, ed. Treatise on Invertebrate Paleontology Part N, 3. Kansas: The Geological Society of America and the Universtity of Kansas, 1016–1136

Stuiver M, Reimer P J. 1993a. Extended ^{14}C data base and revised calib 3.0 ^{14}C age calibration program. Radiocarbon, 35(1): 215–230, doi: 10.1017/S0033822200013904

Table A4.1. The Holocene relative mean sea level (rmsl) indicators, derived from the sediments, on the west coast of Bohai Bay

	Basic information			Temporal distribution								Spatial distribution		
No.	Locality, stratigraphy and environment, material dated, sampling depth / ground surface elevation / (averaged) sample elevation	Coordinate	Lab code	Measured ^{14}C date	$\delta^{13}C$ /‰PDB	Conventional ^{14}C age/a BP	Calibrated ^{14}C age: median probability/2σ range/cal a BP	Status of material dated	Sub-sample	RTC /cal a	Age of rmsl: single value /range/cal ka BP)	Elevation of the observed rmsl/m	Corrections of tectonics/ self-compaction/water withdrawal /m	Elevation of rmsl after corrections for the three local factors /m
1	Zhakou, shelly layer, single valves of undetermined shells, about 2/-/about −1.75 m	39.4°N, 117.8°E	GC175A	*5 410±250*	*−2.68*	*5 769±253*	6 375/ 6 966−5 789	reworked	no	−600	*5.775/ 6.36−5.19*	−1.75±1	+0.58/ +0.78/ +0.20	−0.19±1
2	Lizigu, swamp, upper peaty layer, mud, articulated *Arconaia contorta* (?), about 2 m/about +1 m/−1 m	39.5°N, 117.4°E	CG1394	*3 990±80*	*−27*	*4 199±90*	4 715/ 4 473−4 446, 4 893−4 525, 4 960−4 898	*in situ* (?)	no	−	4.715/ 4.960−4.446	−2.26±0.05	+0.47/ +0.78/ +0.12	−0.89±0.05
3	*idem,* marine sediments, wood branch on the top, 2.3 m/about +1 m/about −1.3 m		CG-?	*6 680±110*	*−27*	*6 696±117*	7 567/ 7 355−7 333, 7 387−7 374, 7 791−7 414	reworked	no	−	7.567/ 7.791−7.333	−2.60±0.5	+0.75/ +0.90/ +0.12	−0.83±0.5
4	Maomaojiang, intertidal shelly layer, single valves of *Mactra veneriformis* mainly, about 2 m/-/about 0 m *idem,* single valves of *M. veneriformis* mainly, about 2.3 m/-/about 0 m	39.4°N, 117.7°E	CG187, TD5	*5 320±75, 6 350±105*	*−2.68*	*5 679±85, 6 709±112*	6 274/ 6 481−6 019; 7 395/ 7 604−7 162	reworked	no	−600	*5.674/ 7.00−5.42*	0±1.5	+0.56/ +0.78/ +0.12	+1.46±1.5
5	Dawuzhuang, oyster reef, Section 9, the bottom of the overlying mud, semi-	39.4°N, 117.9°E	BA 091202	−	−	4 810±35	5 520/ 5 558−5 471, 5 604−5 568	reworked	no	−	5.520/ 5.604−5.471	−2.23±0.7	+0.55/ +1.95/ +0.52	+0.79±0.7

continued from Table A4.1

No.	Basic information: Locality, stratigraphy and environment, material dated, sampling depth / ground surface elevation / (averaged) sample elevation	Coordinate	Lab code	Temporal distribution: Measured ^{14}C date	$\delta^{13}C$ /‰PDB	Conventional ^{14}C age/a BP	Calibrated ^{14}C age: median probability/2σ range/cal a BP	Status of material dated	Sub-sample	RTC /cal a	Age of rmsl: single value /range/cal ka BP)	Spatial distribution: Elevation of the observed rmsl/m	Corrections of tectonics/ self-compaction/water withdrawal /m	Elevation of rmsl after corrections for the three local factors /m
8	*idem,* bottom of garlic-structured clay, articulated shells of *Glauconome primeana*, 2−2.1 m/+1.6 m/−0.45 m		AA 45905	−	−4.8	3 428±49	3 505/ 3 680−3 345	*in situ*	no	−	3.505/ 3.680−3.345	−0.45±0.5	+0.35/ +0.78/ +0.70	+1.38 ±1.5
9	Xingtuo Pit, the lower portion of intertidal zone, fine sandy-silty mud, articulated *Mactra veneriformis* shells, 3.8−4.0 m/about +1.6 m/about −2.3 m		AA 45904	−	−4.5	4 169±52	4 489/ 4 720−4 275, 4 766−4 753	*in situ*	no	−	4.489/ 4.766−4.275	−0.7±0.5	+0.45/ +1.52/ +0.87	+2.14±0.5
10	Core H1, basal peat, peaty mud, 16.57−16.63 m/+1.6 m/−15.0 m	39.3°N, 117.6°E	00Y078	*8 562±100*	*−27*	*8 530±108*	9 520/ 9 793−9 270, 9 816−9 808, 9 865−9 848, 9 885−9 877	*in situ*	no	−660	*8.860/ 9.22−8.61*	−16.26±0.05	+0.88/ +4.81/ +0.87	−9.7±0.05
11	Core H3, intertidal muddy sediments, single valves of *Potamocorbula laevis*, 4.4 m/+1.315 m/−3.09 m	39.3°N, 117.7°E	Beta 358164	3 640±30	−6.4	3 950±30	4 191/ 4 377−4 009	reworked	no	−600	*3.591/ 3.77−3.41*	−3.09±0.5	+0.36, +1.46, +1.40	+0.13±0.5
12	Core HD21, lagoon-salt marsh, articulated *Saliqua pulchella*, 1.1−1.2 m/+0.71	39.4°N, 117.6°E	AA 45902	−	−7.6	1 579±48	1 310/ 1 473−1 173	*in situ*	no	−	1.310/ 1.473−1.173	−1.74±0.5	+0.13/ +0.40/ +0.45	−0.76±0.5

continued from Table A4.1

	Basic information			Temporal distribution								Spatial distribution		
No.	Locality, stratigraphy and environment, material dated, sampling depth / ground surface elevation / (averaged) sample elevation	Coordinate	Lab code	Measured ^{14}C date	$\delta^{13}C$ /‰PDB	Conventional ^{14}C age/a BP	Calibrated ^{14}C age: median probability/2σ range/cal a BP	Status of material dated	Sub-sample	RTC /cal a	Age of rmsl: single value /range/cal ka BP)	Elevation of the observed rmsl/m	Corrections of tectonics/ self-compaction/water withdrawal /m	Elevation of rmsl after corrections for the three local factors /m
16	Core HG81, basal peat, peaty mud, 16.65−16.68 m/about +2 m/−14.67 m	39.2°N, 117.8°E	06Y084	*8 160±250*	*−27*	*8128±253*	9 040/ 9 539−8 430	*in situ*	no	−660	*8.380/ 8.88−7.77*	−15.93±0.05	+0.84/ +4.83/ +1.05	−9.21±0.05
17	Core Beining Park, basal peat, plant debris (?), 16.89−17.09 m/about +2.46 m/about −14.53 m	39.2°N, 117.2°E	ZK601-I	*8 035±120*	*−27*	*8035±120*	8 902/ 9 271−8 592	*in situ*	no	−	8.902/ 9.271−8.592	−15.79±0.05	+0.89/ +4.93/ +0.37	−9.6±0.05
18	Core CH114, basal peat, peaty mud, 12.0−12.1 m/about −3.90 m/about −15.95 m	39.1°N, 117.9°E	BA 081875	−	−	8415±35	9 455/ 9 351−9 320, 9 522−9 400	*in situ*	no	−660	*8.795/ 8.86−8.66*	−17.21±0.05	+0.88/ +4.61/ +1.12	−10.6±0.05
19	Core CH115, basal peat, charcoals and carbonized twigs, 17.41−17.43 m/−3.90 m/about −21.32 m	39.1°N, 117.9°E	BA 081878	−	−	8 805±35	9 833/ 9 946−9 682, 10 008−9 993, 10 127−10 063	*in situ* (?)	yes	−	*9.833/ 10.127−9.682*	−22.58±0.05	+0.98/ +5.75/ +1.12	−14.73±0.05
20	Core HDZ, basal peat, peaty mud, 18.05−18.15 m/about +2.5 m/−15.6 m	39.1°N, 117.7°E	TD408	*8 120±160*	*−27*	*8 088±165*	8 998/ 9 436−8 587	*in situ*	no	−660	*8.338/ 8.78−7.93*	−16.86±0.05	+0.83/ +4.67/ +0.17	−11.19±0.05
21	*idem,* basal peat, peaty mud, 18.81−19.0 m/about +2.5 m/−16.41 m	39.1°N, 117.7°E	TD409	*8 645±130*	*−27*	*8 613±136*	9 644/ 9 357−9 316, 9 962−9 399, 10 044−9 985, 10 152−10 052	*in situ*	no	−660	*8.984/ 9.49−8.65*	−17.67±0.05	+0.90/ +4.90/ +0.17	−11.7±0.05

continued from Table A4.1

No.	Basic information: Locality, stratigraphy and environment, material dated, sampling depth / ground surface elevation / (averaged) sample elevation	Coordinate	Lab code	Temporal distribution: Measured ^{14}C date	$\delta^{13}C$ /‰PDB	Conventional ^{14}C age/a BP	Calibrated ^{14}C age: median probability/2σ range/cal a BP	Status of material dated	Sub-sample	RTC /cal a	Age of rmsl: single value /range/cal ka BP)	Spatial distribution: Elevation of the observed rmsl/m	Corrections of tectonics/ self-compaction/water withdrawal /m	Elevation of rmsl after corrections for the three local factors /m
25	Chuanganglu Pit, Section 7, Shell Bed B, articulated *Potamocorbula laevis*, 4.8/-/about −2.91 m	38.8°N, 117.5°E	Beta 363624	2 070±30	−3.7	2 420±30	2 271/ 2 427−2 114	reworked	yes	−	2.271/ 2.427−2.114	−2.91±1	+0.22/ +1.87/ +2.0	+1.18±1
26	Chuanganglu Pit, Section 4, carbonized, fine plant twig, about 4/-/−2.46 m	38.8°N, 117.5°E	Beta 352331	2 830±30	−26.0	2 810±30	2 911/ 2 999−2 844	reworked	no	−	2.911/ 2.999−2.844	−3.76±0.5	+0.29/ +1.56/ +2.0	+0.09±0.5
27	*idem,* Section 4, the bottom of Shell Bed A, articulated *Mactra chinensis*, about 4.4/-/−2.86 m	38.8°N, 117.5°E	Beta 352328	1 320±30	−1.3	1 710±30	1 436/ 1 558−1 300	reworked	yes	−	*1.436/ 1.558−1.300*	−2.86±1	+0.14/ +1.72/ +2.0	+1±1
28	Chuanganglu Pit, Section 5, the mid-upper part of Shell Bed A, articulated *Sinonovacula constricta*, about 4/-/−2.46 m	38.8°N, 117.5°E	Beta 352325	1 570±30	−6.6	1 870±30	1 620/ 1 786−1 482	*in situ*	yes	−	*1.620/ 1.786−1.482*	−3.76±0.5	+0.16/ +1.56/ +2.0	−0.04±0.5
29	Chuanganglu Pit, Section 1, coarse shell hash layer at the lower part of Shell Bed 1, *Nassarius* sp., about 4.2/-/about −2.4 m	38.8°N, 117.5°E	Beta 335910	1 520±30	−3.0	1 880±30	1 631/ 1 795−1 494	reworked	yes	−	*1.631/ 1.795−1.494*	−2.4±1	+0.16/ +1.64/ +1.5	+0.9±1
30	*idem,* Section 1, thin shelly lamina at the	38.8°N, 117.5°E	Beta 335912	2 080±30	−1.2	2 470±30	2 339/ 2 516−2 149	reworked	yes	−	*2.339/ 2.516−2.149*	−2.7±1	+0.23/ +1.75/	+1.28±1

continued from Table A4.1

Basic information			Temporal distribution								Spatial distribution		
No.	Locality, stratigraphy and environment, material dated, sampling depth / ground surface elevation / (averaged) sample elevation	Coordinate	Lab code	Measured ^{14}C date	$\delta^{13}C$ /‰PDB	Conventional ^{14}C age/a BP	Calibrated ^{14}C age: median probability/2σ range/cal a BP	Status of material dated	Sub-sample	RTC /cal a	Age of rmsl: single value /range/cal ka BP)	Elevation of the observed rmsl/m	Corrections of tectonics/ self-compaction/water withdrawal /m	Elevation of rmsl after corrections for the three local factors /m
32	*idem,* Section 2, the bottom of Shell Bed A, single valve of *Potamocorbula laevis*, about 5/−/about −3 m		Beta 335911	2 470±30	−2.2	2 840±30	2 794/ 2 934−2 692	reworked	no	−600	*2.194/ 2.33−2.09*	−3.0±0.5	+0.22/ +1.95/ +2.0	+1.17±0.5
33	Chuanganglu Pit, Section 6, Shell Bed C, articulated *Cyclina sinensis*, about 5.5/-/−3.7 m;	38.8°N, 117.5°E	Beta 352323	2 100±30	−1.6	2 480±30	2 355/ 2 542−2 156	reworked	yes	−	*2.318/ 2.542−2.093*	−3.7±1	+0.23/ +1.87/ +2.0	0.4±1
	idem, Section 6, Shell Bed C, articulated *Potamocorbula laevis*, about 5.5/-/−3.7 m;		Beta 363617	2 090±30	−5.9	2 400±30	2 246/ 2 392−2 093							
	idem, Section 6, Shell Bed C, articulated *Mactra chinenesis*, about 5.5/-/−3.7 m		Beta 363620	2 090±30	−1.4	2 480±30	2 355/ 2 542−2 156							
34	*idem,* Section 6, Shell Bed C, copper coin, about 5.5/-/−3.7 m		−	−	−	−	−	*in situ*	−	−	2.119/ 2.171−2.068	−5.0±0.5	+0.21/ +1.87/ +2.0	−0.92±0.5
35	*idem,* Section 6, Shell Bed D, *Dupliaria dussumierii* (?), about 6/-/−4.15 m		Beta 363623	1 950±30	+0.4	2 370±30	2 217/ 2 341−2 060	reworked	yes	−	*2.217/ 2.341−2.060*	−4.15±1	+0.22/ +2.04/ +2.0	+0.11±1
36	Core BT113, single valve of *Potamocorbula laevis*, 4.4 m/+1.436 m/−2.96	38.8°N, 117.5°E	Beta 296005	1 180±30	−0.8	1 580±30	1 310/ 1 436−1 180	reworked	no	−600	*0.710/ 0.83−0.58*	−2.96±1	+0.07/ +1.52/ +1.50	+0.13 ±1

continued from Table A4.1

No.	Basic information			Temporal distribution								Spatial distribution		
	Locality, stratigraphy and environment, material dated, sampling depth / ground surface elevation / (averaged) sample elevation	Coordinate	Lab code	Measured ^{14}C date	$\delta^{13}C$ /‰PDB	Conventional ^{14}C age/a BP	Calibrated ^{14}C age: median probability/2σ range/cal a BP	Status of material dated	Sub-sample	RTC /cal a	Age of rmsl: single value /range/cal ka BP)	Elevation of the observed rmsl/m	Corrections of tectonics/ self-compaction/water withdrawal /m	Elevation of rmsl after corrections for the three local factors /m
40	Core G15, basal peat, peaty mud, 17.95 m/about +2.46 m/−15.49 m	38.7°N, 117.4°E	ZK1465	*8 580±130*	*−27*	*8 548±136*	9 548/ 9 177−9 140, 9 223−9 203, 9 926−9 236, 10 117−10 069	*in situ*	no	−660	*8.888/ 9.46−8.48*	−16.75±0.05	+0.89/ +5.20/ +0.22	−10.44±0.05
41	*idem*, basal peat, peaty mud, 18.65 m/about +2.46 m/−16.19 m		ZK1466	*9 140±120*	*−27*	*9 108±127*	10 288/ 10 595−9 894, 10 650−10 624	*in situ*	no	−660	*9.628/ 9.99−9.23*	−17.45±0.05	+0.96/ +5.41/ +0.22	−10.86±0.05
42	Core BQ1, marine muddy sediments, intercalated coarse shelly layer, *Corbicula fluminea*, 18.22 m/+3.404 m/−14.81 m		BA 04542	−	−	8 620±40	9 462/ 9 576−9 305	reworked	no	−600	*8.862/ 8.97−8.70*	−13.21±0.5	+0.88/ +4.98/ +1.12	−6.23±0.5
43	Core TP23, single valve of *Potamocorbula laevis*, 5.7 m/+1.848 m/−3.85 m	38.7°N, 117.4°E	BA 091539	−	−	3 450±35	3 528/ 3 682−3 376	reworked	no	−600	*2.928/ 3.08−2.77*	−3.85±1	+0.29/ +1.50/ +1.35	−0.71±1
44	*idem*, peat layer, peaty mud, 14.1 m/+1.848 m/−12.25 m		BA 091542	−	−	7 610±40	8 407/ 8 462−8 350, 8 477−8 467, 8 513−8 495	*in situ*	no	−660	*7.747/ 7.85−7.69*	−13.51±0.05	+0.77/ +3.80/ +1.75	−7.19±0.05
45	*idem,* peat layer, peaty mud, 14.2 m/+1.848 m/−12.35 m		BA 091543	−	−	8 160±40	9 096/ 9 149−9 010, 9 254−9 162	*in situ*	no	−660	*8.436/ 8.59−8.35*	−13.61±0.05	+0.84/ +3.83/ +1.75	−7.19±0.05
46	Core Q7, lagoon-salt marsh (?), upper peat	38.7°N, 117.5°E	Beta 358054	450±30	−20.4	530±30	540/ 559−510,	*in situ*	no	−100	*0.440/ 0.53−0.41*	+0.9±0.05	+0.04/ +0.12/	+2.06±0.05

continued from Table A4.1

	Basic information			Temporal distribution								Spatial distribution		
No.	Locality, stratigraphy and environment, material dated, sampling depth / ground surface elevation / (averaged) sample elevation	Coordinate	Lab code	Measured ^{14}C date	$\delta^{13}C$ /‰PDB	Conventional ^{14}C age/a BP	Calibrated ^{14}C age: median probability/2σ range/cal a BP	Status of material dated	Sub-sample	RTC /cal a	Age of rmsl: single value /range/cal ka BP)	Elevation of the observed rmsl/m	Corrections of tectonics/ self-compaction/water withdrawal /m	Elevation of rmsl after corrections for the three local factors /m
50	Core QX01, lagoon-salt marsh, organic mud (<180 μm), 5.52 m/+5.16 m/−0.36 m	38.7°N, 116.8°E	Beta 329647	4 260±30	−22.5	4 300±30	4 858/ 4 892−4 829, 4 908−4 899, 4 917−4 913, 4 960−4 924	*in situ*	no	−1 320	*3.538/ 3.64−3.51*	−1.66±0.5	+0.35/ +1.76/ +1.0	+1.45±0.5
51	*idem,* lagoon-salt marsh, organic mud (<180 μm), 6.35 m/+5.16 m/−1.19 m		Beta 329644	4 990±50	−23.6	5 010±50	5 750/ 5 900−5 644	*in situ*	no	−1 320	*4.430/ 4.58−4.32*	−2.45±0.05	+0.44/ +1.82/ +1.0	+0.81±0.05
52	*idem,* lagoon-salt marsh, organic mud (<180 μm), 7.2 m/+5.16 m/−2.04 m		Beta 329643	5 090±30	−25.0	5 090±30	5 813/ 5 831−5 748, 5 912−5 843	*in situ*	no	−1 320	*4.493/ 4.59−4.43*	−3.34±0.5	+0.45/ +2.11/ +1.0	+0.22±0.5
53	*idem,* lagoon-salt marsh, plant debris (>180 μm), 8.2 m/+5.16 m/−3.04 m		Beta 329641	5 820±30	−24.6	5 830±30	6 647/ 6 732−6 554	*in situ*	yes	−	6.647/ 6.732−6.554	−4.34±0.5	+0.66/ +2.45/ +1.0	−0.23±0.5
54	*idem,* lagoon-salt marsh, basal peat, plant debris (>180 μm), 8.7 m/+5.16 m/−3.54 m		Beta 329642	6 020±40	−24.3	6 030±40	6 875/ 6 763−6 755, 6 981−6 778	*in situ*	yes	−	*6.875/ 6.981−6.755*	−4.8±0.05	+0.69/ +2.62/ +1.0	−0.49±0.05
55	*idem,* lagoon-salt marsh, basal peat, plant debris (>180 μm), 9.16 m/+5.16 m/−4.0 m		Beta 329645	6 160±40	−27.4	6 220±40	7 117/ 7 133−7 006, 7 250−7 140	*in situ*	yes	−	*7.117/ 7.250−7.006*	−5.26±0.05	+0.71/ +2.77/ +1.0	−0.78±0.05
56	*idem,* lagoon-salt marsh, basal peat,		Beta 329640	7 010±30	−25.3	7 010±30	7 855/ 7 771−7 763,	*in situ*	yes	−	*7.855/ 7.935−7.763*	−7.53±0.5	+0.78/ +3.22/	−2.53±0.5

continued from Table A4.1

Basic information			Temporal distribution							Spatial distribution		
No.	Locality, stratigraphy and environment, material dated, sampling depth / ground surface elevation / (averaged) sample elevation	Coordinate	Lab code	Measured ^{14}C date	$\delta^{13}C$ /‰PDB	Conventional ^{14}C age/a BP	Calibrated ^{14}C age: median probability/2σ range/cal a BP	Status of material dated	Sub-sample	RTC /cal a	Age of rmsl: single value /range/cal ka BP)	Elevation of the observed rmsl/m	Corrections of tectonics/ self-compaction/water withdrawal /m	Elevation of rmsl after corrections for the three local factors /m
60	*idem.* gleysoil (?), plant debries (>180 μm), 7.39−7.40 m/+4.38 m/−3.01 m		Beta 353796	NA	NA	5 930±30	6 752/ 799−6 671, 6 844−6 816	*in situ*	yes	−	*6.752/ 6.844−6.671*	−3.01±1	+0.67/ +2.17/ +0.90	+0.73±1
61	*idem.* organic mud, plant debris (>180 μm), 8.63−8.65 m/+4.38 m/−4.26 m		Beta 353798	6 440±40	−26.7	6 410±40	7 350/ 7 420−7 271	*in situ*	yes	−	*7.350/ 7.420−7.271*	−5.52±0.05	+0.73/ +2.59/ +0.90	−1.3±0.05
62	Core QX02, intercalated organic mud (<180 μm), 5.68 m/+3.57 m/−2.11 m	38.6°N, 117. 0°E	Beta 332792	5 430±30	−24.0	5 450±30	6 247/ 6 300−6 204	*in situ*	no	−1 320	*4.927/ 4.98−4.88*	−3.41±0.5	+0.49/ +1.78/ +0.95	−0.19±0.5
63	*idem,* intercalated organic mud, plant debris (>180 μm), 7.27 m/+3.57 m/−3.70 m		Beta 333329	6 360±30	−25.7	6 350±30	7 283/ 7 218−7 176, 7 331−7 240, 7 373−7 356, 7 413−7 390	*in situ*	yes	−	*7.283/ 7.413−7.176*	−5.0±0.5	+0.73/ +2.10/ +0.95	−1.22±0.5
64	*idem,* plant debris (>180 μm), 8.98 m/+3.57 m/−5.41 m		Beta 333330	6 620±30	−26.3	6 600±30	7 494/ 7 522−7 434, 7 564−7 532	*in situ*	yes	−	*7.494/ 7.564−7.434*	−6.71±0.5	+0.75/ +2.71/ +0.95	−2.3±0.5
65	Core Yugong 3, basal peat, peaty mud, 14.72−14.92 m/about +1.26 m/−13.56 m	38.5°N, 117.6°E	CG70	*9 120±180*	*−27*	*9 088±184*	10 240/ 9 640−9 635, 10 711−9 661	*in situ*	no	−660	*9.580/ 10.05−8.97*	−14.82±0.05	+0.96/ +4.59/ +0.06	−9.21±0.05
66	Core 8-1, lagoon-salt marsh behind chenier, gleysol horizon, *Gyraulus* sp. and *Assiminea* sp.,	38.2°N, 117.8°E	AA 45899	−	−7.0	2 869±56	2 827/ 3 018−2 689	*in situ*	yes	−	*2.827/ 3.018−2.689*	+0.13±0.03	+0.28/ +0.60/ +0.15	+1.16±0.03

Continued form Table A4.1

No.	Notes
	Explainations of the indicative meaning, RTC, the three spatial corrections and changes from the previous work (Li et al., 2015)
1	It is a shelly layer intercalated in intertidal muddy sediments (SQG, 1980). Two estimated sampling elevations were −2 m and −1.5 m (Han and Meng, 1996), so an average −1.75 m is used in this study. RTC was given (Li et al., 2015). "□" −1.75 m, msl (−1.75±1) m while error was ±1.5 m in Li et al. (2015).
2	An organic mud was formed in lagoon-swamp left by marine regression. This thin muddy layer, with fresh water mollusks including this dated *Arcomaia contorta* (?) and antler of *Elaphodus davidianus*, laid on the marine influenced sediments with oyster and razor clam shells (Zhao et al., 1989). Sampling depth and corresponding elevation were estimated on local topographic map (Zhao et al., 1989). "┬" −1m and (1.26±0.05) m (Table A3) should be subtracted for restoring msl, i.e., msl (−2.26±0.05) m. However, msl was (−2.5±0.5) m in Li et al. (2015) because MTL and MSL were confused at that time.
3	This thin twig was mixed into top part of marine sediments, buried by the upper peat layer, from which the sample CG1394 was obtained (Zhao et al., 1989). "┬" −1.3 m, (1.3±0.5) m should be subtracted (Table A3), i.e., msl (−2.6±0.5) m. However, 1.5 m was chosen in Li et al. (2015).
4	It was a shelly layer intercalated into intertidal muddy sediments (Han et al., 1980; Peng et al., 1980; Peng et al., 1984; Li and Zhao, 1990). The samples, taken from the lower to bottom part of the layer, indicate intertidal environemnt. However, the two ages are more than 1 100 cal a different and only sampling depths were given in the literature but without elevation. Correponding elevation has to be converted from topographic map. "□" 0 m, msl (0±1.5) m (Li et al., 2015).
5	This twig, 10 cm-long and 1.5 cm in diameter, was found mixed in the intertidal muddy sediments, immediately (only 1 cm) above the reef top. Foraminifera (abbreviated as "forams" below) analysis indicates that the muddy sample (10 g, dry), taken exactly from the same position with this twig, contains 14 different species and total 796 tests, mainly *Ammonia beccarii* vars., *Elphidium nakanokawaense* and *E. magellanicum* dominantly, indicating sea water influence in intertidal zone closing to estuary. Upwards, 10−20 cm above the reef-top, the mud consists of 18 species and about 1 600 tests, including *A. beccarii, E. nakanokawaense* and *A. takanabensis*. Both forams samples indicate the mid- to upper part of intertidal zone (Liu, 2010). Moreover, sedimentary facies analysis shows the mud sediments, overlying on the reef, remained intertidal environment for its lower 1.5 m thickness and further upward gradually changed to lagoon and salt marsh environment (Liu, 2010; Wang, 2012; Wang et al., 2011c). Elevation of the sampling position, −2.229 m, was given by Total Station measurement relative to the National Vertical Datum 1985 (Liu, 2010) (see the sea level indicator BA110343 for further details). So, "□" −2.23 m and directly indicates msl (−2.23±0.7) m. This reconstructed msl is same as Li et al. (2015) while the vertical error is changed from ±1.5 m to ±0.7 m in this study. RTC is not necessary because it is a macro plant fossil.
6	This terrigenous, 50−60 cm thick, peaty layer is 0.5−1 m below the ground surface and the sample was taken from the top part of the layer (IOA, 1983; Peng et al., 1980). Elevation of ground surface, about +2 m, is estimated from local topographic map by this study. The sampling position indicating "┬" about +1.25 m; two samples give a time range of 1988−956 cal a BP. After RTC it becomes about 1.33−0.85 cal ka BP. Contemporaneous msl was (−0.01±0.05) m, i.e., subtracting (−1.26±0.05) m (Table A3). However, (1.8±0.5) m was subtracted in Li et al. (2015).
7	The sampling layer shows a sudden increase of forams tests from less than a few hundred 60 cm below to about 3 630 at this position, where *Pseudononinella variabilis* and *Ammonia beccarii* vars. dominated, of which about 2 000 tests were picked out for AMS dating. On the other hand, 30 cm above, forams tests decreased to several tens only (Li et al., 2004; Wang et al., 2010). So, it indicates a flooding intrusion event of high sea water. "┬" +1.02 m, msl (−0.28±0.5) m, i.e., 1.3 m (an indicative meaning for sample deposited at MHHW in paleo bayhead, Table A3) is subtracted from +1.02 m. However, it was regarded as an equivalent of the upper peat, so 1.8 m was subtracted for msl reconstruction in Li et al. (2015).
8	The shells still kept their vertical growth position and were articulated (Li et al., 2004; Wang et al., 2010), and indicating intertidal muddy environment with freshwater input (Zhang, 2008; Okutani, 2000). RTC is not necessary for these in situ shells. "□" −0.45 m, msl (−0.45±0.5) m (Li et al., 2015).
9	Based on sedimentary facies analysis, forams study (Li et al., 2004) and the ecological description for this species (Zhang, 2008; Okutani, 2000), it was in the middle to lower intertidal and the upper subtidal zones. Five forams samples, from 2.8−4.8 m in depth, show 23 species and about 450 tests in average for each sample and maximum 30 species and 4 800 tests, mainly *Quinqueloculina akneriana rotunda, Elphidium magellanicum, E. nakanokawaense, Ammonia beccarii* vars. (Li et al., 2004). Ostrocoda of 2.5−4.5 m were mainly composed of *Sinocytherdea impreaa, Tanella opima, Spinileberis sinensis, Eucyther serrata, Laxoconcha binhaiensis* and totally 46 species with about 1 800 valves in average for each sample, indicating mid- to lower part of intertidal zone) (Lin et al., 2004). "⊥" −2.3 m, msl (−0.7±0.5) m, i.e., adding (1.6±0.5) m (Table A3). RTC is not necessary for the *in situ* articulated shells. In Li et al. (2015), msl was (−0.8±0.5) m because 1.5 m was simply added.
10	Only rarely marine influenced Ostracoda *Neomonoceratina dongtaiensis* and *Sinocytheridea impressa* were found in the middle to upper part of this basal peat layer (Lin et al., 2004) but

continued from Table A4.1

No.	Notes
13	Facies analysis indicates that the sedimentary environment of U5, from which this sample was taken, had changed from open intertidal to lagoon-salt marsh, caused by continuously increased accumulations of fluvial sediments (Chen et al., 2014). Forams show both *Ammonia beccarii* vars. and *Elphidium magellanicum* decreased but *E. hugesi foraminosum, E. kiangsuensis, Pseudononionella variabilis* and *Cribrononion porisuturalis* increased. Ostracoda assemblage shows *Albileberis sheyangensis, Bicornucythere bisanensis, Neomonoceratina dongtaiensis, N. triangulata* and *Trachyleberis niitsumai* disappered but *Sinocytheridea impressa* and *Loxoconcha binhaiensis* increased. All these indicate the sampling position was in the upper part of intertidal depth in lagoon-salt marsh environment (Chen et al., 2016).“┬” +1.03 m. msl (−0.12±0.5) m, i.e., (1.15±0.5) m should be subtracted because it is located in the northeast periphery (Table A3). However, it was mistakenly regarded as an equivalent of the upper peat, so 1.8 m was subtracted for msl reconstruction in Li et al. (2015).
14	This is a 10 cm-thick shell hash layer in marine facies U4, also with single valves of *Chlamus forreri* and other marine shells. Forams show *A. beccarii* vars. was domimant, while *E. magellanicum* decreased but *Protelphid turberculatum* and *Quinqueloculina akneriana* increased (Chen et al., 2014, 2016), indicating the lower limit of MLLW. “┴” −7.22 m. msl (−5.72±0.5) m, i.e., (1.5±0.5) m should be added because it is in the northeast periphery (Table A3). RTC was given. Although (1.5±0.5) m was also added in Li et al. (2015), it was considered as a half of MHHW−MLLW as a general value for the whole coast of the west Bohai Bay. However, there was lack of awareness of difference between MTL and MSL, and tidal regime difference beween bayhead and pheriphery at that time in Li et al. (2015).
15	The charcoal grains, >180 μm, picked out from a shelly layer, consisting of *C. pestigris, P. laevis* and *Dosinia* sp., intercalated into U3. It was formed in intertidal zone (Chen et al., 2014, 2016). RTC is not needed because of large charcoal grains. “□” −15.65 m, msl (−15.65±0.5) m while was (−15.65±1.5) m (Li et al., 2015).
16	Although terrigenous *Bithynia* sp. and *Gyraulus* sp. shells were found about 30 cm below this layer, broken *Crasostrea* shell and other marine shell fragments appeared 60 cm above it (Liu, 2007). So, it can be roughly recognized at MHHW level, i.e., “┬” −14.67 m, msl (−15.93±0.05) m (subtracting (1.26±0.05) m, Table A3), though msl was (−16.4±0.5) m in Li et al. (2015), i.e., subtracting (1.8±0.5) m when the sampling elevation was roughly determined as −14.6 m. RTC was given (Li et al., 2015).
17	Although it was immediately under the marine sediments the ground elevation +4 m (IOA, 1983) is doubtful, i.e., without definite indication of which elevation system was used. This study guesses it should be the 1950 Dagu System (the local system). So, 1.543 m is subtracted from the original +4 m. Thus, “┬” −14.53 m, msl (−15.79±0.05) m, i.e., subtracting (1.26±0.05) m (Table A3) though (1.8±0.5) m was subtracted in Li et al. (2015). RTC is not needed because the sample was described as plant peat (IOA, 1983) though it was given in Li et al. (2015).
18	Scattered fragments of marine diatom *Coscinodiscus* spp. were found in this peat layer, i.e., upper part of the diatom Assemblage Zone 1. This basal peat layer was eroded at 11.2 m by overlying marine mixed deposits of black-brown shell hash of *Chlamus farreri* (?), *Crassostrea* sp. and *Anomia chinesis*, with silty sand, consisting of diatom Zone 2, including *Cyclotella striata/stylorum, Coscinodiscus perforates, C. subconcavus, Actinoptychus undulates, C. argus, C. radiates, Thalassionema nitzschioides* and *Grammatophora oceanica* (Shang, 2011). Sedimentary facies analysis and diatom assemblages indicate this basal peat had been slightly influenced by sea water as salt marsh environment and then eroded by shallow sea deposits⑨ (Shang, 2011). So, “┬” −15.95 m. msl (−17.21±0.05) m, i.e., (1.26±0.05) m should be subtracted because at bayhead (Table A3). RTC was given (Li et al., 2015). However, (1.8±0.5) m was subtracted in Li et al. (2015).
19	This 2 cm-thick bulk sample, then subdivided into two subsamples, was taken from a dark muddy peaty layer in depth of 17.4−17.6 m. This layer consists of *Gyraulus* sp., *Cincinnatia alticonula, Stenothyra glabra* and *Assiminea lutea,* and seeds, semi-carbonized plant debris, and fresh water Ostracoda *Cypris decaryi*, *Candonirlla albicans*, *Ilyocypris radiate* and *I. subbiplicata* but without forams, indicating this is fresh water peat (unpublished data of the authors’ group). However, Assiminea sp. appeared in overlying mud at 15.05−17.4 m, indicating the beginning of sea water influence. This subsample of charcoals and twigs is about 1 330 cal a younger than another subsample: 11 167 cal a BP/BA081877, shells of *Gyraulus* sp. and *Bithynia* sp. (Li et al., 2015). On the other hand, this peaty layer was gradually formed from the underlying hard mud, i.e., the late Pleistocene soil horizon formed in LGM (Last Glacial Maximum). This *in situ* characteristic and being much younger than another subsample mean that RTC is not necessary. “┬” −21.32 m and (1.26±0.05) m should be subtracted (Table A3). So, msl (−22.58±0.05) m. However, (1.8±0.5) m was subtracted in Li et al. (2015).
20	Although marine sediments existed immediately above this basal peat layer, elevation of the borehole is approximately estimated only (Li and Zhao, 1990; Wang and Tian, 1999). So, “┬” −15.6 m, msl (−16.86±0.05) m (Table A3). However, it was (−17.4±0.5) m in Li et al. (2015) because (1.8±0.5) m was subtracted. RTC was given (Li et al., 2015).

continued from Table A4.1

No.	Notes
25	It is also a beach face layer and about 130 cal a younger than another subsample of single valve of *Mactra chinensis*: 2 397 cal a BP/Beta363625 (Li et al., 2015; Shang et al., 2015; 2016). The sampling position is about 75 cm below the average top elevation of −2.16 m. So, "□" −2.91 m, msl (−2.91±1) m. RTC is not necessary. The reconstructed msl is more accuracy than (−3±1.5) m in Li et al. (2015).
26	It is a totally 30 cm-thick, horizontally alternative deposits between shelly hash laminae and muddy laminae with very fine, carbonized herbaceous twigs. It was formed in between the Shell Bed A and the overlying salt marsh-lagoonal mud (Shang et al., 2016), indicating a remained influence of sea water. It might indicate high waters rather than the intertidal as Li et al. (2015) used. The sampling position is 30 cm below the average top elevation of −2.16 m. So, "┬" −2.46 m and msl should be (−3.76±0.5) m, i.e., (1.3±0.5) m is subtracted (Tables A2 and A3). However, it was believed as intertidal environment and reconstruceted msl was (−2.46±1.5) m in Li et al. (2015). RTC is not necessary because it is macro plant though RTC calibration was given in Li et al. (2015).
27	This is a beach face in intertidal depth, Shell Bed A, and about 1 260−0 cal a younger than another two subsamples of single valves of *Moerella* sp.: 2 695 cal a BP/Beta352329, and *Potamocorbula laevis*: 1 436 cal a BP/Beta352330 (Li et al., 2015; Shang et al., 2015, 2016). The sampling position is 70 cm below the average top elevation of −2.16 m. Thus, "□" −2.86 m, msl (−2.86±1) m though msl was (−2.86±1.5) m in Li et al. (2015). RTC is not necessary (Li et al., 2015).
28	This *in situ* razor clam is still in vertical position and articulated. The species is in lower, or middle to lower, intertidal environment based on conchologists such as Okutani (2000) and Zhang (2008). However, sedimentalogically, this individual probably survived in a small depression with poured high waters in the Shell Bed A, top layer of the Holocene marine sediments (Shang et al., 2016), therefore, it may roughly indicate high position of the intertidal environment rather than its normally growing environment. It was 210−70 cal a younger than another two subsamples of the same layer as *Umbonium* sp.: 1 830 cal a BP/Beta352327, and single valve of *Scapharca kagoshimensis*: 1 689 cal a BP/Beta352326 (Li et al., 2015). The sampling position is about 30 cm below the average top elevation of −2.16 m (Li et al., 2015; Shang et al., 2015, 2016). So, "┬" −2.46 m and msl (−3.76±0.5) m (i.e., subtracting (1.3±0.5) m, Table A3), while msl was (−2.46±1.5) m in Li et al. (2015) because the conchlogists' idea was simply followed. RTC is not necessary (Li et al., 2015).
29	This shell bed, as a cover of the Holocene marine sediments, was formed in intertidal zone and it is about 390 cal a younger than another subsample of single valve *Potamocorbula laevis*: 2019 cal a BP/Beta335908 (Shang et al., 2015, 2016). So, "□" −2.4 m, msl (−2.4±1) m (Table A3), though it was (−2.4±1.5) m (Li et al., 2015). RTC is not necessary.
30	It was in the intertidal flat during the Holocene marine regression period and is about 470 cal a younger than another subsample of single valve of *Corbicula*: 2 812 cal a BP/Beta335909 and RTC is not necessary. Elevation of the outcrop was Total Station and RTK measured relative to the National Vertical Datum 1985. "□" −2.7 m, msl (−2.7±1) m while it was (−2.7±1.5) m (Li et al., 2015).
31	It was a 10 cm-thick, coarse shelly layer, having high-angle foreset bedding, in the top part of Shell Bed A, Section 2, and is about 650−290 cal a younger than another two subsamples of single valve of *Scapharca kagoshimensis* (1 830 cal a BP/Beta335913) and shell hash (2 198 cal a BP/Beta335914) (Shang et al., 2016; Li et al., 2015). In this pit (about 200 m×120 m, cf., Shang et al., 2016), top elevations of the Holocene marine sediments and the ground surface were Total Station measured and then connected with the National Vertical Datum 1985 by RTK, showing the average elevation (−2.16±0.2) m (simply as −2.2 m) for top of the Holocene marine sediments (12-spot average, but only six sites were shown in Shang et al. (2016) and +1.93 m of the local ground surface elevation, unpublished data of the authors' group). In this paper, elevations of sea level indicators in this pit were then calculated as a vertical distance from the average top elevation (−2.16±0.2) m (or (−2.2±0.2) m). As to this sample, it was probably formed by MHHW. "┬" −2.2 m. So, (1.3±0.5) m should be subtracted and msl (−3.5±0.5) m. RTC is not necessary compared with another two subsamples (Li et al., 2015). However, msl was (−2.2±1.5) m because it was approximately regarded as intertidal depth and without further compensation for msl reconstruction in Li et al. (2015).
32	It was formed in intertidal environment (Li et al., 2015; Shang et al., 2016). Sampling position is about 80 cm lower than the average top elevation of −2.16 m in this site. "□" about −3.0 m, msl (−3.0±0.5) m. RTC was given (Li et al., 2015). The indicative meaning was same while error was ±1.5 m in Li et al. (2015).
33	These three articulated shells, as three subsamples, taken from the same thin shelly layer in the shell beach, Shell Bed C, show the exactly same or highly overlapping ages of their 2σ range, and are about 1 130 cal a younger than the fourth subsample of single valve of *Dosinia corrugate*: 3 450 cal a BP/Beta352324 (Li et al., 2015; Shang et al., 2015, 2016). The sampling position is about 1.5 m below the average top elevation of −2.16 m (Li et al., 2015). This layer is considered as shelly beach in intertidal environment. So, "□" −3.7 m, msl (−3.7±1) m. Such three subsamples give the same ages and are 1 150 cal a younger than the fourth one, RTC is therefore not necessary (Li et al., 2015). In Li et al. (2015), vertical error

continued from Table A4.1

No.	Notes
38	Definitely marine influenced shelly hash layer with *Scapharca kagoshimensis* was found only 0.8 m above this peaty layer. This basal peat was formed in coastal salt marsh based on seismic investigations and sedimentary analysis (Tian et al., 2017). So, it was just above high waters. "┬" −17.2 m, msl (−18.46±0.05) m (Table A3). RTC was given (Li et al., 2015).
39	11.3−11.45 m: marine shell layer, with >10 cm fragmentary shells of *Crassostrea* sp., eroded the underlying sediments. 11.45−12.6 m: mud, without definite marine-influenced evidence. So, this sample, taken from the peaty layer of 12.6−12.7 m, approximately shows that corresponding msl must be lower. It is about 630 cal a younger than another subsample (portion <180 μm): 8 899 cal a BP/Beta355822, so RTC is not necessary (Li et al., 2015). "┬" −10.97 m, and (1.26±0.05) m was subtracted (Table A3), so msl (−12.23±0.05) m. Howwver, (1.8±0.5) m was subtracted in Li et al. (2015).
40	This basal peat layer was immediately overlaid by Holocene marine sediments with suddenly increasing of forams and marine ostracoda, 100−200 individuals, respectively, per sample (Wang et al., 1986). However, the borehole elevation could be only approximately estimated as +4 m relative to the local datum and so 1.543 m is therefore subtracted by this study to convert to the National Vertical Datum 1985 system. So, "┬" −15.49 m, and (1.26±0.05) m should be subtracted (Table A3), i.e., msl (−16.75±0.05) m. RTC was given (Li et al., 2015). However, the ground elevation was estimated as +2 m of the local datum and 1.8 m was subtracted by Li et al. (2015) and thus, reconstructed msl was even about 2.5 m lower than this study.
41	It was taken from the lower part of the same basal peat layer with the sample ZK1465 (Wang et al., 1986). This sample was even less marine-influenced than the overlying one (ZK1465), So, "┬" −16.19 m, msl (−17.45±0.05) m, i.e., subtracting (1.26±0.05) m (Table A3). However, msl was (−19.96±0.5) m in Li et al. (2015), see the notice of indicator ZK1465. RTC was given (Li et al., 2015).
42	It was taken from the lower part of Bed 2. This bed, yellowish brown (10YR 4/3) silt, is composed of *Potamocorbula laevis, Scapharca subcrenata, Arcopsis* sp., *Sinonovacula aonstricta* and *Nassarius* sp., with brackish water species such as *Corbicula fluminea, Parafossarulus exiguous, Assiminea latericea*. Forams increased to >5 000 tests while marine ostracoda reached to >1 760 valves per sample. This was a fluctuation of sea level rise named as Ib④, formed in estuary in intertidal depth to subtidal depth (Yan et al., 2006a, b). So, it may indicate "┴" −14.81 m, msl −13.21 m, i.e., adding (1.6±0.5) m (Table A3). RTC was given (Li et al., 2015). However, (1.5±0.5) m, a half of mean high tidal range, was simply added in Li et al. (2015).
43	It was deposited on the top part of Holocene marine sediments, with abundant shell hash mixed in mud, indicating intertidal environment following marine regression process (unpublished data of the authors; Sun et al., 2011). "□" −3.85 m, msl (−3.85±1) m (Table A3). RTC was given (Li et al., 2015).
44	This and the following data all have a few forams, including *Elphidium nakanokawaense* and *Ammonia beccarii*, which suggest a coming of sea water (unpublished data of the authors' group). So, "┬" −12.25 m, msl (−13.51±0.05) m, i.e., (1.26±0.05) m should be subtracted (Table A3). RTC was given (Li et al., 2015). However, (1.8±0.5) m was subtracted in Li et al. (2015).
45	This is same as the overlying BA091542 (unpublished data of the authors' group). "┬" −12.35 m, msl (−13.61±0.05) m, i.e., (1.26±0.05) m should be subtracted (Table A3). However, 1.8 m was subtracted in Li et al. (2015). RTC was given (Li et al., 2015).
46	Many shelly hash and scattered articulated *Mactra chinensis* (?) were also found in this peaty layer and the layer was considered as the upper peat layer, i.e., "┬" +2.16 m. So, msl (+0.9±0.05) m (Table A3). RTC was given (Li et al., 2015). However, (1.8±0.5) m was subtracted in Li et al. (2015).
47	Forams at the sampling position of 16.3 m show less than 50 tests but rapidly booming upward to >500 tests at 16 m. It indicates an ongoing rising-fluctuation of sea level. Unfortunately, there is only a test-counting but without species identification. So, it is better to think it was in intertidal zone, i.e., "□" −12.84 m, msl (−12.84±1) m. RTC was given (Li et al., 2015). The sampling position was considered at low tidal environment and 1.5 m, as a half range between MHHW and MLLW, was added to restore msl as (−11.34±0.5) m in Li et al. (2015). However, difference between MTL and MSL was not realized three years ago.
48	As an intercalated thin peaty layer, it was found in the lower part of Holocene marine muddy sediments. Based on facies analysis, this layer was in salt marsh in intertidal depth with forams tests nearly 350 a sample. Although it was perhaps reworked peaty-concentrated layer, this subsample (>180 μm) is about 420 cal a younger than another one (i.e., the portion <180 μm): 9 287 cal a BP/Beta358055 (Li et al., 2015). Therefore, RTC seems to be not necessary. "□" −13.76 m, msl (−13.76±1) m (Table A3), though the error was ±1.5 m in Li et al. (2015).
49	It immediately overlay on the early Holocene terrigenous, yellowish brown mud, with a small amount of forams (<50 tests), indicating onset of marine transgression. "┬" −15.39 m, msl

continued from Table A4.1

No.	Notes
53	It is a faint, darkish layer belonging to the start of Forams Zone V-1. A very small amount of forams of *Nonion glabrum* (12 tests) and *Ammonia beccarii* (1 test) was found in a 20 g dry sample taken from this layer, showing brackish environment (Wang et al., 2015). This subsample was about 360 cal a younger than another subsample (portion <180 μm): 7 005 cal a BP/Beta331456 (Li et al., 2015). "┬" −3.04 m, msl (−4.34±0.5) m (subtracting (1.3±0.5) m, Table A3). It was classified to the "upper peat layer" in Li et al. (2015), or more precisely, a layer transformed from the immediately underlying hydromorphic gley horizon in salt marsh-lagoon environment behind shoreline and was occasionally inundated by high water.
54	A faint darkish layer in the bottom of Zone IV, 8.7−7.8 m. Two samples were without forams and only one sample had 13 tests, and colour become yellowish with weakly mottling structure, all indicating increased terrestrial influence, i.e., sea level drops for a short time. So, this sample was in the upper part of intertidal zone in between MHHW and MHW and can be treated as an intercalated organic-rich layer. It was about 210 cal a younger than another subsample (portion <180 μm): 7 088 cal a BP/Beta331457 (Li et al., 2015). So, "┬" −3.54 m and (1.26±0.05) m (Table A3) should be subtracted, i.e., msl (−4.8±0.05) m. However, 1.8 m was subtracted in Li et al. (2015).
55	Zone III, 9.2−8.7 m in depth and 2 forams samples show 68 and 338 tests, respectively, and *Nonion glabrum* dominated (Wang et al., 2015;). About 1 050 cal a younger than another subsample (portion <180 μm): 8 162 cal a BP/Beta331458 (Li et al., 2015). Downwards, core logging and forams study of Zone II, 10.6−9.2 m, having 7 forams samples with tests in between 0−18, showing a saltmarsh occasionally influenced by high water. So this sample can also be roughly treated as an intercalated organic-rich layer. "┬" −4.0 m, msl (−5.26±0.05) m, though (1.8±0.5) m was subtracted in Li et al. (2015).
56	Although freshwater diatoms were still dominant such as *Eunotia* spp. and *Synedra unla*, more marine and brackish species, including planktonic *Cosinodiscus* spp. and *Actinocyclus* spp., were found. The freshwater diatoms also changed from benthic (e.g., *Eunotia* spp. and *S. unla*) to planktonic taxa (e.g., *Melosira* spp.). On the other hand, forams in this sample downward to the basal peat at about 13.1 m, 8 010 cal a BP (Beta329646) were very rare for 4 forams samples (0−3 tests per sample). However, forams sadenly boomed from above 11.2 m upward (Wang et al., 2015). Therefore, this sample itself can be reconnized as being highwater influenced and indicating an arrival of sea water to the area. This subsample is about 160 cal a younger than another subsample (portion <180 μm): 8 016 cal a BP/Beta331455 (Li et al., 2015). So, "┬" −6.23 m, msl (−7.53±0.5) m (i.e., subtracting (1.3±0.5) m, Table A3) and RTC was given (Li et al., 2015). However, 1.8 m was subtracted in Li et al. (2015).
57	It was a peaty layer, with fragments of *Gyraulus* sp. and small $CaCO_3$ concretions, formed in lagoon-salt marsh environment and may indicate a maximum height of MHHW (unpublished data of the authors' group). RTC is not necessary because only the plant debris was used for dating. "┬" +1.47 m, and (1.26±0.05) m (Table A3) should be subtracted because it shows influence by MHHW. So, msl (+0.21±0.05) m. However, (1.8±0.5) m was subtracted in Li et al. (2015).
58	A dark organic layer, 4.9−5.1 m, was formed in salt marsh-lagoonal muddy environment and this sample was taken from the very top of the layer. Forams in this layer have >500 tests a 20 g dry sample and then sharply decreased upward to less than 50 in the overlying sediments, implying an end of seawater fluctuation upwards. So, this layer was probably influenced by MHHW. "┬" −0.53 m, subtracting (1.3±0.5) m to restore msl, i.e., msl (−1.83±0.5) m. RTC is not needed (Li et al., 2015). However, 1.8 m was subtracted in Li et al. (2015).
59	6−7.9 m: mud, dull yellow orange (10YR 7/2), clearly mottling structure with scattered Fe/Mn nodules of mm scale. This is different with both underlying and overlying brownish gray mud (10YR 5/1) and indicating more oxidized environment. Conchologically, this razor clam usually lives in mid- and lower intertidal zone with fresh water input, according to Zhang (2008) and Okutani (2000). The ^{13}C value, −9.5‰PDB, of this clam shell supports freshwater poured in. On the other hand, forams had suddenly booming from about 7.4 m, i.e., 12 cm below the clam position, upward, indicating this articulated razor shell was also seawater influenced. So, most probably, this razor clam lived in lagoon-salt marsh within intertidal depth where both high tidal waters and freshwater can pour into. So, "□" −2.9 m, msl (−2.9±1) m. However, it was considered to be survived by high waters and 1.8 m was subtracted for msl reconstruction in Li et al. (2015). Indeed, survived by high waters was true but it was in intertidal depth.
60	A 1 cm-thick gleysol horizon, light grey, 10YR 7/1, was in muddy sediment. Forams started to bloom from this position upward till 6.7 m in depth, within which five forams samples all show >500 tests, indicating seawater came from this horizon. 820 cal a younger than another subsample (part <180 μm): 7 572 cal a BP/Beta355244 (Li et al., 2015). So, this horizon can be considered as a sudden but endurable filling of high sea waters into lagoon-salt marsh (see explanation of Beta 353808). "□" −3.01 m, msl (−3.01±1) m. However, this age is about 630 a younger than the overlying razor clam (Beta353808). A doubt remains with this reversal time sequence. It is a new indicator in this study.
61	Forams analysis indicates a sudden high sea water fluctuation with >500 tests a sample at about 8.8 m, i.e., only a decimeter lower than this sampling position. It means this sample was high tide influenced. It is 955 cal a younger than another subsample (<180 μm): 8 305 cal a BP/Beta355245 (Li et al., 2015). "┬" −4.26 m, as being an equivalent of basal peat, so

continued from Table A4.1

No.	Notes
64	The diatom assemblage at 9.0−8.39 m shows from more benthic to more planktonic species upwards, indicating marine inundation had started (Wang et al., 2015). However, abundance of foraminifera had decreased from >500 tests in about 9.2 m to disappeared in this sampling depth of 8.98 m, then reoccurred at about 8.6 m (i.e., about 40 cm above this sample). So, it can be roughly considered as only influenced by high waters. "┬" about 5.41 m, and (1.3±0.5) m should be subtracted because is was an intercalated organic layer indicating high waters (Table A3). So, msl (−6.71±0.5) m. This is about 460 cal a younger than another subsample (<180 μm): 7952 cal a BP/Beta332794 (Li et al., 2015), so RTC is not needed. This is a new indicator in this study.
65	It is composed of euryhaline forams, brackish ostracoda and molluscan shells (Peng et al., 1984) and so it was influenced by high sea waters. The borehole elevation of +2.8 m (Peng et al., 1984) was classified to the National Vertical Datum 1985 in Li et al. (2015). Nevertheless, in this study, it is reconsidered as the local datum only and 1.543 m has to be subtracted. So, "┬" −13.56 m, msl (−14.82±0.05) m, i.e., subtracting (1.26±0.05) m (Table A3). RTC was given (Li et al., 2015).
66	This is about 10 560 cal a younger than another subsample of bulk organic mud (gley horizon): 13 477 cal a BP/KIK12257 (Wang et al., 2004; Li et al., 2015), from which the *in situ* gastropoda shells were picked out and dated (Wang et al., 2003). "┬" +1.23 m, msl (+0.13±0.03) m, i.e., subtracting (1.1±0.03) m because it was located in the ancient southwest periphery as an upper peat layer (Fig. A1 and Table A3). However, 1.8 m was subtracted in Li et al. (2015). RTC correction is not necessary (Li et al., 2015).
67	This basal peat was eroded by marine muddy sediments, in which *Potamocorbula* sp., *Scapharca subcrenata, Mactra veneriformis, Assiminea* sp., *Nassarius* sp., *Corbicula* sp. and *Ammonia beccarii, Elphidium advenum* and *Quinqueloculina seminula* were found (Li et al., 2006). "┬" −12.48 m, msl (−13.58±0.03) m, i.e., (1.1±0.03) m was subtracted as it was basal peat in the ancient southwest periphery (Fig. A1 and Table A3). RTC seems to be not necessary because it was *in situ* and mainly charcoals though it was given in Li et al. (2015).

Note: The measured ^{14}C dates, signified in italics in Column 4, were changed from their original dates with the Libby half life of 5 730 a by subdiving 1.029 in this study. The ^{13}C values, signified in italics in Column 5, were either recommended by Mook and van de Plassche (1986) or used with the local empirical mean value of −2.68‰ PDB (Wang, 1994; Wang and van Strydonck, 1997; Li et al., 2015) for the marine shells. Correspondingly, such calibrated approximate conventional ages in Column 6 were given in italics.

Table A4.2. Holocene relative mean sea level (rmsl) indicators, derived from the shelly cheniers, in the west coast of Bohai Bay

	Basic information			Teomporal distribution								Spatial distribution		
No.	Locality, stratigraphy and environment, material dated, sample-depth / ground surface elevation / (averaged) sample elevation	Coordinate	Lab code	Measured ^{14}C date	$\delta^{13}C$ /‰PDB	Conventional ^{14}C age/a BP	Calibrated ^{14}C age: median probability/2σ range/cal a BP	Status of material dated	Sub-sample	RTC /cal a	Age of rmsl: single value/ range/cal ka BP	Elevation of the observed rmsl/m	Corrections of tectonics /self-compaction/ water withdrawal/ m	Elevation of rmsl after corrections for the three local factors/m
68	Qingtuozi, shelly chenier, Section 1, *Umbonium* sp., 2.90/-/about−0.20 m	39.1°N, 117.8°E	Beta 305314	1 940±30	−3.6	2 290±30	2 123/ 2 292−1 972	reworked	no	−600	*1.523/ 1.69−1.37*	−1.4±0.5	+0.15/ +1.13/ +1.57	+1.45±0.5
69	*idem,* shelly chenier, Section 4, single valves of *Potamocorbula laevis,* about 2/-/about +0.22 m		Beta 305312	2 180±30	−0.2	2 590±30	2 505/ 2 677−2 341	reworked	no	−600	*1.905/ 2.07−1.74*	−0.98±0.5	+0.19/ +0.78/ +1.57	+1.56±0.5
70	Xinlicun, chenier, single valves of undetermined shells, about 1.5/-/about +1 m	39.1°N, 117.4°E	GC 172(2)	*3 040±120*	*−2.68*	*3 399±127*	3 476/ 3 827−3 138	reworked	yes	−600	*2.876/ 3.23−2.54*	−0.2±0.5	+0.29/ +0.58/ +0.25	+0.92±0.5
71	Jugezhuang, shelly chenier, Eijkelkamp core Site JN341-2, very bottom of chenier, single valves of *Mactra veneriformis,* about 4/-/−0.4 m	39.0°N, 117.3°E	BA 101095	−	−	3 350±25	3 417/ 3 285−3 270, 3 560−3 290	reworked	yes	−	*3.417/ 3.560−3.270*	−1.0±0.5	+0.34/ +1.56/ +1.75	+2.65±0.5
72	*idem,* Site JN341-2, very top of the underlying mud, single valves of *M. veneriformis* and *Scapharca*		BA 101097	−	−	3 500±25	3 590/ 3 753−3 438	reworked	yes	−	3.590/ 3.753−3.438	−1.2±0.5	+0.36/ +1.56/ +1.75	+2.47±0.5

continued from Table A4.2

	Basic information			Teomporal distribution								Spatial distribution		
No.	Locality, stratigraphy and environment, material dated, sample-depth / ground surface elevation / (averaged) sample elevation	Coordinate	Lab code	Measured ^{14}C date	$\delta^{13}C$ /‰PDB	Conventional ^{14}C age/a BP	Calibrated ^{14}C age: median probability/2σ range/cal a BP	Status of material dated	Sub-sample	RTC /cal a	Age of rmsl: single value/ range/cal ka BP	Elevation of the observed rmsl/m	Corrections of tectonics /self-compaction/ water withdrawal/ m	Elevation of rmsl after corrections for the three local factors/m
75	Apple Garden, Shanggulin, shelly chenier, top of the underlying mud, single valves of *Scapharca kagoshimensis* and *Mactra veneriformis,* about 4/-/about −1.5 m	38.8°N, 117.5°E	UtC7038	−	−1.70	1 850±35	1 597/ 1 760−1 430	reworked	yes	−	*1.597/ 1.760−1.430*	−1.5±0.5	+0.10/ +1.56/ +1.56	+1.72±0.5
76	*idem.* chenier, above the front-base, *Umbonium* sp. and Terebridae, -/-/about −1 m		UtC2240	−	0.0	2 350±100	2 190/ 2 478−1 894	reworked	yes	−	*2.19/ 2.478−1.894*	−1±0.5	+0.22/ +1.56/ +1.56	+2.34±0.5
77	Papadi, Shanggulin, shelly chenier, middle part, articulated *Mactra veneriformis,* 1.2 m/about +2 m/+0.8 m	38.8°N, 117.5°E	UtC7037	−	−4.03	2 125±40	1 919/ 2 096−1 701	reworked	no	−	1.919/ 2.096−1.701	−0.5±0.5	+0.19/ +0.47/ +1.56	+1.72±0.5
78	*idem.* shelly chenier, bottom, just above its subsurface at its seaward side, *Umbonium* sp., 2 m/about +2 m/0 m		98Y075	*2 410±140*	*−2.68*	*2 769±146*	*2 705/ 3 080−2 319*	*in situ*	no	−	*2.28/ 2.66−1.90*	0±0.5	+0.23/ +0.78/ +1.56	+2.57±0.5
79	Gongnongcun, Shanggulin, shelly	38.8°N, 117.5°E	03Y79	−	−	*850±80*	605/ 767−468	*in situ*	no	−	0.605/ 0.767−0.468	−0.5±0.5	+0.06/ +1.56/	+2.68±0.5

continued from Table A4.2

Basic information			Teomporal distribution							Spatial distribution		
No.	Locality, stratigraphy and environment, material dated, sample-depth / ground surface elevation / (averaged) sample elevation	Coordinate	Lab code	Measured ^{14}C date	$\delta^{13}C$ /‰PDB	Conventional ^{14}C age/a BP	Calibrated ^{14}C age: median probability/2σ range/cal a BP	Status of material dated	Sub-sample	RTC /cal a	Age of rmsl: single value/ range/cal ka BP	Elevation of the observed rmsl/m	Corrections of tectonics /self-compaction/ water withdrawal/ m	Elevation of rmsl after corrections for the three local factors/m
81	*idem,* shelly chenier, about 0.5 m above the rear-base of subsurface, single valves of undetermined shells, -/-/about +1 m		CG73	*2 020±100*	*−2.68*	*2 379±108*	2 225/ 2 573−1 917	reworked	no	−600	*1.625/ 1.97−1.31*	+0.2±0.5	+0.16/ +0.78/ +0.17	+1.31±0.5
82	Zhaizhuang, shelly chenier, top of the underlying mud, articulated *Sinonovacula constricta*, 4−5 m/-/about −3 m	38.6°N, 117.2°E	CG328	*5 130±85*	*−2.68*	*5 489±94*	6 070/ 6 295−5 845	*in situ*	no	−	6.070/ 6.295−5.845	−3±0.5	+0.61/ +1.75/ +0.09	−0.55±0.5
83	Zhangjuhe, shelly chenier, bottom, shells, 1.8/-/about +0.6 m	38.6°N, 117.6°E	YS265	*2 495±65*	*−2.68*	*2 854±76*	2 819/ 3 064−2 609	reworked	no	−600	*2.219/ 2.46−2.01*	−0.7±0.5	+0.22/ +0.70/ +0.15	+0.37±0.5
84	Houtangpu, shelly chenier, Eijkelkamp core, chenier foot above its front-base, *Umbonium* sp. and Terebridae, −2/-/about −0.5 m	38.5°N, 117.6°E	UtC2237	−	+0.7	820±90	586/ 762−426	reworked	no	−100	0.486/ 0.66−0.32	−0.5±0.5	+0.05/ +0.78/ +0.15	+0.48±0.5
85	Zhaojiapu, a thin shelly layer remained in the present-day muddy intertidal flat,	38.5°N, 117.6°E	SH200	*1 030±60*	*−2.68*	*1 389±72*	1 121/ 1 281−937	reworked	no	−100	1.021/ 1.18−0.83	+0.48±0.5	+0.10/ 0/ +0.10	+0.68±0.5

continued from Table A4.2

Basic information				Teomporal distribution								Spatial distribution		
No.	Locality, stratigraphy and environment, material dated, sample-depth / ground surface elevation / (averaged) sample elevation	Coordinate	Lab code	Measured ^{14}C date	$\delta^{13}C$ /‰PDB	Conventional ^{14}C age/a BP	Calibrated ^{14}C age: median probability/2σ range/cal a BP	Status of material dated	Sub-sample	RTC /cal a	Age of rmsl: single value/ range/cal ka BP	Elevation of the observed rmsl/m	Corrections of tectonics /self-compaction/ water withdrawal/ m	Elevation of rmsl after corrections for the three local factors/m
87	Jilingbo, shelly chenier, undetermined shells, 1.45/-/about +0.5 m	38.4°N, 117.7°E	SH247	*2 860±70*	*−2.68*	*3 219±81*	3 255/ 3 482−2 988	reworked	no	−600	*2.655/ 2.88−2.39*	−0.8±0.5	+0.26/ +0.56/ +0.21	+0.23±0.5
88	Wuditai, shelly chenier, undetermined shells, 1.1/-/about +1.1 m	38.4°N, 117.5°E	GC-?	*3 920±120*	*−2.68*	*4 279±127*	4 629/ 4 969−4 243	reworked	no	−600	*4.029/ 4.37−3.64*	−0.2±0.5	+0.40/ +0.43/ +0.10	+0.73±0.5
89	Yangjiapu, shelly chenier, undetermined shells, 1.05/-/about +1.1 m	38.4°N, 117.7°E	YS248	*2 205±70*	*−2.68*	*2 564±81*	2 477/ 2 724−2 253	reworked	no	−600	*1.877/ 2.12−1.65*	−0.2±0.5	+0.19/ +0.41/ +0.09	+0.49±0.5
90	Qianmiaozhuang, shelly chenier, middle-upper part, single valves of *Meretrix meretrix*, about 2.5/-/about +1.8 m	38.3°N, 117.4°E	CG 176(1)	*4 205±105*	*−2.68*	*4 564±112*	5 013/ 5 319−4 675	reworked	yes	−	*5.013/ 5.319−4.675*	+0.5±0.5	+0.50/ +0.97/ +0.05	+2.02±0.5
91	*idem.* shelly chenier, lower part, single valves of *Meretrix meretrix* and *Mactra veneriformis,* about 3.3/-/about +0.35 m		CG177	4 740±105	*−2.68*	*5 099±112*	*5 648/ 5 336−5 334, 5 370−5 349, 5 906−5 384*	reworked	no	−600	5.048/ 5.30−4.73	−0.85±0.5	+0.50/ +1.29/ 0.05	+0.99±0.5
92	Laolangtuozi, Pit 1, shelly chenier, top of the underlying mud, Terebridae and	38.3°N, 117.8°E	AA 45901	−	−1.6	1 687±52	1 416/ 1 566−1 272	reworked	no	−600	0.816/ 0.96−0.67	−0.6±0.5	+0.08/ +1.94/ +0.12	+1.54±0.5

Continued form Table A4.2

No.	Notes
	Explainations of the indicative meaning, RTC, the three spatial corrections and changes from the previous work (Li et al., 2015)
68	Redeposited on the middle part of subsurface of chenier (Su, 2012; Shang et al., 2013). Elevation of the sampling position was measured by Total Station connected with the National Vertical Datum 1985 benchmark (Su, 2012). "┬" −0.20 m, msl (−1.4±0.5) m, i.e., subtracting (1.2±0.5) m as it was above the mid-subsurface (Table A3). However, it was roughly treated as being formed in intertdal depth only and thus reconstructed msl is (−0.2±1.5) m in Li et al. (2015). RTC was given (Li et al., 2015).
69	Redeposited on the middle part of subsurface of chenier (Su, 2012; Shang et al., 2013). Elevation of the sampling position was measured by Total Station connected with the National vertical Datum 1985 benchmark (Su, 2012). "┬" +0.22 m, msl (−0.98±0.5) m, i.e., subtracting (1.2±0.5) m because it was above the mid-subsurface (Table A3). RTC was given (Li et al., 2015). However, it was simply judged to be just in intertidal depth in Li et al. (2015).
70	Detailed information is lacking except its approximate elevation It is treated to be taken from above the mid-subsurface, so (1.2±0.5) m should be subtracted, i.e., msl (−0.2±0.5) m (Table A3). However, it was simply considered at intertidal zone in Li et al. (2015). RTC was given (Li et al., 2015).
71	It was just above the chenier subsurface at its middle to seaward side. 720−310 cal a younger than another 3 subsamples: 3 731 cal a BP/BA101094, 3 766 cal a BP/BA101093 and 4 140 cal a BP/BA101112 (Su, 2012; Shang et al., 2016). Forams assemblages, for the lower part of chenier and the immediately underlying muddy sediments, indicate that the uppermost 1 m of the muddy sediments was dominantly composed of *Ammonia beccarii, A. confertitesta, A. granuloumbilica, Elphidium simplex, A. granuloumbilic*a and *Pseudononionella variabilis,* based on four forams samples. Upwards in the mud column to closing the chenier subsurface, the assemblage shows size of the reworked individuals increased, i.e., tests become bigger and much broken. These suggest the chenier subsurface was subject to erosion and close to MHW environment (Li et al., 2016b; Su, 2012). Elevation of the ground surface was Total Station measured and then connected to the National Vertical Datum 1985 (Su, 2012). "┬" −0.4 m, msl (−1.0±0.5) m, i.e., 0.6 m could be subtracted because the sampling position is just in between the forepart and the mid-subsurface (the former is without vertical compensation but 1.2 m should be subtracted for the latter, Table A3). However, 1.8 m was subtracted in Li et al. (2015) since the compensation value of 1.8 m for basal peat was misused.
72	The sampling position was in between the mid-subsurface and the forepart. 720−340 cal a younger than another 3 subsamples: 3 927 cal a BP/BA101096, 4 089 cal a BP/BA101113 and 4 313 cal a BP/BA101098 (Su, 2012; Shang et al., 2016). Forams assemblages (Li et al., 2016; Su, 2012) and indicative meaning can be referred to the indicator BA101095 aforementioned. "┬" −0.6 m, msl (−1.2±0.5) m (Table A3). However, 1.8 m was subtracted in Li et al. (2015) because the compensation value of 1.8 m for basal peat was misused.
73	This age is 510 cal a younger than another subsample of *Nassarius* sp.: 5 318 cal a BP/BA110864 (Shang et al., 2016; Li et al., 2015; Su, 2012) though *Crassostrea* shells are usually able to bear stronger or longer reworking processes. Total Station measurement, connecting with RTK leveling, was given for elevation of the sampling position, which is only about 10 cm above the mid-subsurface (Su, 2012). So, (1.2±0.5) m should be subtracted, i.e., msl (−0.81±0.5) m (Table A3). However, the sampling position was just simply determined as intertidal depth in Li et al. (2015).
74	It was just above the subsurface at chenier's seaward margin, indicating intertidal environment (Su, 2012; Li et al., 2015). "□" −0.14 m, msl (−0.14±0.5) m (Table A3) and RTC was given (Li et al., 2015). The vertical error was ±1.5 m in Li et al. (2015).
75	The sample, lying on the top of the underlying mud, is only 10 cm beneath the chenier subsurface at its fore-base (Wang et al., 2000c). This age is about 590−900 cal a younger than another two, 2 190 cal a BP/UtC2240 and 2 505 cal a BP/Beta305320, obtained from the bottom of the chenier at its fore-base (Li et al., 2015; Shang et al., 2013a). Elevation of the sampling position, about −1.5 m, was measured relative to a local benchmark. Considering all the three were reworked, this age as the youngest is chosen by this study indicating "□" at −1.5 m, so msl (−1.5±0.5) m (Table A3). RTC is not given because the age used was much younger than another two. Notes 6 ages of the chenier, including 2 190 cal a BP and 2 506 cal a BP, in this site are 550−1 100 cal a older than this age from the underlying mud. In general, ages in chenier may be older than those from the underlying mud because of reworking, but the time-gap of 550−1 100 cal a is too much. Therefore, it raised doubt that this age, 1 597 cal a BP, may be slightly younger. Thus, the following age, UtC2240, is still retained though both ages give self-contradictory time determination for the two indicators.
76	Another sample was taken from the similar position but age of 2 505 cal a BP/Beta305320. Therefore, RTC is not necersary. Elevation of subsurface at the fore-base here is −1.4 m and this sample was taken from about −1 m (Su et al., 2011). "□" −1 m, msl (−1±0.5) m (Table A3).
77	The dated *M. veneriformis* specimen, with very fresh shell surface decoration and still articulated, were mixed with wrecked single valves of *Scapharca* sp., *Dosinia* sp. and *Meretrix* sp. Although the dated *M. veneriformis* shells were also reworked, they must not be far away from their original living place and were quickly dumped into the chenier in here (Wang et al.,

continued from Table A4.2

No.	Notes
79	Although 8 shell samples were dated in this site (Wang et al., 2007), only this *in situ* articulated razor clam sample is a most believable indicator. Conchologically, this species lives in mid to lower intertidal depth (Zhang, 2008; Okutani, 2000). The sampling elevation is estimated based on the measurement in Apple Garden, about 2 km north along the same chenier ridge (Shang et al., 2013). "□" −0.5 m, msl (−0.5±0.5) m (Table A3) though it was (−0.5±1.5) m in Li et al. (2015).
80	The sample, with definite sampling depth and elevation, was taken from the very bottom of chenier and its sampling position is closed to the present-day high tidal shoreline (Xu, 1994; Xu et al., 1986). Normally, chenier foot wadges seaward below the shoreface of late muddy sediments, so this suggests the sampling position is above the fore-base along its traverse section (i.e., a section perpendicular to the strike direction of chenier chain; Wang and van Strydonck, 1997). So, msl (+0.9±0.5) m (Table A3), though it was (+0.9±1.5) m in Li et al. (2015). RTC was given (Li et al., 2015).
81	Landward subsurface in the sampling position is about +1 m (Wang, 1994), while the sampling position is about 0.5 m above it (Zhao et al., 1980), i.e., about +1.5 m. So, msl (+0.2±0.5) m, i.e., subtracting (1.3±0.5) m (Table A3), while it was (−0.4±0.5) m in Li et al. (2015) because elevation was mistakenly cited from literature. RTC was given (Li et al., 2015).
82	Three radiocarbon-dated shell samples are available in this site (Zhao and Zhang, 1981). Based on Zhao and Zhang (1981) and personal discussion with the author, only this *in situ* articulated razor clam sample is believable but the another two were picked up from the upper part of chenier. However, Zhao and Zhang (1981) only indicated this razor shell was taken 4−5 m below the ground surface, while radiocarbon lab gave the sampling elevation as +1.5 m (Peng et al., 1984). However, local topographic map shows the ground surface here is about +1.5 m. So, Peng et al.' estimation is wrong (we guess Peng et al. confused ground surface elevation with the sampling elevation for this sample) and thus this study uses the sampling elevation as about −3 m (considering sampling depth of 4−5 m). "□" −3 m, msl (−3±0.5) m (Table A3). However, sampling elevation was +1.5 m in Li et al. (2015) because simply accepted Peng et al.' +1.5 m. RTC is not necessary (Li et al., 2015).
83	This sample was taken from the very bottom of chenier, i.e., just above the subsurface, with an approximate sampling elevation of +0.6 m (Xu, 1994). Beneath the subsurface here, underlying mud is composed of *Ammonia beccarii* vars., *A. annectens*, *Candoniella albicans* and pollen assemblage Chenopodiaceae-*Pinus*-*Pteredum*. On the other hand, *A. beccarii* vars., *A. annectens* and Chenopodiaceae-*Querecus* were found from the surficial muddy sediment along the present-day high tidal shoreline in the same site. So, the bottom material of chenier here was formed at high tidal environment influenced by fresh water input (Xu and Liu, 1991; Xu, 1994). "┬" +0.6 m, msl (−0.7±0.5) m, i.e., (1.3±0.5) m was subtracted (Table A3). RTC was given. However, Li et al. (2015) put the sampling position simply in intertidal depth without further compensation for msl reconstruction.
84	The sampling position is about 1 m above the chenier subsurface at its seaward margin of −1.5 m in elevation. Chenier foot was fully wedged into muddy tidal flat. Sediments in this part were composed of alternation between shelly hash laminae and muddy laminae, with penecontemporaneous deformation structure, and much dark-staining downwards, indicating intertidal environment (Wang et al., 2000a, b). The subsurface tilted seaward for about 2.8 m within about 100 m distance from its landward to seaward margin (Wang et al., 2000a, b; Su, 2012). So, "□" −0.5 m, msl (−0.5±0.5) m (Table A3) and RTC was given (Li et al., 2015).
85	Nowadays, it was found as a linear shoal, only 10 cm thick, consisting of well-sorted, very fine shell hash, about 2 200 m out of the present-day shoreline. This remaining shoal is about 70−80 m wide and about 10 cm beneath the intertidal flat surface of clayey silt and floating mud. Elevation was measured relative to local bench mark (Xu et al., 1986; Xu, 1994). This shoal was probably a remnant of Chenier S-T (Sui-Tang) (Wang et al., 2000b; Shang et al., 2016). RTC was given. "□" +0.48 m, msl (+0.48±0.5) m. However, msl was (+0.48±1.5) m in Li et al. (2015).
86	Due to landward digging by local fishermen from the sea side of chenier here, the core portion of chenier was exposed and a bulk sample was taken from the lower part, about 1 m above the subsurface. Elevation of subsurface in the sampling position is about +0.8 m based on comparison with the present-day MHHW shoreline which is 31 m east of the sampling pit (Wang, 1994). This is similar with subsurface elevation of +0.657 m measured by Xu and Liu (1991) and Xu (1994) in this site. So, "┬" +1.8 m, msl (+0.6±0.5) m (Table A3). This subsample is 100 cal a younger than another subsample of *Umbonium* sp. and Terebridae: 679 cal a BP/UtC2238 (Wang, 1994; Wang and van Strydonck, 1997; Shang et al., 2016; Li et al., 2015). However, the elevation of sampling position was roughly determined as (+2±1.5) m and thought to be msl directly in Li et al. (2015).
87	It was taken from lower-middle part of chenier and elevation was approximately obtained from topographic map (Xu, 1994). So, "┬" +0.5 m, msl (−0.8±0.5) m (Table A3). RTC was given. As indicator YS265, the sampling position was only simply recognized as intertidal depth in Li et al. (2015).
88	It was taken from the lower part of chenier because still having 0.4 m-thick shelly sediments below this sampling poition, and elevation was approximately obtained from topographic

continued from Table A4.2

No.	Notes
92	This underlying mud is dull yellowish brown (10YR 5/3) clay, indicating much oxidized environment in the upper part of intertidal flat⑰ (Wang et al., 2003). However, the authors thought previously it was formed just in intertidal depth (Li et al., 2015), but now it is further restricted to the upper part of intertidal zone. So, "┬" +0.7 m and (1.3±0.5) m should be subtracted (Table A3), i.e., msl (−0.6±0.5) m. However, msl was reconstructed as (+0.7±1.5) m in Li et al. (2015). RTC was given (Li et al., 2015). Elevations of three indicators, including the following two, in this site were leveled relative to a local benchmark with National Vertical Datum 1985 (Wang et al., 2003).
93	This gastropoda sample, picked from fine shelly hash, immediately lying on the chenier subsurface, is about 10 cm above the sample AA45901⑰. It was thought to be formed in intertidal depth (Li et al., 2015) but now in this paper is restricted to the upper intertidal zone. So, "┬" +0.8 m, msl (−0.5±0.5) m (Table A3). RTC was given (Li et al., 2015).
94	The sample was taken just above the subsurface at the mid- to rear part of the chenier[17]. So, "┬" +1.7 m, msl (+0.4±0.5) m, i.e., (1.3±0.5) m should be subtracted (Table A3). However, 1.8 m was subtracted from the sampling elevation in Li et al. (2015) because it was incorrectly treated as an equivalent of the peat layer. RTC was given (Li et al., 2015).

Note: The measured ^{14}C dates, signified in italics in Column 4, were changed from their original dates with the Libby half life of 5 730 a by subdiving 1.029 in this study. The ^{13}C values, signified in italics in Column 5, were either recommended by Mook and van de Plassche (1986) or used with the local empirical mean value of −2.68‰PDB (Wang, 1994; Wang and van Strydonck, 1997; Li et al., 2015) for the marine shells. Correspondingly, such calibrated approximate conventional ages in Column 6 were given in italics.

⑰Wang Hong, Li Jianfen, Zhang Yufa, et al. 2002. The present-day geological processes (deposition, erosion and shoreline migrations) and accurate dating on muddy coast (in Chinese), 1–77

Table A4.3. Holocene relative mean sea level (rmsl) indicators, derived from the oyster reefs, in the west coast of Bohai Bay

	Basic information			Temporal distribution								Spatial distribution		
No.	Locality, stratigraphy and environment, material dated, sample-depth / ground surface elevation / (averaged) sample elevation	Coordinate	Lab code	Measured ^{14}C date	$\delta^{13}C$ /‰PDB	Conventional ^{14}C age/a BP	Calibrated ^{14}C age: median probability/2σ range/cal a BP	Status of material dated	Sub-sample	RTC /cal a	Age of rmsl: single value/ range/cal ka BP	Elevation of the observed rmsl/m	Corrections of tectonics /self-compaction/water withdrawal /m	Elevation of rmsl after corrections for the three local factors /m
95	Mengzhuang oyster reef, articulated *C. gigas,* 4.5 m/-/about −2.5 to −3.3 m (?)	39.4°N, 117.8°E	TD342	*5 070±115*	*−2.68*	*5 429±122*	6 008/ 6 280−5 704	*in situ*	no	−	6.008/ 6.280−5.704	−2.65±0.7	+0.60/ +1.75/ +0.37	+0.07±0.7
96	Dawuzhuang, oyster reef, Section 6, top, articulated *C. gigas,* about 4.5/-/about −2.58 m	39.4°N, 117.9°E	BA 091172	−	−	5 360±35	5 926/ 6 096−5 752	*in situ*	no	−	5.926/ 6.096−5.752	−2.43±0.7	+0.59/ +1.75/ +0.60	+0.51±0.7
97	Dawuzhuang, oyster reef, Section 1, top, articulated *C. gigas,* 0−0.3 m below the top surface, about 5/-/−3.22 to −3.5 m	39.4°N, 117.9°E	BA 110343	−	−	5 625±35	6 223/ 6 365−6 061	*in situ*	yes	−	6.223/ 6.365−6.061	−3.07±0.7	+0.62/ +1.95/ +0.60	+0.1±0.7
98	Shizhuang, oyster reef, top (?), articulated *Crassostrea gigas,* about 4/about +2.5 m/−1.4 to −2 m;	39.4°N, 117.5°E	TD344	*5 860±95*	*−2.68*	*6 219±103*	6 879/ 7 161−6 613	*in situ*	no	−	6.414/ 7.161−5.614	−1.55±0.7	+0.64/ +1.56/ +0.11	+0.76±0.7
	Jiangzhuang-Shizhuang oyster reef, articulated *C. gigas,* about 4/about +2.5 m/−1.4 to −2 m		CG181	5 020±140	*−2.68*	*5 379±146*	5 950/ 6 267−5 614	*in situ*	no	−				
99	Lingtou, oyster reef, top, articulated *C. gigas,* 3.1−3.3	39.3°N, 117.6°E	BA 110339	−	−	3 980±30	4 234/ 4 404−4 069	*in situ*	yes	−	4.234/ 4.404−4.069	−2.08±0.7	+0.42/ +1.25/ +0.62	+0.21±0.7

continued from Table A4.3

Basic information			Temporal distribution								Spatial distribution		
No.	Locality, stratigraphy and environment, material dated, sample-depth / ground surface elevation / (averaged) sample elevation	Coordinate	Lab code	Measured ^{14}C date	$\delta^{13}C$ /‰PDB	Conventional ^{14}C age/a BP	Calibrated ^{14}C age: median probability/2σ range/cal a BP	Status of material dated	Sub-sample	RTC /cal a	Age of rmsl: single value/ range/cal ka BP	Elevation of the observed rmsl/m	Corrections of tectonics /self-compaction/water withdrawal /m	Elevation of rmsl after corrections for the three local factors /m
103	Konggang, oyster reef, a transition zone between reef-top and the overlying mud, articulated *Trapezium liratum,* about 5.5/-/−2.85 to −2.90 m	39.1°N, 117.4°E	BA 101110	−	−	3 800±25	3 980/ 4 140−3 825	*in situ*	yes	−	3.980/ 4.140−3.825	−2.7±0.7	+0.40/ +1.87/ +1.05	+0.62±0.7
104	*idem*, reef-top, articulated *C. gigas,* about 5.5/-/about −2.9 to −3.0 m; *idem*, the same individual of BA101108	39.2°N, 117.4°E	BA 101108, Beta 305302	− 3 440±30	− −3.9	3 800±25, 3 790±30	3 980/ 4 140−3 825; 3 967/ 4 140−3 811	*in situ*	yes	−	3.973/ 4.140−3.811	−2.78±0.7	+0.40/ +1.87/ +1.05	+0.54±0.7
105	Binhaihu, oyster reef, top, articulated *C. gigas,* about 3.3/-/about 3.15 to −3.5 m	39.2°N, 117.6°E	BA 110340	−	−	2 265±30	2 088/ 2 276−1 939	*in situ*	yes	−	2.088/ 2.276−1.939	−3.16±0.7	+0.21/ +1.29/ +0.75	−0.91±0.7
106	Core CH79, oyster reef, articulated *C. gigas,* 8.75−8.80 m/−3.4 m/about −12.18 m	39.2°N, 117.9°E	BA 08822	−	−	6 935±35	7 588/ 7 702−7 466	*in situ*	no	−	7.588/ 7.702−7.466	−10.58±0.5	+0.76/ +3.78/ +1.87	−4.17±0.5
107	*idem*, articulated *C. gigas,* 9.90−9.95 m/−3.4 m/−13.33 m		BA 08823	−	−	7 275±40	7 912/ 8 048−7 762	*in situ*	no	−	7.912/ 8.048−7.762	−11.73±0.5	+0.79/ +4.13/ +1.87	−4.94±0.5
108	*idem*, articulated *C. gigas,* 11.50−11.55 m/−3.4 m/−14.93 m		BA 08824	−	−	7 625±35	8 268/ 8 388−8 146	*in situ*	no	−	8.268/ 8.388−8.146	−13.33±0.5	+0.83/ +4.63/ +1.87	−6.0±0.5
109	Beitang, oyster reef,	39.1°N,	ZK507-I	975±85	*−2.68*	*1 334±94*	1 067/	*in situ*	no	−	1.067/	−0.85±0.7	+0.10/	+0.22±0.7

Continued form Table A4.3

No.	Notes
	Explainations of the indicative meaning, RTC, the three spatial corrections and changes from the previous work (Li et al., 2015)
95	The sample is about 1 m below the reef top (Wang et al., 1991) while the top elevation is confused as −1.5 m (Wang et al., 1991), −2.3 m or −1.5 m (Han and Meng, 1996). This study uses average of about −2.8 m as the sampling elevation. The age is considered approximately as its top age. So, msl (−2.65±0.7) m while it was (−2±1.5) m in Li et al. (2015). Usually, the reef-top can grow up to MTL but 15 cm lower than the corresponding msl in the study area (see Section 4.3 and Table A3). Thus, all the oyster indicators here have been treated by adding 15 cm to the observed reef-top elevation in order to fulfil the conversion from MTL to msl (the same below).
96	Elevation of this sampling position was not measured and we then use −2.58 m, the 7-spot-average of the reef-top elevations in this site (Li et al., 2015). msl (−2.43±0.7) m.
97	In this big pit, elevation measurement was given by using Total Station connected with the National Vertical Datum 1985. As a result, elevations of the 7 spots on the reef top were obtained, among which the top surface at this sampling position is −3.22 m. Furthermore, totally, 19 top-spots, including another two reef sites in Binhai Lake and Konggang, were leveled and showed that an average undulation of the reef-top is ±0.7 m (Fan et al., 2005a; Liu, 2010; Wang et al., 2011c, 2012a; Shang et al., 2013). This is similar to 0.5−1 m of the top undulation of the modern living oyster reef in Xiaomiaohong site, Jiangsu Province (Zhang, 2004). In this study, ±0.7 m has been used as an error range for the top undulation for all oyster reefs (Li et al., 2015). So, msl (−3.07±0.7) m (Table A3). However, it was (−3.4±0.7) m in Li et al. (2015) because −3.4 m is a rounding value of middle point of the sampling range of −3.22 m to −3.5 m.
98	*C. gigas* were with coexisting *Trapezium* sp., *Assiminea* sp. and *Cerithidea* sp. shells (Peng et al., 1980). Five independent investigations were carried out and five ages, dated by four different labs, were obtained for these two closed reef sites (Peng et al., 1980; ICP, 1987; IOA, 1983; Li and Zhao, 1990). Ages of TD344 and CG181 listed are the oldest and youngest, respectively, among the five (Li et al., 2015). Elevations of the reef top were quite different from about +0.5 m (ICP, 1987), −1.5 m (Wang et al., 1991), −1.4−−1.5 m (Han and Meng, 1996) to about −2 m (Wang et al., 2011c). Considering less precise estimation for the elevations and the inherent undulation of reef top, this study uses −1.7 m, an average of the latter three (Li et al., 2015). So, msl (−1.55±0.7) m in this study (Table A3) while it was (−1.7±1.5) m in Li et al. (2015).
99	This individual was taken from the top of reef in this site. Elevation of ground surface was leveled relative to a local benchmark (Li et al., 2015) and msl (−2.08±0.7) m (Li et al., 2015).
100	The ground elevation is +0.71 m of Core HD21, about 1 km west of this reef site and a 7-spot-average, given by RTK leveling in 2016, is +0.385 m, about 0.5 km north of this reef site (Qin et al., 2017). This is flattened lagoon-salt marsh lowland[18] (Qin et al., 2017; see indicator No. 12). So, the ground elevation in this reef site is about +0.5 m approximately. This sample was taken from the top of the reef, which is 2.8 m below the ground surface① (Shang et al., 2013). So, the reef-top is −2.3 m and msl (−2.15±0.7) m. However, the sampling elevation, about −3.1 m in Li et al. (2015), was only reckoned by an estimation of elevation difference between the reef-tops of Biaokou and this site (the latter is based on Wang et al., 1991).
101	*T. liratu*m is a most important associated species in the *C. gigas* reefs in the study area and this sample was taken from 5 cm below the reef top. Ground elevation was leveled relative to the local benchmark (Wang et al., 2006; Li et al., 2015). msl (−1.67±0.7) m (Li et al., 2015).
102	Top and/or upper part of oyster reef in this site was destroyed by bridge construction and the reef-bottom was not dug out (Wang et al., 1991). So, it is impossible to know from which part of reef column the sample was taken exactly. Approximately, it is considered to be in middle part of the reef body in this site and was in intertidal depth. So, '□' −1.4—1.6 m, msl (−1.5±1.5) m.
103	The sample, in the bottom of transitional zone, was immediately above the reef-top. Another *in situ* subsample is articulated *Ruditapes philippinarum,* which was a later burrowed animal showing reasonably 480 cal a younger age: 3 500 cal a BP/BA101109 (Wang, 2012; Wang et al., 2012a; Li et al., 2015). MTL (−2.85±0.7) m while msl should be (−2.7±0.7) m.
104	The top elevation fluctuated between (−2.70 to −3.16) m based on leveling at 3 spots in this site and the average is −2.93 m (Wang, 2012). A bulk sample, as a part of the ligamental resilium of LV of the same individual, taken from the reef-top, was divided and separately AMS dated by two labs and gave the exact same ages (Wang, 2012; Wang et al., 2012a; Li et al., 2015). msl (−2.78±0.7) m (Li et al., 2015).
105	The top part of reef in this site is composed of intact oyster individuals and oyster hash, also fragments of *Rapana venosa,* and *Trapezium liratum, Mitrella bella* (?), *Pseudoliotia pucchella, Assiminea latericea, Barbatia* sp., *Potamocorbula laevis, Ruditapes philippinarum*. Forams were *Ammonia confertitesta* (dominant species), *Quinqueloculina akneriana rotunda, Protelphidium granosum, Elphidium nakanokawaense.* Ostracoda were *Sinocytheridea impressa, Loxoconcha binhaiensis* and so on. These indicate intertidal environment with occasionally input of freshwater[19] (Fan et al., 2008; unpublished data of the authors' group). Nine spot levelling indicates the top elevation is in between −2.96 to −4.36 m[18] and average

[18]Li Fenglin, Wang Hong, Wang Yunsheng, et al. 2002. Report of Huaidianxiang Sheet (J50E005015, 1: 50 000) (in Chinese), 1–104.

[19]Fan Changfu, Pei Yandong, Wang Fu, et al. 2006. Report of Buried Oyster Reef in Binhaihu Lake, Tianjin (in Chinese), 1–11

continued from Table A4.3

No.	Notes
108	This articulated shell, taken from the reef-bottom, gives an initial age of this reef. Concomitant forams, 3 000−4 000 tests per 20 g dry sample, were composed of mainly *Ammonia beccarii* and shallow sea species such as *A. flevensis, Elphidium limpidum, Pseudoeponides enderssen* and *A. convexdorsa,* indicating estuary environment in lower intertidal to upper subtidal depth (Li, 2010). Downwards, two forams samples, taken from the underlying mud, 12−14.9 m, show mainly *A. beccarii* vars., indicating marine influence had started from this underlying mud and sea water become deeper upwards. So, '⊥' −14.93 m, msl (−13.33±0.5) m, i.e., (1.6±0.5) m should be added (Table A3). However, msl was (−13.43±0.5) m because 1.5 m was simply added in Li et al. (2015).
109	It seems to be taken from the reef top though more detailed information, including elevations for both ground surface and reef top, were deficient in original literature (Zhao et al., 1979). So, msl (−0.85±0.7) m and RTC is not necessary (Li et al., 2015).
110	This possible oyster reef, or at least an oyster bank, existed exceptionally in Chenier Plain (Peng et al., 1980) and with a numerous *Trapezium liratum* (Wang et al., 2007), one of a few coexisting species within *C. gigas* reefs in the area. So, it is probably a less developed reef occurred in Chenier Plain. '□' +1 m, MTL +1 m and msl +1.15 m. The oyster sample is considered *in situ* and RTC is not necessary (Li et al., 2015). It was thought to be chenier with a vertical error of ±1.5 m (Li et al., 2015). Now it is reclassified to oyster reef and vertical error is changed to ±0.7 m as the local reef top undulation.

Note: The measured ^{14}C dates, signified in italics in Column 5, were changed from their original dates with the Libby half life of 5 730 a by subdiving 1.029 in this study. The ^{13}C values, signified in italics in Column 6, were either recommended by Mook and van de Plassche (1986) or used with the local empirical mean value of −2.68‰PDB (Wang, 1994; Wang and van Strydonck, 1997; Li et al., 2015) for the marine shells. Correspondingly, such calibrated approximate conventional ages in Column 7 were given in italics.

Stuiver M, Reimer P J. 1993b. CALIB Rev 3.0.3. Seattle: Quaternary Isotope Lab. Washington: University of Washington

Su Shengwei. 2012. Paleoenvironmental reconstruction of the holocene cheniers in the west coast of Bohai Bay (in Chinese) [dissertation]. Changchun: Jilin University

Su Shengwei, Shang Zhiwen, Wang Fu. 2011. Holocene Cheniers: Spatial and temporal distribution and sea level indicators in Bohai Bay. Geological Bulletin of China, 30(9): 1382–1395

Sun Yiying, Wu P, Huang Guangqing, et al. 2015. Holocene sea-level reconstruction for Guangdong coast and a comparison with GIA model outputs. Quaternary Sciences (in Chinese), 35(2): 281–290

Tian Lizhu, Chen Yanping, Jiang Xingyu, et al. 2017. Post-glacial sequence and sedimentation in the western Bohai Sea, China, and its linkage to global sea-level changes. Marine Geology, 388: 12 –24, doi: 10.1016/j.margeo.2017.04.006

Törnqvist T E, Rosenheim B E, Hu P, et al. 2015. Radiocarbon dating and calibration. In: Shennan I, Long A J, Horton B P, eds. Handbook of Sea-Level Research. West Sussex: John Wiley & Sons, 349–360

Törnqvist T E, van Ree M H M, van't Veer R, et al. 1998. Improving methodology for high-resolution reconstruction of sea-level rise and neotectonics by paleoecological analysis and AMS ^{14}C dating of basal peats. Quaternary Research, 49(1): 72–85, doi: 10.1006/qres.1997.1938

van de Plassche O. 1982. Sea-level change and water-level movements in the Netherlands during the Holocene [dissertation]. Amsterdam: Vrije Universiteit Amsterdam

van de Plassche O. 1986. Sea-Level Research: A Manual for the Collection and Evaluation of Data. Netherlands: Springer

Wang Ying. 1964. The shell coast ridges and the old coastlines of the west coast of the Bohai Bay. Journal of Nanjing University (in Chinese), 8(3): 424–443

Wang Hong. 1994. Palaeoenvironment of Holocene Chenier and Oyster Reefs in the Bohai Bay (China) [dissertation]. Brussel: Vrije Universiteit Brussel

Wang Haifeng. 2012. The Palaeoenvironment reconstruction of Konggang buried oyster reef and the response to the global change, northwest coast of Bohai Bay (in Chinese) [dissertation]. Beijing: China University of Geosciences (Beijing)

Wang Hong, Chen Yongsheng, Tian Lizhu, et al. 2011a. Holocene cheniers and oyster reefs in Bohai Bay: Palaeoclimate and sea level changes. Geological Bulletin of China (in Chinese), 30(9): 1405–1411

Wang Hong, Fan Changfu. 2005. The ^{14}C database (II) on the Circum-Bohai Sea-Coast. Quaternary Sciences (in Chinese), 25(2): 141–156

Wang Hong, Fan Changfu, Li Jianfen, et al. 2006. Holocene oyster reefs on the northwest coast of the Bohai Bay, China. Geological Bulletin of China (in Chinese), 25(3): 315–331

Wang Ying, Ke Xiankun. 1989. Cheniers on the east coastal plain of China. Marine Geology, 90(4): 321 –335, doi: 10.1016/0025-3227(89)90134-5

Wang Hong, Keppens E, Nielson P, et al. 1995. Oxygen and carbon isotope study of the Holocene oyster reefs and paleoenvironmental reconstruction on the northwest coast of Bohai Bay, China. Marine Geology, 124(1–4): 289–302

Wang Hong, Li Fenglin, Fan Changfu, et al. 2004. The ^{14}C database (I) on the Circum-Bohai Sea-Coast. Quaternary Sciences (in Chinese), 24(6): 601–613

Wang Hong, Li Jianfen, Pei Yandong, et al. 2011b. Study of Quaternary geology on the west coast of Bohai Bay. Geological Survey and Research (in Chinese), 34(2): 81–97

Wang Hong, Li Jianfen, Zhang Yufa, et al. 2000a. The younger Cheniers (Shell Banks) on the west coast of the Bohai Bay: Morphology, structure and polygenetic processes. Geological Review (in Chinese), 46(3): 276–287

Wang Haifeng, Pei Yandng, Liu Huimin, et al. 2011c. Holocene oyster reefs: Spatial and temporal distribution and sea level in dicators in Bohai Bay. Geological Bulletin of China (in Chinese), 30(9): 1396–1404

Wang Zhanghua, Ryves D B, Lei Shao, et al. 2018. Middle Holocene marine flooding and human response in the south Yangtze coastal plain, East China. Quaternary Science Reviews, 187: 80 –93, doi: 10.1016/j.quascirev.2018.03.001

Wang Hong, Shang Zhiwen, Li Jianfen, et al. 2010. Holocene shoreline changes and marine impacts on the muddy coast, western Bohai Bay, China. Geological Bulletin of China (in Chinese), 29(5): 627–640

Wang Fu, Shang Zhiwen, Li Jianfen, et al. 2020a. Research status and protection suggestions of suggestions of cheniers on Bohai Bay. Geologyical Survey and Research, 43(4): 293–316

Wang Hong, Van Strydonck M. 1997. Chronology of Holocene cheniers and oyster reefs on the coast of Bohai Bay, China. Quaternary Research, 47(2): 192 –205, doi: 10.1006/qres.1996.1865

Wang Haifeng, Wang Hong, Fan Changfu, et al. 2012a. Konggang oyster reef in Tianjin constrained by both the Mid-Holocene environmental deteriorations and the local neotectonic faults. Geological Bulletin of China (in Chinese), 31(9): 1387–1393

Wang Zhanghua, Zhan Qiang, Long Haiyan, et al. 2013. Early to Mid-Holocene rapid sea-level rise and coastal response on the southern Yangtze delta plain, China. Journal of Quaternary Science, 28(7): 659–672, doi: 10.1002/jqs.2662

Wang Hong, Zhang Jinqi, Zhang Yufa, et al. 2000b. Chronology of the Chenier I and shoreline changes since the last 1ka, on western coast of Bohai Bay. Marine Geology & Quaternary Geology (in Chinese), 20(2): 7–14

Wang Hong, Zhang Yufa, Zhang Jinqi, et al. 2000c. The Chenier II on the western coast of Bohai Bay: Its subdivision and amended time-framework. Acta Geoscientia Sinica (in Chinese), 21(3): 320–327

Wang Ruobai, Zhou Wei, Li Fenglin, et al. 2003. Tectonic subsi-

dence and prospect of ground subsidence control in Tianjin area. Hydrogeology & Engineering Geology (in Chinese), 30(5): 12–17

Wang Zhanghua, Zhuang Chengcheng, Saito Y, et al. 2012b. Early mid-Holocene sea-level change and coastal environmental response on the southern Yangtze delta plain, China: Implications for the rise of Neolithic culture. Quaternary Science Reviews, 35: 51 –62, doi: 10.1016/j.quascirev.2012.01.005

Wang Fu, Zong Yongqiang, Mauz B, et al. 2020b. Holocene sea-level change on the central coast of Bohai Bay, China. Earth Surface Dynamics, 8(3): 679–693, doi: 10.5194/esurf-8-679-2020

Weill P, Tessier B, Mouazé D, et al. 2012. Shelly cheniers on a modern macrotidal flat (Mont-Saint-Michel bay, France)−Internal architecture revealed by ground-penetrating radar. Sedimentary Geology, 279: 173 –186, doi: 10.1016/j.sedgeo.2010.12.002

Woodroffe C D, Curtis R J, McLean R F. 1983. Development of a Chenier Plain, Firth of Thames, New Zealand. Marine Geology, 53(1–2): 1–22

Woodroffe S A, Horton B P. 2005. Holocene sea-level changes in the Indo-Pacific. Journal of Asian Earth Sciences, 25(1): 29–43, doi: 10.1016/j.jseaes.2004.01.009

Xia Dongxing. 1981. Whence comes the high sea-level during the holocene. Haiyang Xuebao (in Chinese), 3(4): 601–609

Xie Zhiren. 1986. The simulation for environment changes since the last 20000 years: Feedback mechanism between climate, sea-level and crust movement (in Chinese) [dissertation]. Nanjing: Nanjing Universtity

Xie Hailan, Xia Yubo, Meng Qinghua, et al. 2019. Study on land subsidence assessment in evaluation of carrying capacity of geological environment. Geological Survey and Research (in Chinese), 42(2): 104–108

Xie Zhiren, Yuan Linwang, Lv Guonian, et al. 2012. Systematic Change on Sea Surface and Land Surface: Reconstruction, Monitoring and Prediction (in Chinese). Beijing: Science Press

Xu Jiasheng. 1994. Cheniers and sea level changes along the Huanghua coast of Bohai Bay. Haiyang Xuebao (in Chinese), 16(1): 68–77

Xu Jiasheng, Liu Kefu, Li Zhaoji, et al. 1986. Development of cheniers and variation of coast line along the western coast of Qikou-Langtuozi in the Bohai Sea since the Dynasties of Tang and Song. In: International Geological Correlation Programme Project No. 200 China Working Group, ed. China Sea Level Changes (in Chinese). Beijing: China Ocean Press, 61–69

Xu Jie, Ma Zongjin, Chen Guoguang, et al. 2005. Estimating times of Quaternary tectonic episodes in the Bohai Sea based on geomorphic features of surrounding mountainous areas. Quaternary Sciences (in Chinese), 25(6): 700–710

Yang Zigeng, Li Youjun, Ding Qiuling, et al. 1979. Some fundamental problems of Quaternary geology of eastern Hebei plain. Acta Geologica Sinica (in Chinese), (4): 263–281

Zhang Renshun. 2004. The geomorphology-sedimentology character of oyster reef in Xiaomiaohong tidal channel, Jiangsu Province. Oceanologia et Limnologia Sinica (in Chinese), 35(1): 1–7

Zhang Hongtao, Zhang Xunhua, Wen Zhenhe, et al. 2010. Geological and Geophysical Map Series of Eastern China Seas and Adjacent Regions. Beijing: China Ocean Press (in Chinese)

Zhao Xitao. 1989. Cheniers in China: An overview. Marine Geology, 90(4): 311–320, doi: 10.1016/0025-3227(89)90133-3

Zhao Songling, Yang Guangfu, Cang Shuxi, et al. 1978. On the marine stratigraphy and coastlines of the western coast of the gulf of Bohai. Oceanologia et Limnologia Sinica (in Chinese), 9(1): 15–25

Zhao Xitao, Zhang Jingwen. 1981. A new evidence on the existence of the forth chenier ridge along the west coast of the Bohai Bay and its C14 dating. Scientia Geologica Sinica (in Chinese), (1): 29

Zhao Xitao, Zhang Jingwen. 1984. Basic characteristics of the Holocene sea level changes along the coastal areas in China. In: Zhao Xitao, ed. Studies on the Evolution of China's Coast. Fuzhou: Fujian Publishing House of Science and Technology Press, 178–186

Zhao Xitao, Zhang Jingwen, Jiao Wenqiang, et al. 1980. Cheniers on the western coast of Bohai Gulf. Chinese Science Bulletin, 25(3): 243–247

Zong Yongqiang. 2004. Mid-Holocene sea-level highstand along the southeast coast of China. Quaternary International, 117(1): 55–67, doi: 10.1016/S1040-6182(03)00116-2

Appendix A:

A1 Tides

Type of tides in the study area was not so clearly classified in the past decades. Earlier study pointed out the whole studying coast is the semidiurnal tides (EBN, 1965). With a boundary along Haihe River Mouth (Fig. A1), where Tanggu gauge station located in, the Bohai Bay coast was divided into unequal semidiurnal pattern in the north and semidiurnal in the south (Liu et al., 1986). Recently, following gradual accumulation of more measured data, the whole coast is thought to be unequal semidiurnal pattern⑥⑦. Such change on type of tides is because the local ratio of $(H_{O_1} + H_{K_1})/H_{M_2}$ is only 0.58−0.64 which is quite close to 0.5, i.e., the boundary between semidiurnal and unequal semidiurnal⑥ (Fig. A1).

Our study has determined the Holocene shorelines, combined by cheniers and earthy mounds (Wang et al., 2010; Shang et al., 2016) and clearly show that the ancient bayhead was located in the Oyster Plain (Fig. A1), in contrast with the modern bayhead along Tanggu−Jiyun River and Qikou−Nanpai River mouths approximately (Fig. A1, Table A1).

Local tidal information⑥⑦ (Liu et al., 1986; EBC, 1989; HPL, 2007; Sun and He, 2013) indicates the tidal ranges (mean range and mean high range) in the bayhead (Tanggu−Jiyun River Mouth to Qikou−Nanpai River Mouth) are approximately 2.42 m and 3.0 m, respectively (Tables A1 and A2). Also, for the bayhead area, MHW is +1.21 m, MHHW is +1.3 m and MLLW is −1.61 m, respectively (Tables A1 and A2). As to the both periphery sides, either tidal ranges or high water levels are commonly /ersely about a decimeter higher (Tables A1 and A2). Note all th re counted from or converted to the Tanggu gauge zero⑥, and ha s study.

Furthermore, we speculate could be very similar to present, if not even smaller (Shennan a spatio-temporal distribution of Holocene shorelines showing ar et al., 2010; Shang et al., 2016) (Fig. A1). paleo northeastern

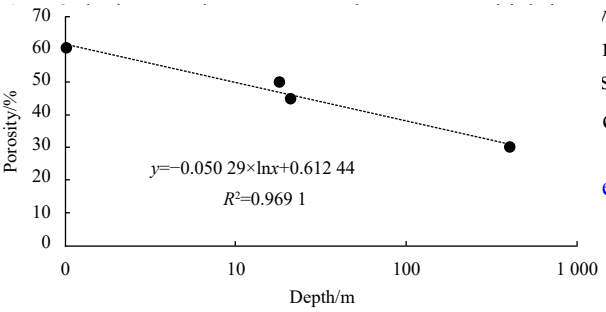

Fig. B1. Regression fit of the local porosity and depth, based on several key layers in Table B1.

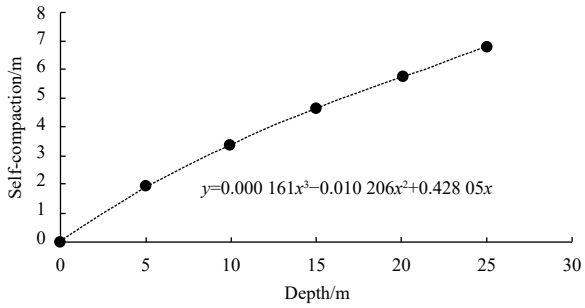

Fig. B2. Relationship between self-compaction and depth in the west coast of Bohai Bay, for depth ⩽25 m only.

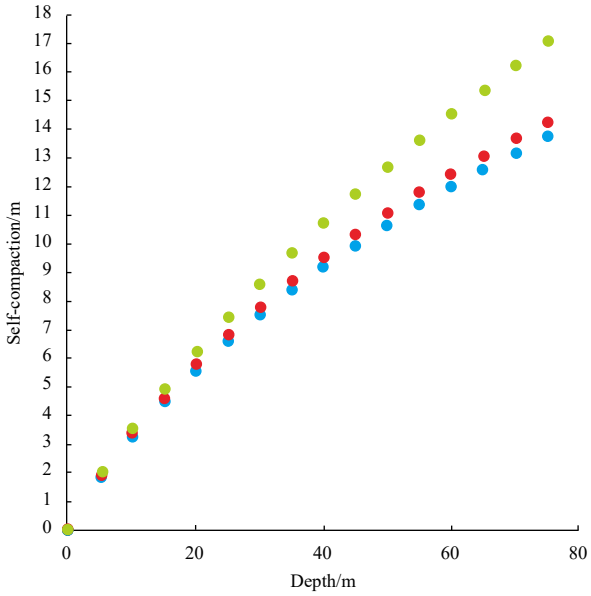

Fig. B3. An Illustration showing comparison between decompacting value trends. For this study, differences are less than 1 m for shallow sediments normally less than 25 m in depth. Red circles: consolidation settlement is 400 m; green circles: consolidation settlement is 1 000 m. Blue circles are drawn by using slightly different values comparing with the red circles for porosity estimates as 45% for the basal peat, 40% for the hard soil horizon and 30% for the base of Quaternary sediments.

Table B1. Estimated porosity for this study, modified from Li et al.③

Key layer	Average depth/m	Porosity/%
Surface	0	60
Basal peat	18	50
Hard soil horizon, LGM	21	45
Subsurface of sediments	400	30

Table B2. Relationship of self-compaction and depth

Depth/m	Self-compaction, Δ (m), model	Self-compaction Δ (m), empirical
0	0.00	0.00
5	1.94	1.91
10	3.39	3.42
15	4.66	4.67
20	5.79	5.77
25	6.83	6.84
30	7.79	7.79
35	8.69	8.71
40	9.53	9.57

periphery is not related with the distribution of the Holocene sea-level indicators (Fig. 2) because this periphery during

Holocene period was far beyond the distribution of the indicators of the study. Estimation for ancient tidal range and high waters for this periphery is indeed not necessary though it is still listed in Table A3.

Two sets of the observational tidal data, 53-a-lomg (1952−2005)⑦ and 40-a-long (1950−1990)⑥ have determined the essential tidal properties, including the height-relationship between the local gauge zero, the local MSL and National MSL (i.e., National Vertical Datum 1985)⑥⑦. All the tidal heights, counted from the local gauge zero, have been converted to the local MSL system. The local mean sea level is +2.62 m while the National Vertical Datum 1985 is +2.64 m above the local gauge zero, respectively⑥⑦.

Notes the local tides reveal that MTL, calculated from the range of MHHW−MLLW, is 15−16 cm lower than the local MSL; or only 2 cm lower than the MSL, calculated from the range of MHW−MLW, in Tanggu Gauge Station at bayhead. Since only 2 cm difference exists between the local MSL and National Vertical Datum 1985, it can be ignored when correlating sea level curve derived by this study with the other sections along the mainland coastaline based on National Vertical Datum 1985. However, a conversion between MTL and MSL has been given for those oyster reef indicators, which took exactly from the very top of reefs.

A2 Summary of the indicative meanings of the three types of indicators

Table A3 quantitatively summarizes all the indicative meanings for sediments (peaty layers and the others), cheniers and oyster reefs in the bayhead and periphery sides, respectively.

A3 Residence time effect

For reworked molluscan shells, there may be a significant time-lag between the organism dying and their final entombment within sediments, cheniers and shelly beds. This difference between the ^{14}C age produced by the analysis of a reworked shells and the depositional time of the layer in which the reworked material was finally laid is called the residence time. This concept has been studied by a number of researchers in the last half century such as Gould and McFarlan (1959), Kowalewski et al. (2000), Giosan et al. (2005) and Nott (2011). Our new result for the study area, based on subsample-comparison of 47 individuals from 17 discrete layers, has been published recently (Shang et al., 2016). As a result, two semi-empirical estimates for the local residence time effect of reworked marine shells have been achieved as 600 cal a for the original ^{14}C dates older than 1 cal ka BP and 100 cal a for the original ^{14}C dates younger than 1 cal ka BP, respectively (Shang et al., 2016). Therefore, for those reworked-shell-derived ^{14}C dates 600 or 100 cal a should be subtracted and such residence-time corrected ages are shown as italics (Table A4.1−A4.3: Column 12). As for those shells *in situ* (still keeping the living condition) or only very shortly transported (still articulated), residence time effect no longer existed or was faint and thus is not necessary for this correction. If there were two or more dates of different subsamples from the same bulk sample, we simply choose the younger/youngest one as its depositional age. In this case, residence time correction was actually given too, and the age was signified in italics also (Table A4.1−A4.3: Column 12).

On the other hand, residence time effect also existed in the ages of reworked plant organic material. Residence time correction has been given to the basal peat layers (Törnqvist et al., 1998; González and Törnqvist, 2009), coastal shal-

low organic sediments (Argyilan et al., 2005), lacustrine sediments (Sirocko et al., 2013; Howarth et al., 2013; Rothacker et al., 2013; Hatté et al., 2013) and coral reefs (Gulliver et al., 2013), based on multi subsamples (or different fractions) within the same single layer and/or from the same bulk sample. In our previous study, 20 bulk samples from Holocene peaty layers of six cores were sieved and divided into two subsamples: >180 μm and <180 μm by Beta Laboratory. The portion, >180 μm, is named organic debris (peat) while the portion, <180 μm, is called organic mud. Then, all these 40 subsamples were AMS ^{14}C dated in the laboratory. Dating results indicate a sole exception that the subsample >180 μm is very slightly older than the subsample <180 μm (the former: 7 487 (7 565−7 430) cal a BP/Beta 329 636, and the latter: 7 466 (7 562−7 422) cal a BP/Beta 331 452) from the same bulk sample (Li et al., 2015).

For all the other 19 groups, subsamples >180 μm are uniformly younger than the counterpart subsamples <180 μm. Range of age difference of these 19 paired subsamples is between 170 cal a to 8 530 cal a, with an arithmetical mean of 1 320 cal a (Li et al., 2015). This meets a basic concept that the finer grains need longer transportation time (Törnqvist et al., 1998; Argyilan et al., 2005; González and Törnqvist, 2009; Rothacker et al., 2013; Sirocko et al., 2013; Howarth et al., 2013; Hatté et al., 2013). Furthermore, in general, an arithmetic mean of the two subsamples' ages can be simply recognized an age of its bulk sample, from which such paired subsamples were subdivided. So, age difference between the subsample >180 μm and a derived approximate age of the bulk sample is attributed to its residence time effect given by the portion <180 μm. Thus, an arithmetically averaged value of 660 cal a as the local calibration age has been obtained (Li et al., 2015). Considering all the previously published dates given by organic-rich material were almost not exceptionally from the bulk samples, so 660 cal a were subtracted and shown as italics too (Li et al., 2015) (Table A4.1−A4.3: Column 12). As to those original dates younger than 2 cal ka BP, a 100 cal a subtraction was used in the light of the reworked shells younger than 1 cal ka BP (Li et al., 2015) (Table A4.1−A4.3: Column 12).

If two or more subsample ages existed for a bulk organic-rich sample, then the younger (or youngest) one, usually given by coarser fraction, is chosen directly as an actual RTC correction. However, sometimes a bulk sample itself is very fine and is composed of only the portion <180 μm. In this case, the AMS ages of <180 μm should be subtracted by 1 320 cal a for its plausible residence time (Li et al., 2015) (Table A4.1−A4.3: Column 12).

A4 Sea level indicators

In total, 15 items are involved for each indicator (Table A4.1−A4.3).

Basic information (Columns 2−4):

(1) Sequence No.

(2) Sample location/stratigraphy and encironment/material dated/sampling position in outcrop or depth in core/the converted sampling elevation against the National Vertical Datum 1985.

(3) Coordinate (N, E).

(4) Lab code.

Temporal distribution (Columns 5−12):

(5) Measured ^{14}C date.

(6) δ^{13}C value if available or recommended δ^{13}C value based on Mook and Waterbolk (1985) or the local empirical value, −2.68‰ PDB, for marine shells (Wang, 1994).

(7) Conventional age. For those previously published data without δ^{13}C values, CALIB 3 program (Stuiver and Reimer, 1993a, 1993b) was firstly used based on the recommended values or the local empirical value for marine shells in order to obtaining approximate conventional age.

(8) Calibrated age (cal a BP, 2σ range) and the median probability were given by CALIB 7 program (Reimer et al., 2013). ΔR= −178±50 a for marine shell samples (Southon et al., 2002) was used.

(9) Status of the material dated: *in situ* or reworked.

(10) Whether subsamples exist: yes or not.

(11) Residence time effect of two sets of semi-empirical values of 600 cal a or 100 cal a for the reworked marine/brackish samples and 660 cal a or 100 cal a for the reworked terrigenous organic-rich samples was corrected for those reworked samples (Shang et al., 2016a; Li et al., 2015). Four exceptions of 1 320 cal a were given for the sample consisting of grain size <180 μm only (Li et al., 2015).

(12) Age used after the aforementioned corrections: single value and 2σ range, and the Italic is for RTC processed.

Spatial distribution (Columns 13−15):

(13) Elevation of the RMSL, derived from the indicative meaning of the observed rsl indicator.

(14) Corrections for the local factors of neotectonics/self-compaction/groundwater withdrawal, as three fold values,

separated by '/'.

(15) Elevation of the RMSL: after the corrections for the three local factors.

Notes

Detailed descriptions include litho- and biostratigraphical evidence, sedimentary facies analysis and comparison between this study and the previous work (Li et al., 2015). Among them, the temporo- and spatial characteristics of each RMSL indicator are shown by Columns (12) and (15), respectively.

Comparing the excel form (Hijma et al., 2015; personal communication, Khan, 2017), the aforementioned 15 items have covered most contents of the almost 80 fields they recommended. Our study still keeps the word version here and will be transformed into excel form later on.

Appendix A References

Argyilan E P, Forman S L, Johnston J W, et al. 2005. Optically stimulated luminescence dating of Late Holocene raised strandplain sequences adjacent to Lakes Michigan and Superior, Upper Peninsula, Michigan, USA. Quaternary Research, 63(2): 122–135

Chen Yongsheng, Li Jianfen, Wang Fu, et al. 2016. Records of Holocene sedimentation environment and relative sea level by the boreholes collected along the present shoreline of the west coast of Bohai Bay, China. Journal of Jilin Univerdity (Earth Science Edition) (in Chinese), 46(2): 499–517

Chen Yongsheng, Wang Hong, Li Jianfen, et al. 2012a. Sedimentary environment since 35 ka and terrestrial-marine interaction revealed by Borehole BT113 in the western coast of Bohai Bay, China. Journal of Jilin University (Earth Science Edition) (in Chinese), 42(Suppl 1): 344–354

Chen Yongsheng, Wang Hong, Pei Yandong, et al. 2012b. Division and its geological significance of the late Quaternary marine sedimentary beds in the west coast of Bohai Bay, China. Journal of Jilin University (Earth Science Edition) (in Chinese), 42(3): 747–759

Chen Yongsheng, Wang Fu, Tian Lizhu, et al. 2014. Holocene sedimentation rates and their response to fluvial supply on the west coast of Bohai Bay. Geological Bulletin of China (in Chinese), 33(10): 1582–1590

EBC (Editorial Board of Coastal Resources). 1989. Coastal Resource in Hebei Province (I) (in Chinese). Shijiazhuang: Hebei Science and Technology Press, 51–84

EBN (Editorial Board of Natural Atlas). 1965. Natural Atlas of People ’s Republic of China (in Chinese). Beijing: Zhonghua Book Company, 97–98

Fan Changfu, Wang Hong, Li Jianfen, et al. 2005. Oyster reefs response to the regional neotectonics and eustatic sea-level, northwest coast of Bohai Bay. Quaternary Sciences (in Chinese), 25(2): 235–244

Fan Changfu, Wang Hong, Pei Yandong, et al. 2008. Palaeoecological environment revealed by the buried Binhaihu Oyster Reef on the northwest coast of Bohai Bay. Marine Geology & Quaternary Geology (in Chinese), 28(1): 33–41

Giosan L, Donnelly J P, Vespremeanu E, et al. 2005. River delta morphodynamics: examples from the Danube Delta. SEPM Special Publication, 83: 393–411

Gould H R, McFarlan E Jr. 1959. Geologic history of the chenier plain, southwestern Louisiana. Gulf Coast Association of Geological Societies Transactions, 9: 261–270

Gulliver P, Palmer S, Perry C, et al. 2013. Are coral clasts from a turbid near-shore reef environment a suitable material for radiocarbon analysis?. Radiocarbon, 55(2): 624–630

Han Y S, Meng G L. 1996. Coast along the Bohai Bay. In: Zhao Xitao, Chen Zongong, Zhu Jiwen, eds. Sea Level Changes in China (in Chinese). Jinan: Shangdong Science Press, 52–70

Hatté C, Bréhéret J G, Jacob J, et al. 2013. Refining the Sarlième Paleolake (France) Neolithic chronology by combining several radiocarbon approaches. Radiocarbon, 55(2–3): 979–992

Howarth J D, Fitzsimons S J, Jacobsen G E, et al. 2013. Identifying a reliable target fraction for radiocarbon dating sedimentary records from lakes. Quaternary Geochronology, 17: 68–80

HPL (Hebei Province Land and Resource Bureau). 2007. Investigations and Assessments on Marine Resources of Hebei Province: Theme Report (1) (in Chinese). Beijing: China Ocean Press, 350–362

ICP (Institute of Culture Preservation). 1987. Report on ^{14}C Dating (WB) I. In: The Radiocarbon Dating Society of Chinese Quaternary Research Association, ed. Contribution to the Quaternary Glaciology and Geology 4 (Speical Issue on ^{14}C Dating) (in Chinese). Beijing: Geological Publishing House, 13–15

IOA (Institute of Archaeology, Chinese Academy of Social Sciences). 1983. Radiocarbon Dating in Chinese Archaeology (in Chinese). Beijing: China Cultural Relics Press, 1–321

Kowalewski M, Serrano G E A, Flessa K W, et al. 2000. Dead delta ’s former productivity: Two trillion shells at the mouth of the Colorado River. Geology, 28(12): 1059–1062

Li Xiuwen, Zhao Fuli. 1990. Report on ^{14}C Dating (TD) I. In: The Radiocarbon Dating Society of Chinese Quaternary Research Association, ed. Contribution to the Quaternary Glaciology and Geology 6 (Speical Issue on ^{14}C Dating). Beijing: Geological Publishing House, 86–102

Lin Fang, Li Fenglin, Li Jianfen, et al. 2004. Holocene ostracoda assemblages and marine transgression-regression cycle in the northwestern coastal area of the Bohai Gulf. Acta Geoscientica Sinica (in Chinese), 25(1): 53–58

Liu Zhiguang. 2007. Holocene environmental changes of the Sanhedao Island and its surrounding area, Tianjin (in Chinese) [dissertation]. Changchun: Jilin University

Luo Baoxin, Wang Yuzhao, Huang Qiupu, et al. 1983. The discovery of the *Picea* and *Coelodont* a antiquitalis symbionsis in Tianjin and its significances. Scientia Geologica Sinica (in Chinese), (2): 160–164

Mook W G, Waterbolk H T. 1985. Handbooks for Archaeologists No.3 Radiocarbon Dating. Strasbourg, France: European Science Foundation, 1-65

Nott J. 2011. A 6000 year tropical cyclone record from Western Australia. Quaternary Science Reviews, 30(5–6): 713–722

Peng Gui, Zhang Jingwen, Chen Yijian. 1984. ^{14}C dating applied in studies of Late Quaternary Bohai transgression with samples of peats and shells from Bohai Sea shore regions. In: Editing Group of the Collection of The First National ^{14}C Dating Conference, ed. Collection of The First National ^{14}C Dating Conference. Beijing: Science Press, 144–149

Peng Gui, Zhang Jingwen, Jiao Wenqiang, et al. 1980. Chronology of Late Quaternary deposits along the coast of the Bohai Bay. Seismology and Geology (in Chinese), 2(2): 71–78

Rothacker L, Dreves A, Sirocko F, et al. 2013. Dating bulk sediments from limnic deposits using a grain size approach. Radiocarbon, 55(2–3): 943–950

Shang Zhiwen. 2011. Characteristics of diatom distribution of the surficial sediments in Tianjin shallow sea area and the implications for Holocene geoenvironmental changes (in Chinese) [dissertation]. Beijing: Chinese Academy of Geological Sciences

Shang Zhiwen, Tian Lizhu, Li Jianfen, et al. 2013. Evolution of the Holocene sedimentary environment and terrestrial-marine interaction revealed by the Borehole CH114 in the west coast of the Bohai Bay of China. Marine Science Bulletin (in Chinese), 32(5): 527–534

Sirocko F, Duetrich S, Veres D, et al. 2013. Multi-proxy dating of Holocene maar lakes and Pleistocene dry maar sediments in the Eifel, Germany. Quaternary Science Reviews, 62: 56–76

SQG (Section of Quaternary Geology and ^{14}C Dating, Institute of Geochemistry, Chinese Academy of Sciences). 1980. Holocene shoreline migrations in the west coast of Bohai Bay. Quaternaria Sinica (in Chinese), 5(1): 64–69

Sun Lianyou, He Guangshun. 2013. General Situation of Coastal and Marine Environments and Resources in Tianjin (in Chinese). Beijing: China Ocean Press, 46–53

Sun Dongyan, Tan Wenbing, Pei Yandong, et al. 2011. Late Quaternary environmental change of Yellow River Basin: An organic geochemical record in Bohai Sea (North China). Organic Geochemistry, 42(6): 575–585

Wang Ying. 1964. The shell coast ridges and the old coastlines of the west coast of the Bohai Bay. Journal of Nanjing University (in Chinese), 8(3): 424–443

Wang Qiang, Gao Xiulin, Li Yude, et al. 1986. The sea-level changes and paleoclimate in west-southern plain of the Bohai Sea since 15×10^4 years. In: International Geological Correlation Programme Project No.200 China Working Group, ed. China Sea Level Changes (in Chinese). Beijing: China Ocean Press, 53–60

Wang Hong, Jiang Yi, Li Jianfen, et al. 2003. ^{14}C, ^{137}Cs and ^{210}Pb dating and accelerated tendency of the present sedimentation rate along the Laolangtuozi coast of the Bohai Bay. Geological Bulletin of China (in Chinese), 22(9): 658–664

Wang Fu, Li Jianfen, Chen Yongsheng, et al. 2015. The record of mid-Holocene maximum landward marine transgression in the west coast of Bohai Bay, China. Marine Geology, 359: 89–95

Wang Qiang, Li Xiuwen, Zhang Zhiliang, et al. 1991. Palaeoceanological significance of Holocene ostracean banks in Tianjin area. Haiyang Xuebao (in Chinese), 13(3): 371–380

Wang Hong, Shang Zhiwen, Li Jianfen, et al. 2010. Holocene shoreline changes and marine impacts on the muddy coast, western Bohai Bay, China. Geological Bulletin of China, 29(5): 627–640

Wang Qiang, Tian Guoqiang. 1999. The neotectonic setting of Late Quaternary transgressions on the eastern coastal plain of China. Journal of Geomechanics (in Chinese), 5(4): 41–48

Wang Qiang, Yuan Guibang, Zhang Shu, et al. 2007. Shelly ridge accumulation and sea-land interaction on the west coast of the Bohai Bay. Quaternary Sciences (in Chinese), 27(5): 775–786

Xia Dongxing, Yu Zhang. 1986. Several questions on the sea level research. Marine Science Bulletin (in Chinese), 5(4): 60–63

Xu Jiasheng, Liu Hezhi. 1991. An Introduction of Coastal Environment for Development in Huanghua Area (in Chinese). Beijing: China Ocean Press, 54–65

Yan Yuzhong, Wang Hong, Li Fenglin, et al. 2006a. Sedimentary environment and sea-level fluctuations revealed by Borehole BQ1 on the west coast of the Bohai Bay, China. Geological Bulletin of China (in Chinese), 25(3): 357–382

Yan Yuzhong, Wang Hong, Li Fenglin, et al. 2006b. Different depositional processes of Boreholes BQ1 and BQ2 in the Late Pleistocene on the west coast of Bohai Bay. Quaternary Sciences (in Chinese), 26(3): 321–326

Zhang Suping. 2008. Atlas of Marine Mollusks in China (in Chinese). Beijing: China Ocean Press, 1–383

Zhao Genmu, Wang Ruobai, Liu Yutian, et al. 1989. A strong earthquake event occurred in ancient time in Beijing-Tianjin-Tangshan area. Seismology and Geology (in Chinese), 11(2): 19–25

Appendix B: Correction for self-compaction

Based on the existed compaction data measured by Li et al. ③ (Table B1), the relationship between the sediment porosity and depth can be expressed as logarithmic equation

$$\Phi(z) = -0.050\,29 \times \ln(z) + 0.612\,44, \tag{B1}$$

and also illustrated as Fig. B1. With the compactable sediment thickness of 400 m and the porosity-depth equation, a numerical model was established to calculate the decompaction value based on the principles of Pico et al. (2016). The empirical relationship between the depth from the present core surface (h) and the decompaction value due to the self-compaction of Holocene and late Pleistocene sediments (Δ) are

$$\Delta = 0.000\,161h^3 - 0.010\,206h^2 + 0.428\,05h, \quad \text{when } h \leqslant 25 \text{ m}; \tag{B2}$$

$$\Delta = 0.000\,0145h^3 - 0.003\,055h^2 + 0.338\,14h, \quad \text{when } 25 \text{ m} < h \leqslant 75 \text{ m}. \tag{B3}$$

Equation (B2), illustrated in Figs B1 and B2, shows the local relationship between porosity and depth. For caution's sake, a depth of 1 000 m as consolidation settlement, if possible, is also considered (Fig. B1) ③. It clearly indicates that for the time scale and depositional depth of this study difference of decompaction values is less than 1 m for varying estimates of consolidation settlement depths (Fig. B3). Therefore, the values given by consolidation depth of 400 m, are used in this study for the shallow sediments (Table B2).